RF MEMS Technology for Radar Sensors

Koen Van Caekenberghe, Ph.D.

May 14, 2010

Overview

Overview

Acronyms

ACC	autonomous cruise control
ADC	analog to digital converter
AESA	active electronically scanned array
ALG	autonomous landing guidance
AMRFS	advanced multifunction radio frequency system
ATM	air traffic management
ATR	automatic target recognition
AWGN	additive white gaussian noise
BCB	benzo-cyclo-butene
BGA	ball grid array
BW	bandwidth
CMOS	complementary metal oxide
CNR	carrier-to-noise ratio
CNT	carbon nanotube
CPS	coplanar strip
CPW	coplanar waveguide
CW	continuous wave
DBF	digital beamforming
DC	direct current
DETSA	dual exponentially tapered slot antenna
DLP	digital light processing
ECM	electret condenser microphone
EIRP	effective isotropically radiated power
ESA	electronically scanned array
EW	electronic warfare
f/D	focal distance over diameter quotient
FBAR	thin film bulk acoustic resonator
FM	frequency modulation
FMCW	frequency modulated continuous wave
FMICW	frequency modulated interrupted continuous wave
FOPEN	foilage penetration
FSS	frequency selective surface
GND	ground
GPR	ground penetrating radar
Gr/T	receive gain over noise temperature quotient
GVD	group velocity dispersion
HEMT	high electron mobility transistor
HKMG	high-k metal gate
HPBW	half-power beamwidth
IC	integrated circuit
IF	intermediate frequency
IFF	identification friend or foe
IL	insertion loss
IMU	inertial measurement unit
IP3	third order intercept point
LCP	liquid crystal polymer
LDMOS	laterally diffused metal oxide semiconductor
LTCC	low temperature co-fired ceramic
MBE	molecular beam epitaxy
MEMS	micro-electromechanical system
MESFET	metal electric semiconductor field effect transistor
MIMO	multiple input, multiple output
MMIC	monolithic microwave integrated circuit
MOEMS	micro-opto-electro-mechanical system
MOSFET	metal oxide semiconductor field effect transistor
MPE-CVD	microwave plasma-enhanced chemical vapor deposition
NF	noise figure
nMOS	n-type metal oxide semiconductor
NRZ	non-return-to-zero
p-i-n diode	pintrinsicn diode
P1dB	1 dB gain compression
PECVD	plasma-enhanced chemical vapor deposition
PESA	passive electronically scanned array
RCS	radar cross section
RF	radio frequency
RF CMOS	radio frequency complementary metal oxide semiconductor
RF MEMS	radio frequency micro-electromechanical system
RFIC	radio frequency integrated circuit
RFID	radio frequency identification
RMS	root mean square
Rx	receive
SAR	synthetic aperture radar
SCP	single chip packaging
SDR	software defined radio
SiC	silicon carbide
SMT	surface mount technology
SNR	signal to noise ratio
SOIMEMS	silicon on insulator micro-electromechanical system
SP4T	single pole 4 throw
SPDT	single pole double throw

Acronyms

SPI	serial peripheral interconnect
SPNT	single pole double throw
SPST	single pole single throw
SSPA	solid state power amplifier
T/R	transmit / receive
TPMS	tire pressure monitoring system
TSV	through silicon via
TTD	true time delay
Tx	transmit
UNCD	ultra nanocrystalline diamond
UWB	ultra wideband
VED	vacuum electronics device
WAIM	wide angle impedance matching
WLP	wafer level packaging

Introduction

FMCW radar:
FM ranging [1–3]

- Range:

$$R = c\frac{T_c}{2}\frac{\Delta f}{f_m}$$

- Velocity:

$$v = \frac{\mathrm{d}\,R}{\mathrm{d}\,t}$$

Pulse-Doppler radar:
pulse-delay ranging [1–3]

- Range:

$$R = c\frac{\Delta\,t}{2}$$

- Velocity:

$$v = \frac{f_D\,\lambda_0}{2}$$

- Blind zone:

$$R_b = c\,(\tau_p + t_s)/2$$

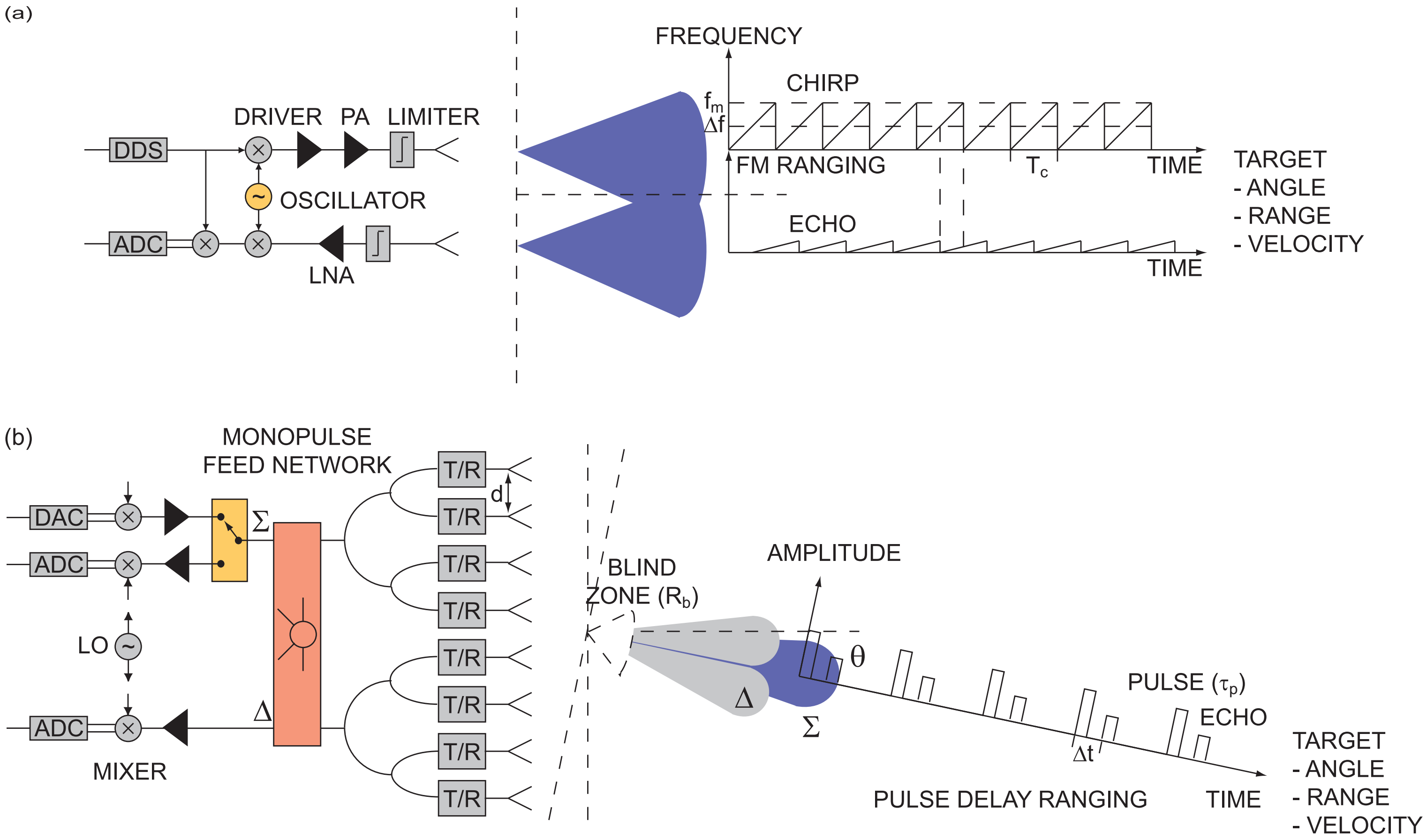

Figure 1: (a) A monostatic frequency modulated continuous wave (FMCW) radar. (b) A monostatic monopulse-Doppler radar based on an RF beamforming active electronically scanned array.

Electronically Scanned Arrays

Figures of merit [4–7]:

- Bandwidth
  - Radar range resolution:

    $r = \frac{c}{2\,BW}$

- Beam pointing error:

  $\Delta^2 = \Phi^2 \frac{\sum A_i^2\, x_i^2}{\left(\sum A_i\, x_i^2\right)^2}$

- EIRP $\times\, G_r/T$
  - Radar range equation:

    $R_{max} = \sqrt[4]{\frac{\lambda_0^2\, EIRP\; G_r/T\; \sigma}{64\,\pi^3\, k_B\; BW\; SNR_{min}}}$

  - Scan loss:

    $\frac{G}{G_0} = \frac{(\cos\theta)^n}{1+\delta^2+\Phi^2}$

- Field of view:

  $\frac{d}{\lambda_0} \le \frac{1}{1+\sin\theta_{max}}$

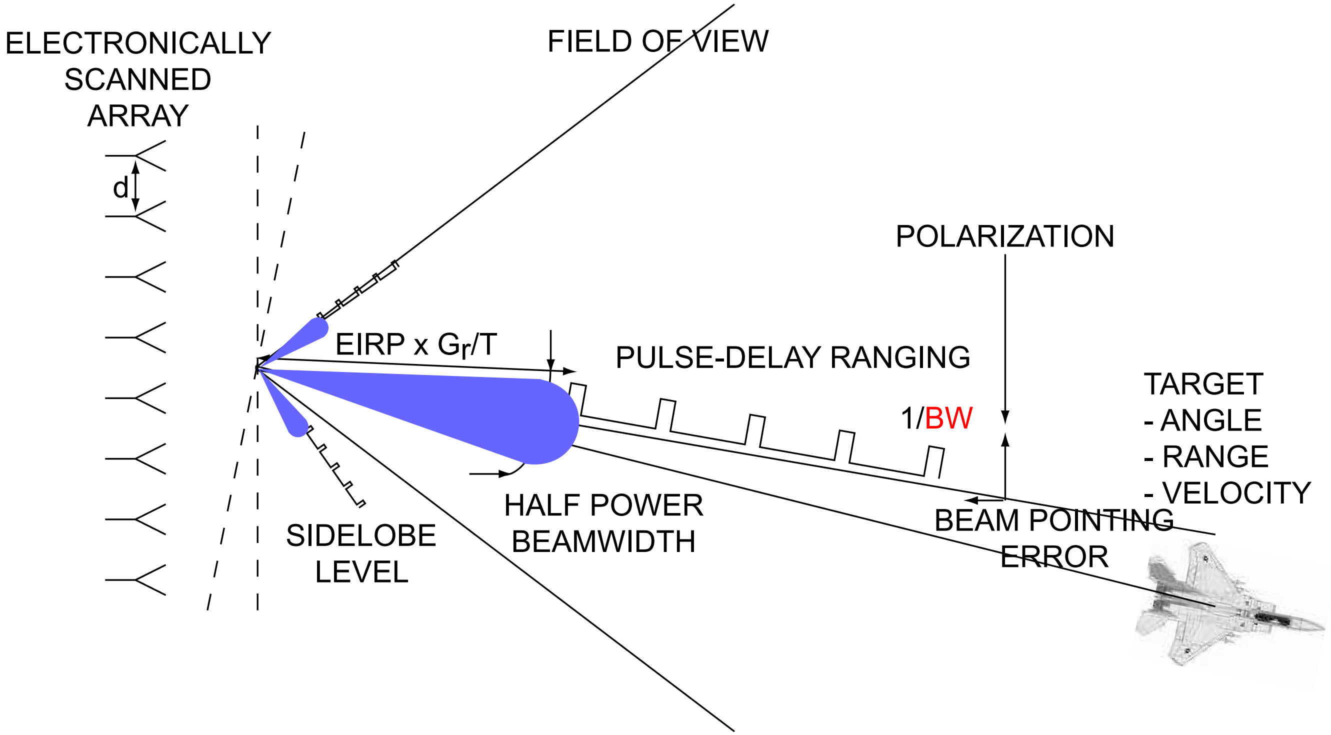

Figure 2: Figures of merit for an electronically scanned array set the radar's ability to search and track targets.

Electronically Scanned Arrays

Figures of merit [4–7]:

- Bandwidth
  - Radar range resolution:

$$r = \frac{c}{2\,BW}$$

- Beam pointing error:

$$\Delta^2 = \Phi^2 \frac{\sum A_i^2\, x_i^2}{\left(\sum A_i\, x_i^2\right)^2}$$

- EIRP $\times\, G_r/T$
  - Radar range equation:

$$R_{max} = \sqrt[4]{\frac{\lambda_0^2\, EIRP\; G_r/T\; \sigma}{64\,\pi^3\, k_B\; BW\; SNR_{min}}}$$

  - Scan loss:

$$\frac{G}{G_0} = \frac{(\cos\theta)^n}{1+\delta^2+\Phi^2}$$

- Field of view:

$$\frac{d}{\lambda_0} \leq \frac{1}{1+\sin\theta_{max}}$$

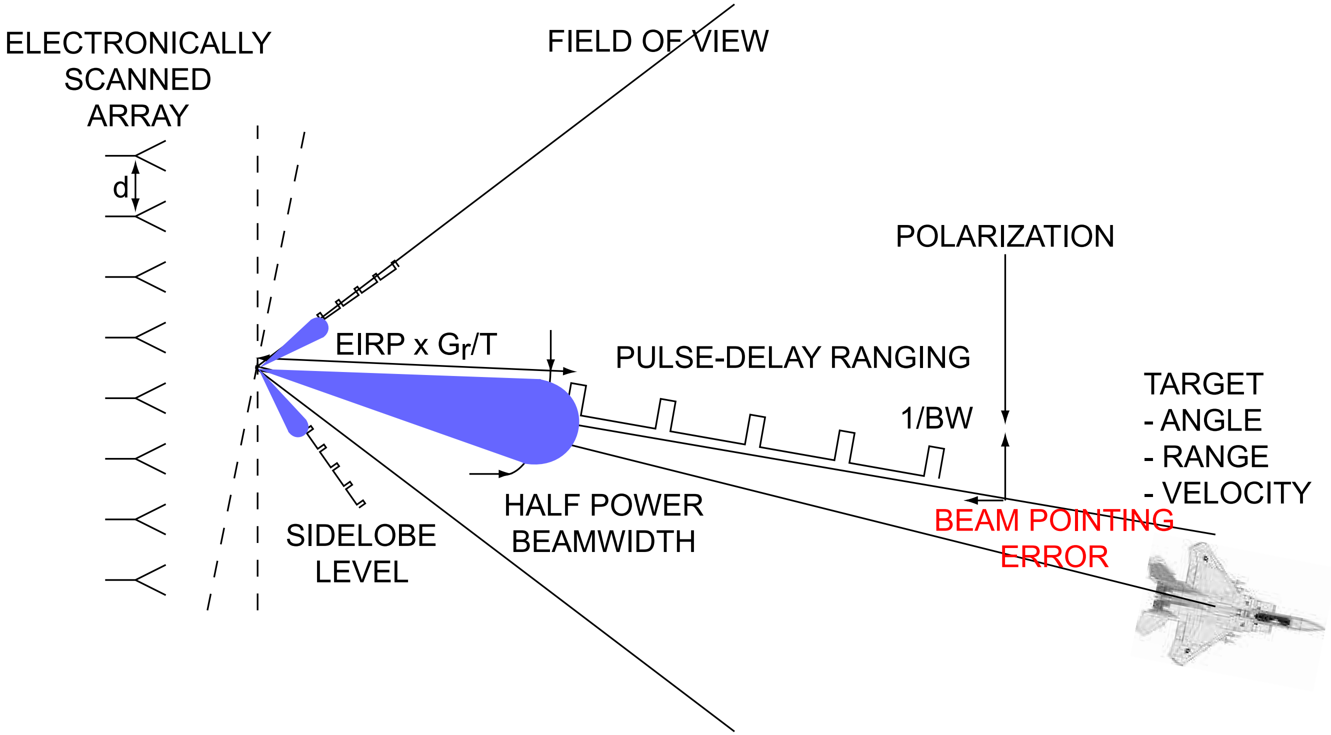

Figure 2: Figures of merit for an electronically scanned array set the radar's ability to search and track targets.

Electronically Scanned Arrays

Figures of merit [4–7]:

- Bandwidth
  - Radar range resolution:

    $r = \frac{c}{2\,BW}$

- Beam pointing error:

  $\Delta^2 = \Phi^2 \frac{\sum A_i^2\, x_i^2}{\left(\sum A_i\, x_i^2\right)^2}$

- EIRP $\times\ G_r/T$
  - Radar range equation:

    $R_{max} = \sqrt[4]{\frac{\lambda_0^2\, EIRP\ G_r/T\ \sigma}{64\,\pi^3\, k_B\ BW\ SNR_{min}}}$

  - Scan loss:

    $\frac{G}{G_0} = \frac{(\cos\theta)^n}{1+\delta^2+\Phi^2}$

- Field of view:

  $\frac{d}{\lambda_0} \leq \frac{1}{1+\sin\theta_{max}}$

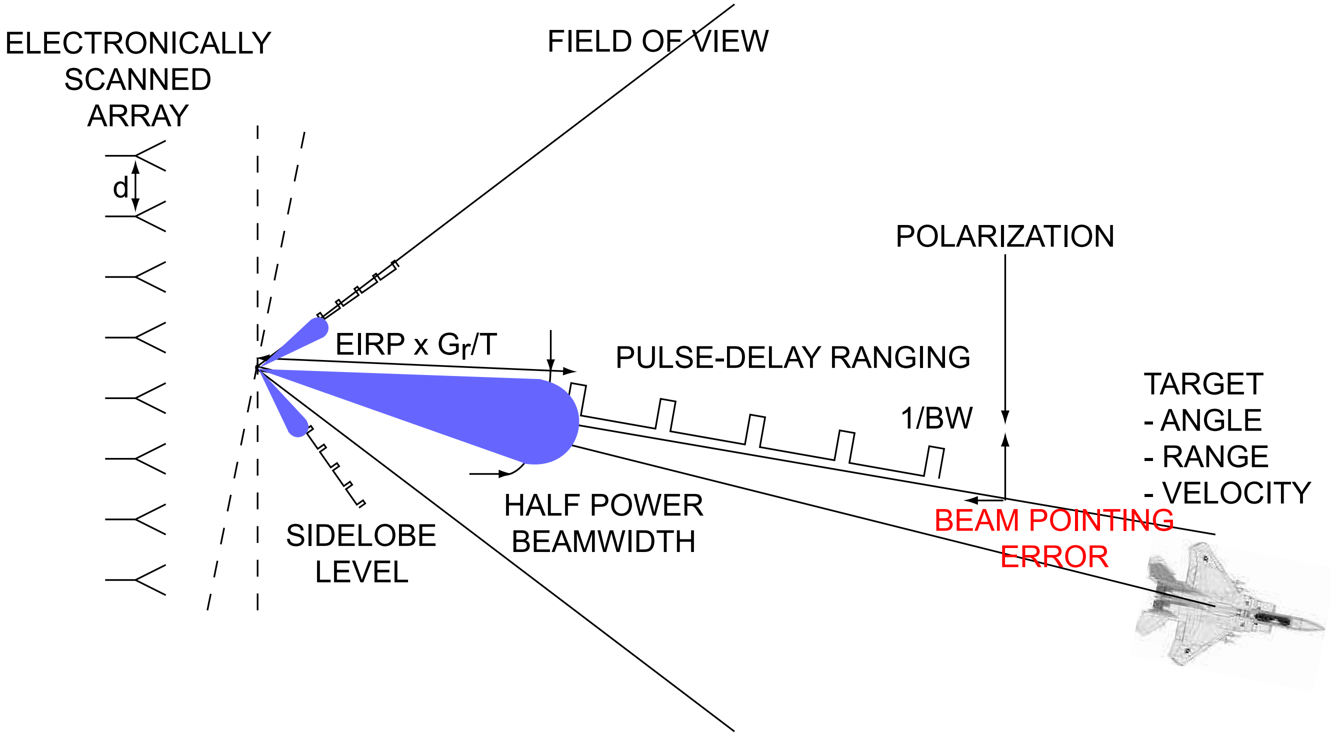

Figure 2: Figures of merit for an electronically scanned array set the radar's ability to search and track targets.

- Amplitude error variance:

  $\hat{\delta}^2 = S^2_{A_{ATT}} + S^2_{A_{PS}}$

- Phase error variance:

  $\hat{\Phi}^2 = S^2_{P_{ATT}} + S^2_{P_{PS}} + \frac{1}{3}\,\frac{\pi^2}{2^{2P}}$

Figures of merit [4–7]:

- Bandwidth
  - Radar range resolution:

    $r = \frac{c}{2\,BW}$

- Beam pointing error:

  $\triangle^2 = \Phi^2 \frac{\sum A_i^2\, x_i^2}{\left(\sum A_i\, x_i^2\right)^2}$

- EIRP $\times$ G_r/T
  - Radar range equation:

    $$R_{max} = \sqrt[4]{\frac{\lambda_0^2\, EIRP\, G_r/T\, \sigma}{64\,\pi^3\, k_B\, BW\, SNR_{min}}}$$

  - Scan loss:

    $\frac{G}{G_0} = \frac{(\cos\theta)^n}{1+\delta^2+\Phi^2}$

- Field of view:

  $\frac{d}{\lambda_0} \leq \frac{1}{1+\sin\theta_{max}}$

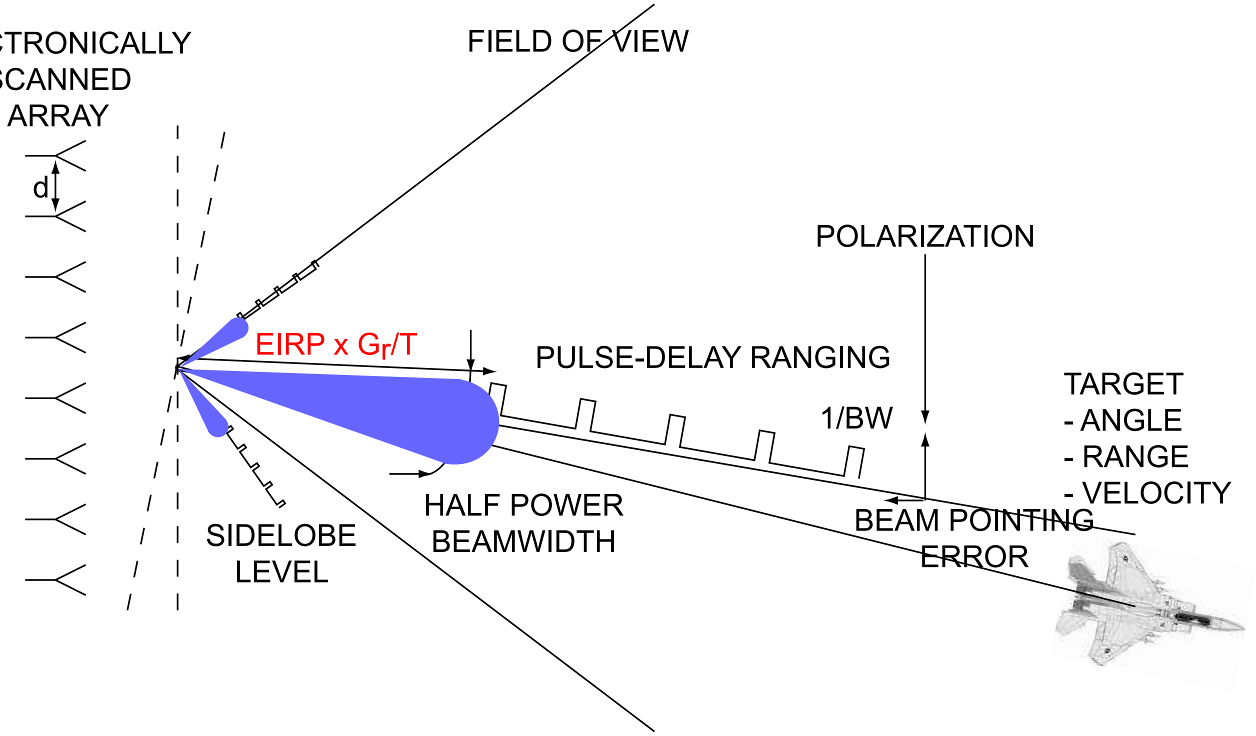

Figure 2: Figures of merit for an electronically scanned array set the radar's ability to search and track targets.

Electronically Scanned Arrays

Figures of merit [4–7]:

- ☐ Bandwidth
  - – Radar range resolution:

    $r = \frac{c}{2\,BW}$

- ☐ Beam pointing error:

  $\triangle^2 = \Phi^2 \frac{\sum A_i^2\, x_i^2}{\left(\sum A_i\, x_i^2\right)^2}$

- ☐ EIRP $\times\ G_r/T$
  - – Radar range equation:

    $R_{max} = \sqrt[4]{\frac{\lambda_0^2\, EIRP\; G_r/T\; \sigma}{64\,\pi^3\, k_B\; BW\; SNR_{min}}}$

  - – Scan loss:

    $\frac{G}{G_0} = \frac{(\cos\theta)^n}{1+\delta^2+\Phi^2}$

- ☐ Field of view:

  $\frac{d}{\lambda_0} \leq \frac{1}{1+\sin\theta_{max}}$

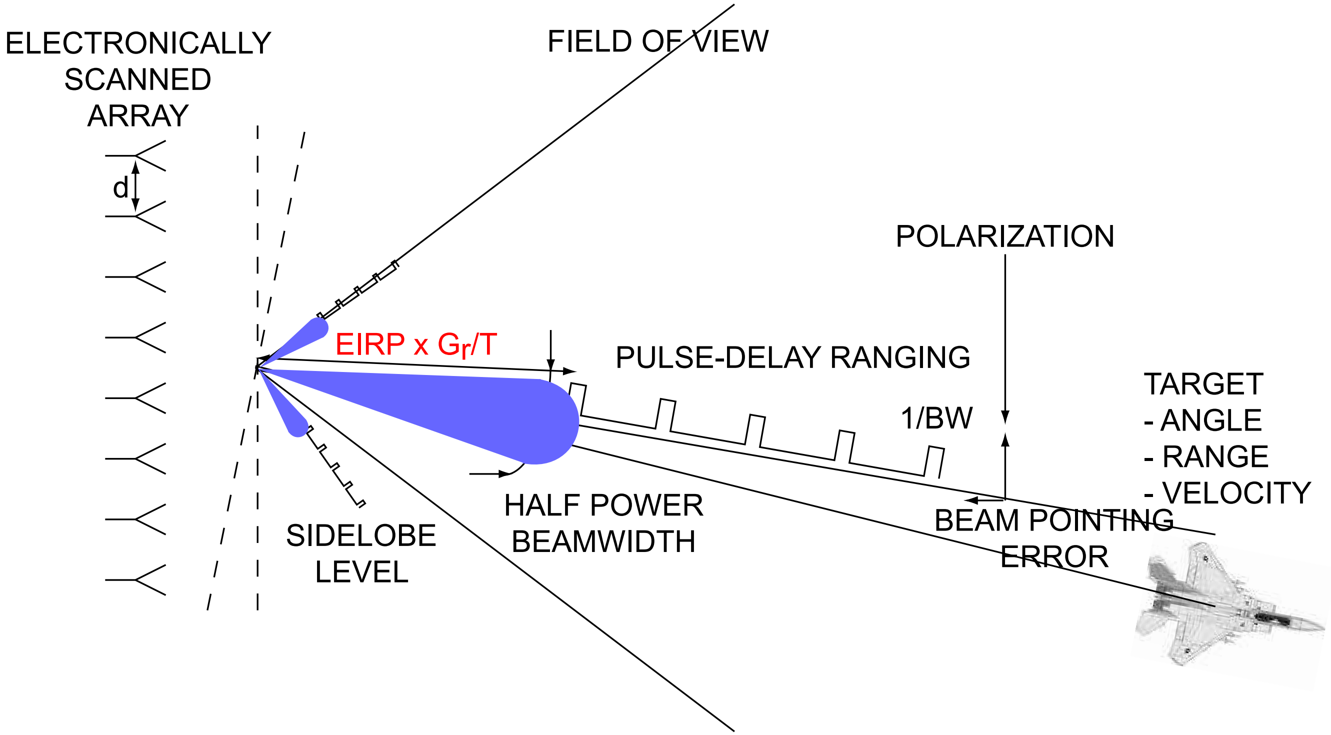

Figure 2: Figures of merit for an electronically scanned array set the radar's ability to search and track targets.

Figures of merit [4–7]:

- Bandwidth
  - Radar range resolution:

$$r = \frac{c}{2\,BW}$$

- Beam pointing error:

$$\triangle^2 = \Phi^2 \frac{\sum A_i^2\, x_i^2}{\left(\sum A_i\, x_i^2\right)^2}$$

- EIRP $\times\, G_r/T$
  - Radar range equation:

$$R_{max} = \sqrt[4]{\frac{\lambda_0^2\, EIRP\; G_r/T\; \sigma}{64\,\pi^3\, k_B\; BW\; SNR_{min}}}$$

  - Scan loss:

$$\frac{G}{G_0} = \frac{(\cos\theta)^n}{1+\delta^2+\Phi^2}$$

- Field of view:

$$\frac{d}{\lambda_0} \le \frac{1}{1+\sin\theta_{max}}$$

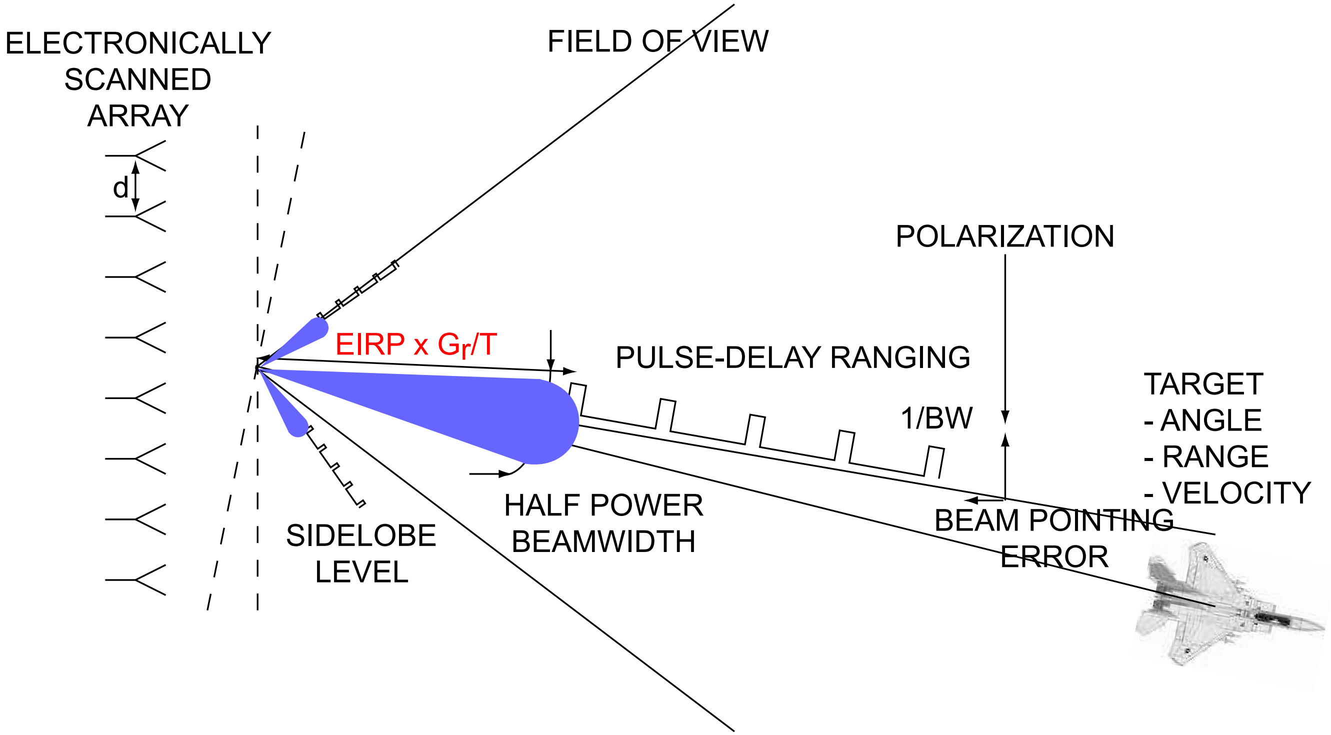

Figure 2: Figures of merit for an electronically scanned array set the radar's ability to search and track targets.

- Amplitude error variance:

$$\hat{\delta}^2 = S^2_{A_{ATT}} + S^2_{A_{PS}}$$

- Phase error variance:

$$\hat{\Phi}^2 = S^2_{P_{ATT}} + S^2_{P_{PS}} + \frac{1}{3}\,\frac{\pi^2}{2^{2P}}$$

Electronically Scanned Arrays

Figures of merit [4–7]:

- Bandwidth
  - Radar range resolution:

    $r = \frac{c}{2\,BW}$

- Beam pointing error:

  $\triangle^2 = \Phi^2 \frac{\sum A_i^2\, x_i^2}{\left(\sum A_i\, x_i^2\right)^2}$

- EIRP $\times\, G_r/T$
  - Radar range equation:

    $R_{max} = \sqrt[4]{\frac{\lambda_0^2\, EIRP\; G_r/T\; \sigma}{64\,\pi^3\, k_B\; BW\; SNR_{min}}}$

  - Scan loss:

    $\frac{G}{G_0} = \frac{(\cos\theta)^n}{1+\delta^2+\Phi^2}$

- Field of view:

  $\frac{d}{\lambda_0} \leq \frac{1}{1+\sin\theta_{max}}$

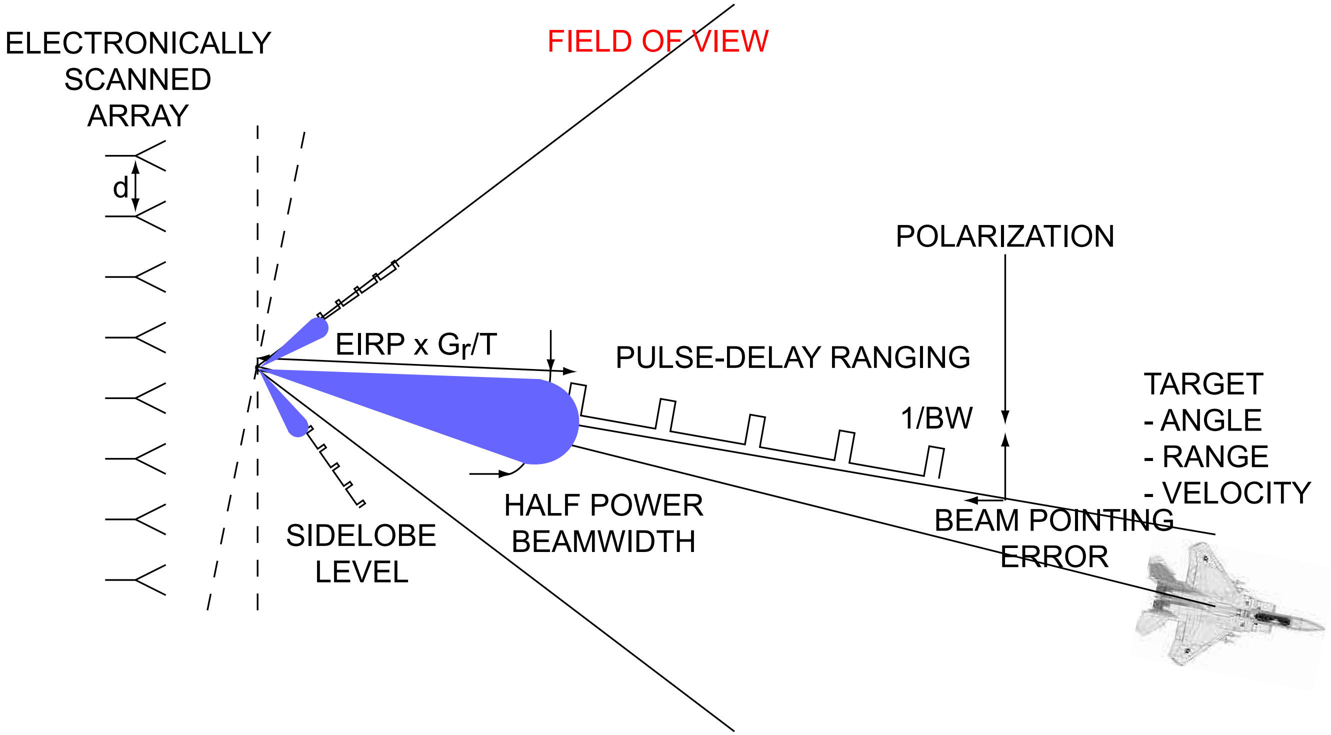

Figure 2: Figures of merit for an electronically scanned array set the radar's ability to search and track targets.

Electronically Scanned Arrays

Figures of merit (continued):

- Half-power beam width:

  $HPBW = 0.886\, B_b \, \frac{\lambda_0}{L}$
- Phase center stability
- Polarization purity
- Radar cross section
- Scalability (2-D, 3-D)
- Sidelobe level:

  $SL_{dB} = 10\, log_{10} \frac{\delta^2 + \Phi^2}{N\, \epsilon_A}$
- Size
- Thermal dissipation
- Weight

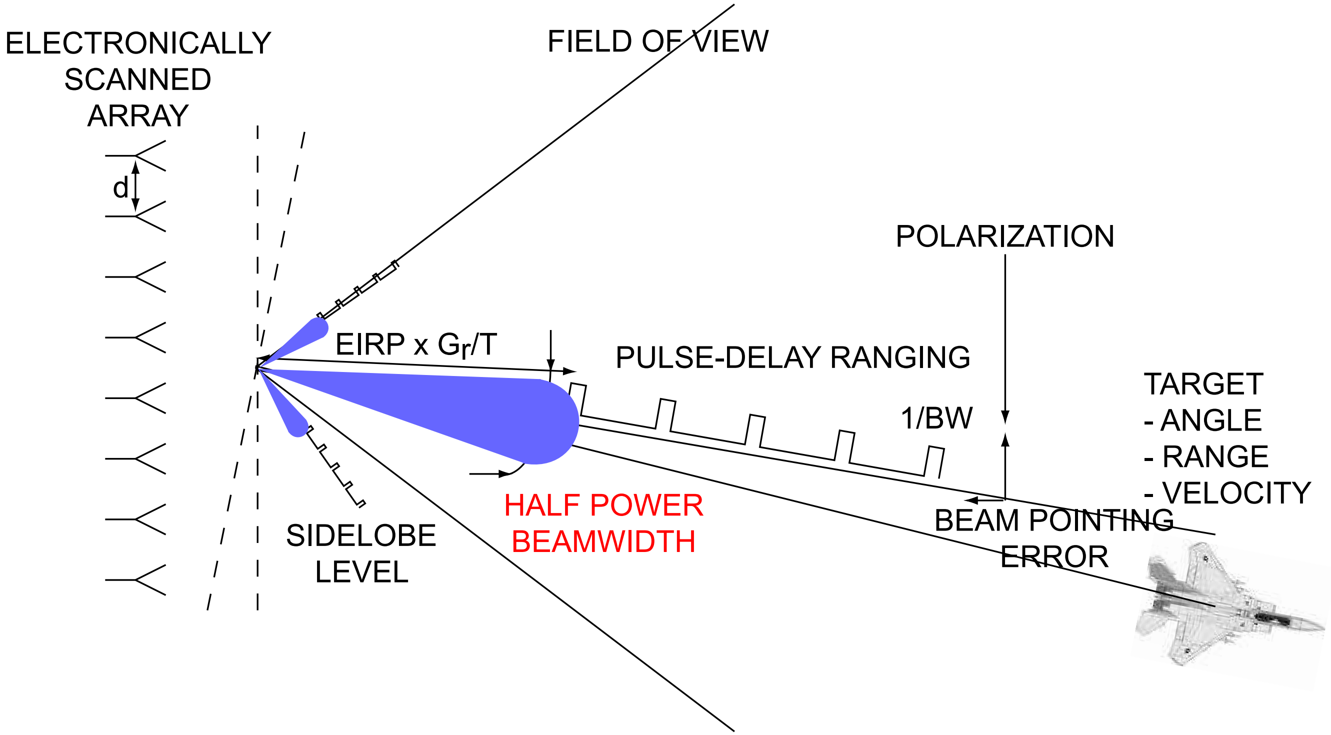

Figure 3: Figures of merit for an electronically scanned array set the radar's ability to search and track targets.

Figures of merit (continued):

- Half-power beam width:

  $HPBW = 0.886\, B_b\, \frac{\lambda_0}{L}$
- Phase center stability
- Polarization purity
- Radar cross section
- Scalability (2-D, 3-D)
- Sidelobe level:

  $SL_{dB} = 10\, log_{10}\, \frac{\delta^2 + \Phi^2}{N\, \epsilon_A}$
- Size
- Thermal dissipation
- Weight

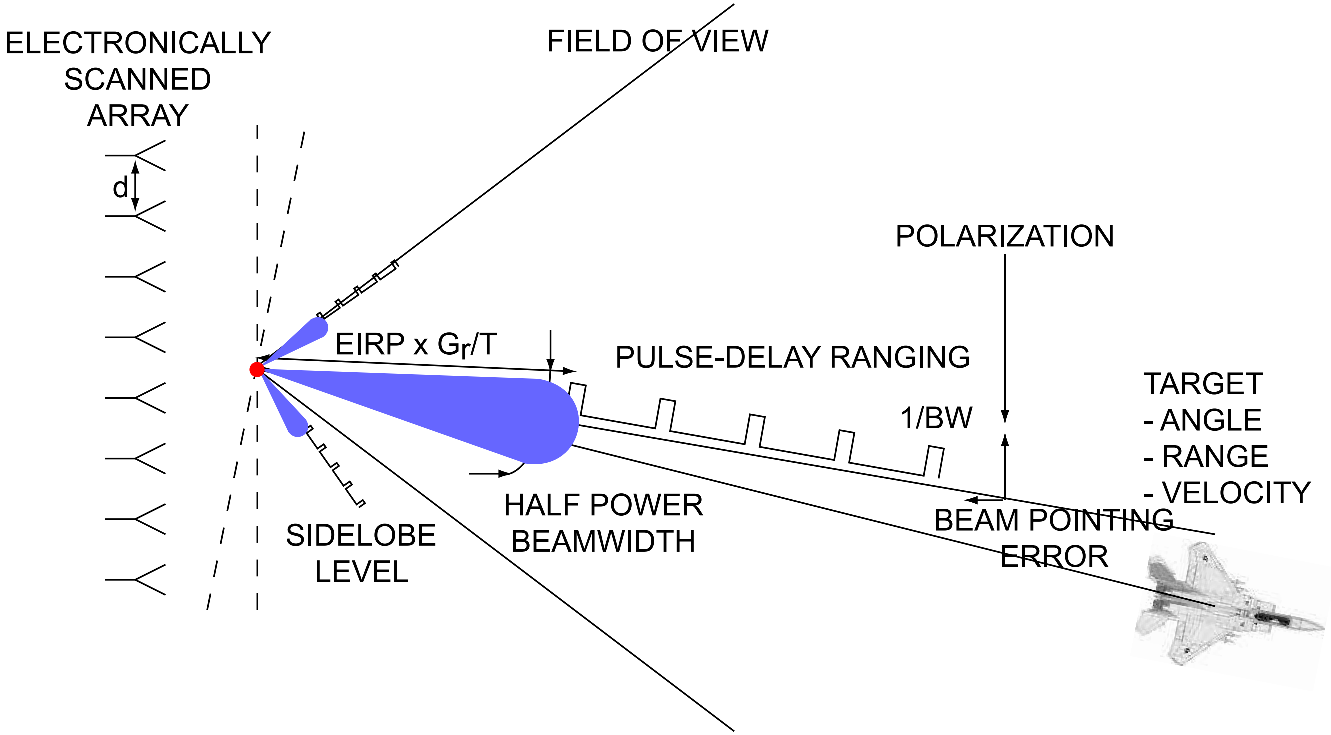

Figure 3: Figures of merit for an electronically scanned array set the radar's ability to search and track targets.

Figures of merit (continued):

- Half-power beam width:

  $HPBW = 0.886\, B_b\, \frac{\lambda_0}{L}$
- Phase center stability
- Polarization purity
- Radar cross section
- Scalability (2-D, 3-D)
- Sidelobe level:

  $SL_{dB} = 10\, log_{10}\, \frac{\delta^2 + \Phi^2}{N\, \epsilon_A}$
- Size
- Thermal dissipation
- Weight

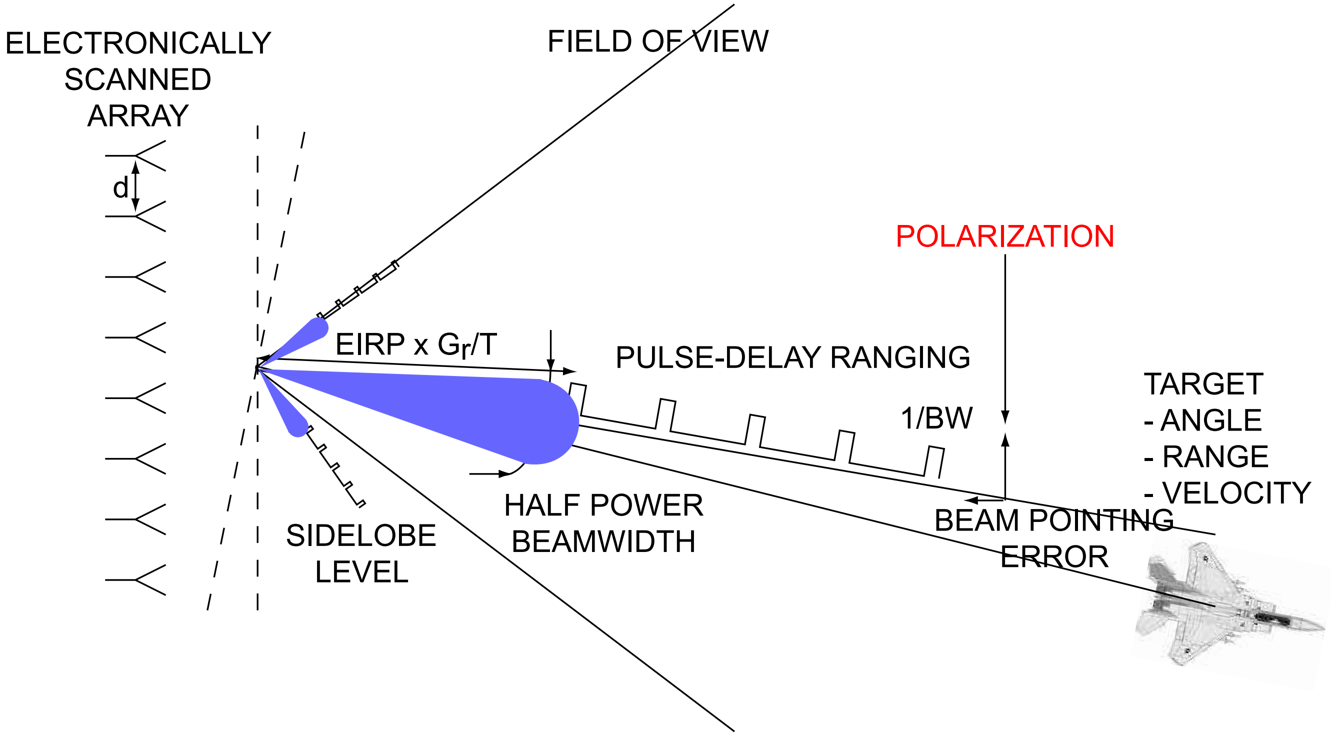

Figure 3: Figures of merit for an electronically scanned array set the radar's ability to search and track targets.

Electronically Scanned Arrays

Figures of merit (continued):

- Half-power beam width:
  $HPBW = 0.886\, B_b\, \frac{\lambda_0}{L}$
- Phase center stability
- Polarization purity
- Radar cross section
- Scalability (2-D, 3-D)
- Sidelobe level:
  $SL_{dB} = 10\, log_{10} \frac{\delta^2 + \Phi^2}{N\, \epsilon_A}$
- Size
- Thermal dissipation
- Weight

Electronically Scanned Arrays

Figures of merit (continued):

- Half-power beam width:

  $HPBW = 0.886\, B_b\, \frac{\lambda_0}{L}$

- Phase center stability
- Polarization purity
- Radar cross section
- Scalability (2-D, 3-D)
- Sidelobe level:

  $SL_{dB} = 10\, log_{10} \frac{\delta^2 + \Phi^2}{N\, \epsilon_A}$

- Size
- Thermal dissipation
- Weight

Electronically Scanned Arrays

Figures of merit (continued):

- Half-power beam width:

  $HPBW = 0.886\, B_b\, \frac{\lambda_0}{L}$

- Phase center stability
- Polarization purity
- Radar cross section
- Scalability (2-D, 3-D)
- Sidelobe level:

  $SL_{dB} = 10\, log_{10}\, \frac{\delta^2 + \Phi^2}{N\, \epsilon_A}$

- Size
- Thermal dissipation
- Weight

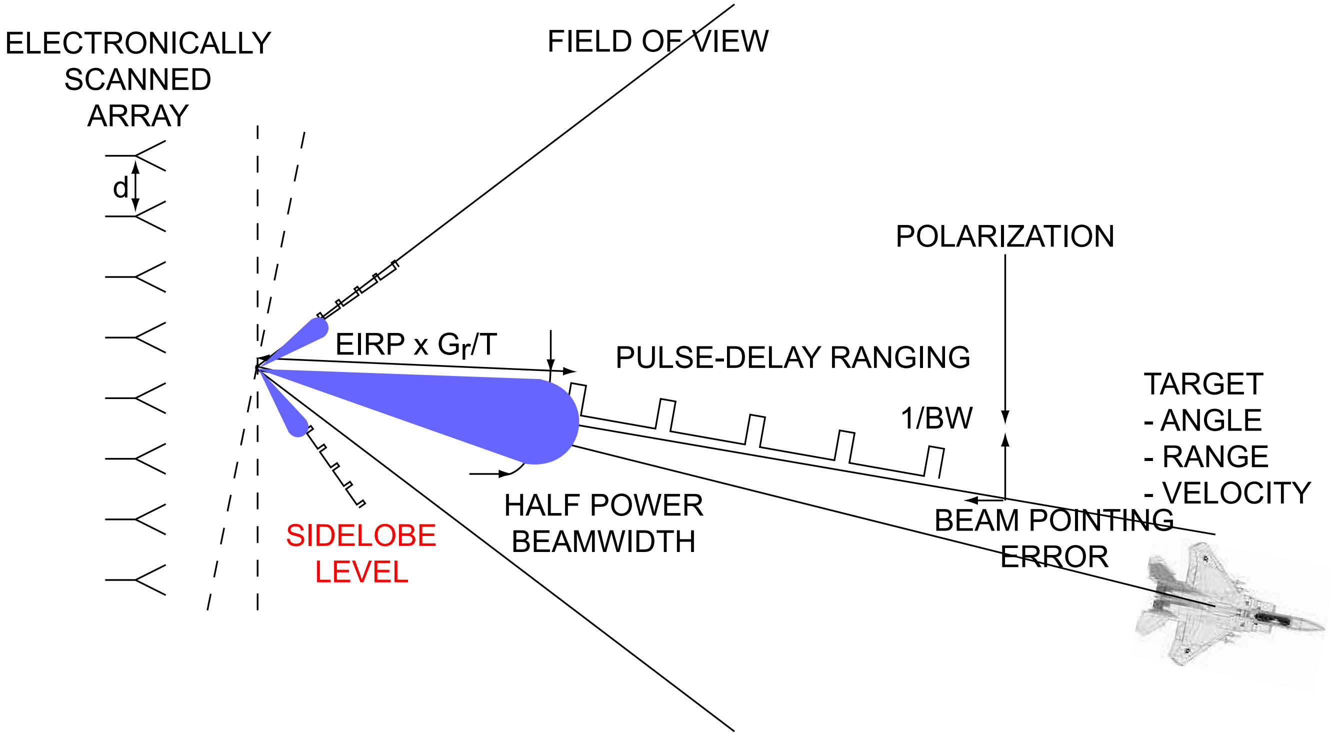

Figure 3: Figures of merit for an electronically scanned array set the radar's ability to search and track targets.

Figures of merit (continued):

- ☐ Half-power beam width:

  $HPBW = 0.886\, B_b\, \frac{\lambda_0}{L}$

- ☐ Phase center stability
- ☐ Polarization purity
- ☐ Radar cross section
- ☐ Scalability (2-D, 3-D)
- ☐ Sidelobe level:

  $SL_{dB} = 10\, log_{10}\, \frac{\delta^2 + \Phi^2}{N\, \epsilon_A}$

- ☐ Size
- ☐ Thermal dissipation
- ☐ Weight

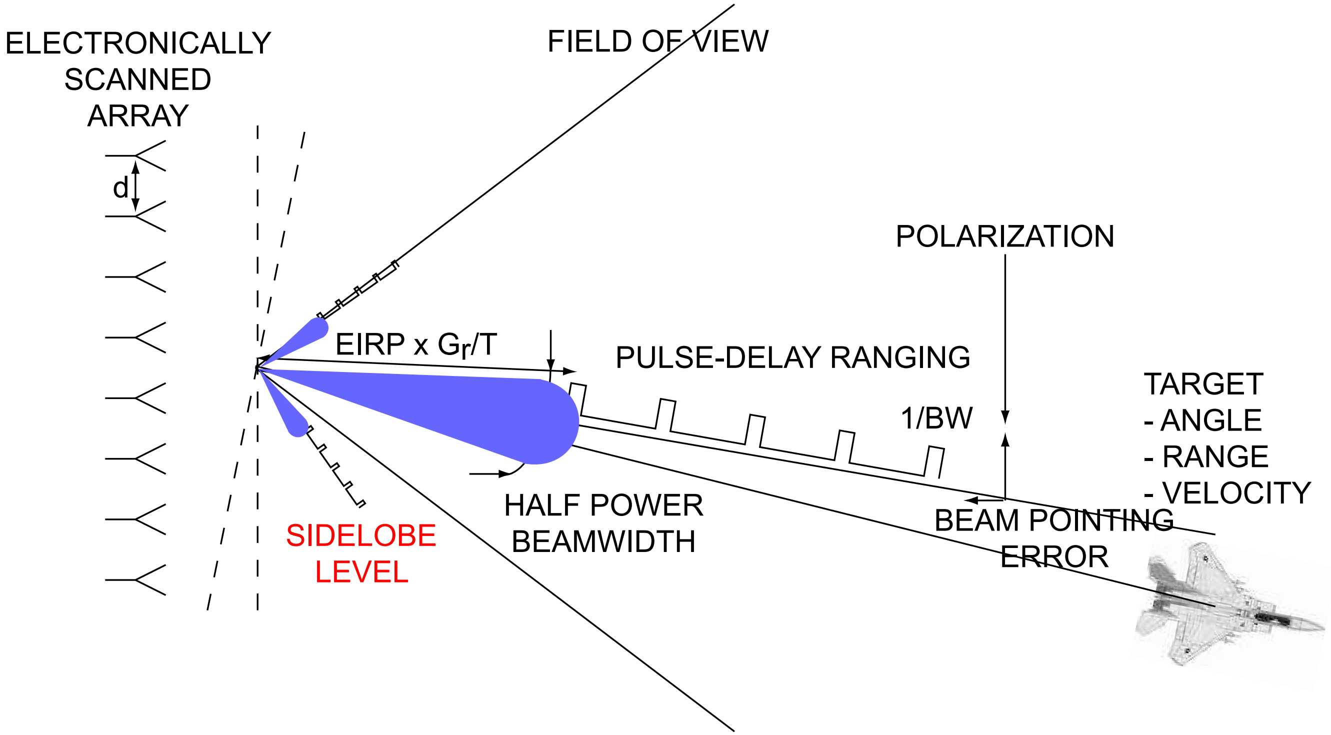

Figure 3: Figures of merit for an electronically scanned array set the radar's ability to search and track targets.

- ☐ Amplitude error variance:

  $\hat{\delta}^2 = S^2_{A_{ATT}} + S^2_{A_{PS}}$

- ☐ Phase error variance:

  $\hat{\Phi}^2 = S^2_{P_{ATT}} + S^2_{P_{PS}} + \frac{1}{3}\, \frac{\pi^2}{2^{2P}}$

Figures of merit (continued):

- Half-power beam width:
  $HPBW = 0.886\, B_b\, \frac{\lambda_0}{L}$
- Phase center stability
- Polarization purity
- Radar cross section
- Scalability (2-D, 3-D)
- Sidelobe level:
  $SL_{dB} = 10\, log_{10} \frac{\delta^2 + \Phi^2}{N\, \epsilon_A}$
- Size
- Thermal dissipation
- Weight

Electronically Scanned Arrays

Figures of merit (continued):

- Half-power beam width:
  $HPBW = 0.886\, B_b\, \frac{\lambda_0}{L}$
- Phase center stability
- Polarization purity
- Radar cross section
- Scalability (2-D, 3-D)
- Sidelobe level:
  $SL_{dB} = 10\, log_{10} \frac{\delta^2 + \Phi^2}{N\, \epsilon_A}$
- Size
- Thermal dissipation
- Weight

Electronically Scanned Arrays

Figures of merit (continued):

- Half-power beam width:

  $HPBW = 0.886\, B_b\, \frac{\lambda_0}{L}$

- Phase center stability
- Polarization purity
- Radar cross section
- Scalability (2-D, 3-D)
- Sidelobe level:

  $SL_{dB} = 10\, log_{10} \frac{\delta^2 + \Phi^2}{N\, \epsilon_A}$

- Size
- Thermal dissipation
- Weight

Electronically Scanned Arrays

Design trade-offs are necessary in the selection of:

- Aperture: real beam or synthetic aperture (SAR)
- Antenna: connected or folded dipole, microstrip, tapered slot, or waveguide antenna
- Beamforming: digital (DBF), IF, optical, RF
- Feed network: constrained (corporate, series) or space-fed (lens array, reflect array). Extensions include monopulse feeds and calibration networks.
- Grid: periodic (hexagonal, rectangular, or triangular) or aperiodic (sparse)
- Manufacturing: 2-D arrays: brick, stick, tile [8] or tray, 3-D arrays: geodesic dome, multifaceted (pyramidal frusta)
- Polarization: vertical (taking advantage of Brewster angle for ground-based and naval platforms), polarimetric (all-weather, foilage penetration (FOPEN), SAR/ATR)
- RF power amplification: active (SSPA) [9], passive subarrays, passive (VED)
- Scanning: frequency-, space-, or time-orthogonal waveform-coherent pencil beams, or multiple input multiple output (MIMO) waveform-orthogonal wide beams

Electronically Scanned Arrays

Design trade-offs are necessary in the selection of:

- ☐ Aperture: real beam or synthetic aperture (SAR)
- ☐ Antenna: connected or folded dipole, microstrip, tapered slot, or waveguide antenna
- ☐ Beamforming: digital (DBF), IF, optical, RF
- ☐ Feed network: constrained (corporate, series) or space-fed (lens array, reflect array). Extensions include monopulse feeds and calibration networks.
- ☐ Grid: periodic (hexagonal, rectangular, or triangular) or aperiodic (sparse)
- ☐ Manufacturing: 2-D arrays: brick, stick, tile [8] or tray, 3-D arrays: geodesic dome, multifaceted (pyramidal frusta)
- ☐ Polarization: vertical (taking advantage of Brewster angle for ground-based and naval platforms), polarimetric (all-weather, foilage penetration (FOPEN), SAR/ATR)
- ☐ RF power amplification: active (SSPA) [9], passive subarrays, passive (VED)
- ☐ Scanning: frequency-, space-, or time-orthogonal waveform-coherent pencil beams, or multiple input multiple output (MIMO) waveform-orthogonal wide beams

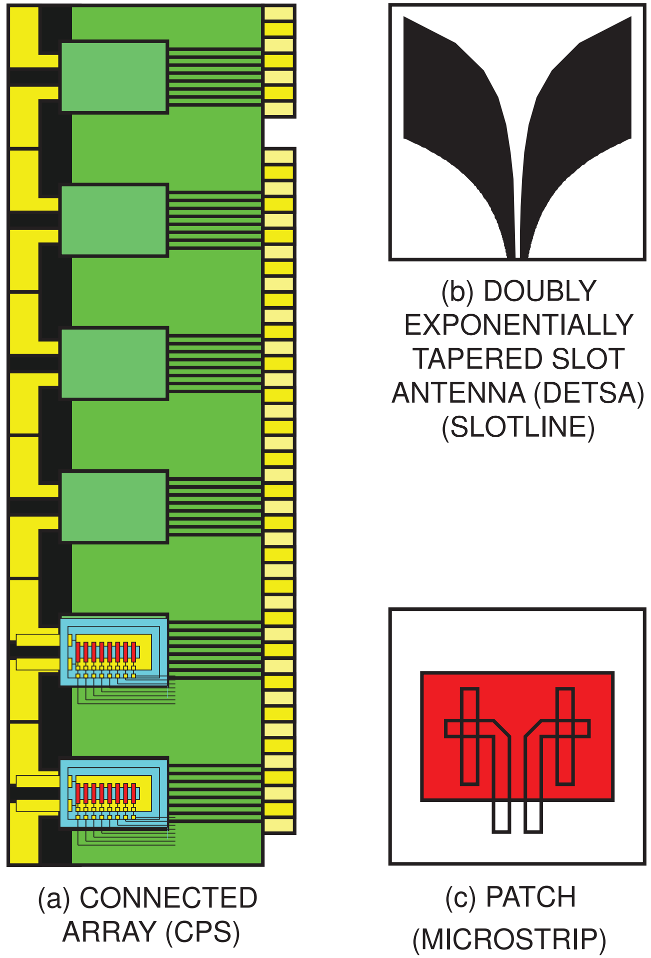

Figure 3: Antennas: (a) Connected array, (b) DETSA, and (c) microstrip.

Electronically Scanned Arrays

Design trade-offs are necessary in the selection of:

- Aperture: real beam or synthetic aperture (SAR)
- Antenna: connected or folded dipole, microstrip, tapered slot, or waveguide antenna
- Beamforming: digital (DBF), IF, optical, RF
- Feed network: constrained (corporate, series) or space-fed (lens array, reflect array). Extensions include monopulse feeds and calibration networks.
- Grid: periodic (hexagonal, rectangular, or triangular) or aperiodic (sparse)
- Manufacturing: 2-D arrays: brick, stick, tile [8] or tray, 3-D arrays: geodesic dome, multifaceted (pyramidal frusta)
- Polarization: vertical (taking advantage of Brewster angle for ground-based and naval platforms), polarimetric (all-weather, foilage penetration (FOPEN), SAR/ATR)
- RF power amplification: active (SSPA) [9], passive subarrays, passive (VED)
- Scanning: frequency-, space-, or time-orthogonal waveform-coherent pencil beams, or multiple input multiple output (MIMO) waveform-orthogonal wide beams

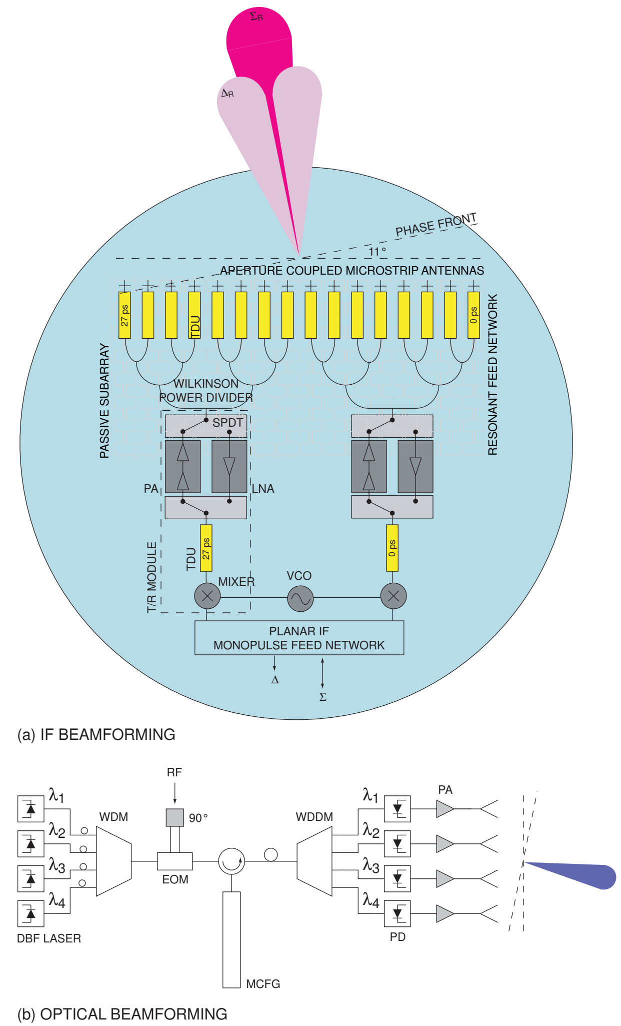

Figure 3: Beamforming networks: (a) IF, and (b) optical

Electronically Scanned Arrays

Design trade-offs are necessary in the selection of:

- Aperture: real beam or synthetic aperture (SAR)
- Antenna: connected or folded dipole, microstrip, tapered slot, or waveguide antenna
- Beamforming: digital (DBF), IF, optical, RF
- Feed network: constrained (corporate, series) or space-fed (lens array, reflect array). Extensions include monopulse feeds and calibration networks.
- Grid: periodic (hexagonal, rectangular, or triangular) or aperiodic (sparse)
- Manufacturing: 2-D arrays: brick, stick, tile [8] or tray, 3-D arrays: geodesic dome, multifaceted (pyramidal frusta)
- Polarization: vertical (taking advantage of Brewster angle for ground-based and naval platforms), polarimetric (all-weather, foilage penetration (FOPEN), SAR/ATR)
- RF power amplification: active (SSPA) [9], passive subarrays, passive (VED)
- Scanning: frequency-, space-, or time-orthogonal waveform-coherent pencil beams, or multiple input multiple output (MIMO) waveform-orthogonal wide beams

Electronically Scanned Arrays

Design trade-offs are necessary in the selection of:

- Aperture: real beam or synthetic aperture (SAR)
- Antenna: connected or folded dipole, microstrip, tapered slot, or waveguide antenna
- Beamforming: digital (DBF), IF, optical, RF
- Feed network: constrained (corporate, series) or space-fed (lens array, reflect array). Extensions include monopulse feeds and calibration networks.
- Grid: periodic (hexagonal, rectangular, or triangular) or aperiodic (sparse)
- Manufacturing: 2-D arrays: brick, stick, tile [8] or tray, 3-D arrays: geodesic dome, multifaceted (pyramidal frusta)
- Polarization: vertical (taking advantage of Brewster angle for ground-based and naval platforms), polarimetric (all-weather, foilage penetration (FOPEN), SAR/ATR)
- RF power amplification: active (SSPA) [9], passive subarrays, passive (VED)
- Scanning: frequency-, space-, or time-orthogonal waveform-coherent pencil beams, or multiple input multiple output (MIMO) waveform-orthogonal wide beams

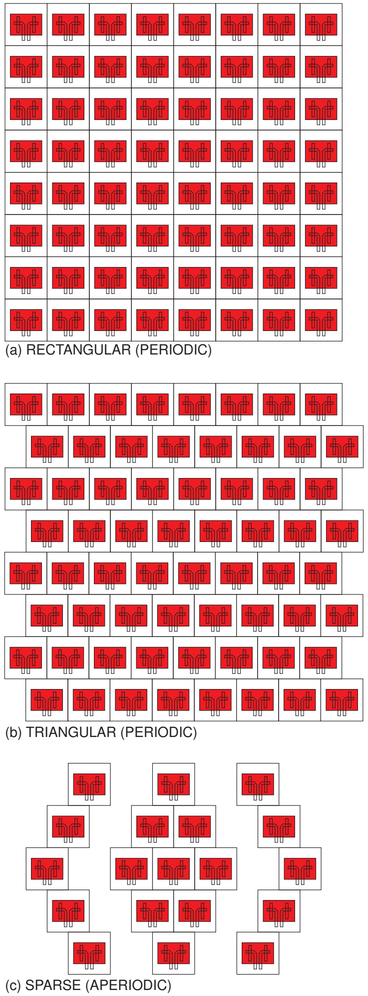

Figure 3: Grid: (a) rectangular (periodic), (b) triangular (periodic), (c) sparse (aperiodic).

Electronically Scanned Arrays

Design trade-offs are necessary in the selection of:

- □ Aperture: real beam or synthetic aperture (SAR)
- □ Antenna: connected or folded dipole, microstrip, tapered slot, or waveguide antenna
- □ Beamforming: digital (DBF), IF, optical, RF
- □ Feed network: constrained (corporate, series) or space-fed (lens array, reflect array). Extensions include monopulse feeds and calibration networks.
- □ Grid: periodic (hexagonal, rectangular, or triangular) or aperiodic (sparse)
- □ Manufacturing: 2-D arrays: brick, stick, tile [8] or tray, 3-D arrays: geodesic dome, multifaceted (pyramidal frusta)
- □ Polarization: vertical (taking advantage of Brewster angle for ground-based and naval platforms), polarimetric (all-weather, foilage penetration (FOPEN), SAR/ATR)
- □ RF power amplification: active (SSPA) [9], passive subarrays, passive (VED)
- □ Scanning: frequency-, space-, or time-orthogonal waveform-coherent pencil beams, or multiple input multiple output (MIMO) waveform-orthogonal wide beams

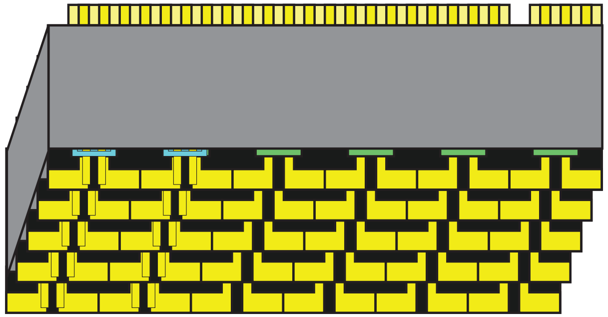

Figure 3: Manufacturing: brick assembly.

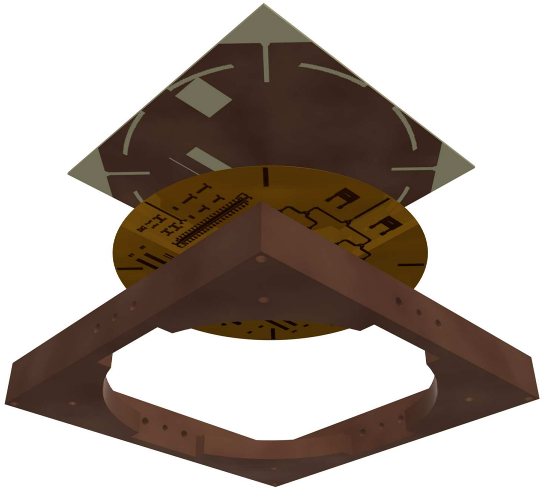

Figure 4: Manufacturing: tile assembly.

Electronically Scanned Arrays

Design trade-offs are necessary in the selection of:

- Aperture: real beam or synthetic aperture (SAR)
- Antenna: connected or folded dipole, microstrip, tapered slot, or waveguide antenna
- Beamforming: digital (DBF), IF, optical, RF
- Feed network: constrained (corporate, series) or space-fed (lens array, reflect array). Extensions include monopulse feeds and calibration networks.
- Grid: periodic (hexagonal, rectangular, or triangular) or aperiodic (sparse)
- Manufacturing: 2-D arrays: brick, stick, tile [8] or tray, 3-D arrays: geodesic dome, multifaceted (pyramidal frusta)
- Polarization: vertical (taking advantage of Brewster angle for ground-based and naval platforms), polarimetric (all-weather, foilage penetration (FOPEN), SAR/ATR)
- RF power amplification: active (SSPA) [9], passive subarrays, passive (VED)
- Scanning: frequency-, space-, or time-orthogonal waveform-coherent pencil beams, or multiple input multiple output (MIMO) waveform-orthogonal wide beams

Electronically Scanned Arrays

Design trade-offs are necessary in the selection of:

- Aperture: real beam or synthetic aperture (SAR)
- Antenna: connected or folded dipole, microstrip, tapered slot, or waveguide antenna
- Beamforming: digital (DBF), IF, optical, RF
- Feed network: constrained (corporate, series) or space-fed (lens array, reflect array). Extensions include monopulse feeds and calibration networks.
- Grid: periodic (hexagonal, rectangular, or triangular) or aperiodic (sparse)
- Manufacturing: 2-D arrays: brick, stick, tile [8] or tray, 3-D arrays: geodesic dome, multifaceted (pyramidal frusta)
- Polarization: vertical (taking advantage of Brewster angle for ground-based and naval platforms), polarimetric (all-weather, foilage penetration (FOPEN), SAR/ATR)
- RF power amplification: active (SSPA) [9], passive subarrays, passive (VED)
- Scanning: frequency-, space-, or time-orthogonal waveform-coherent pencil beams, or multiple input multiple output (MIMO) waveform-orthogonal wide beams

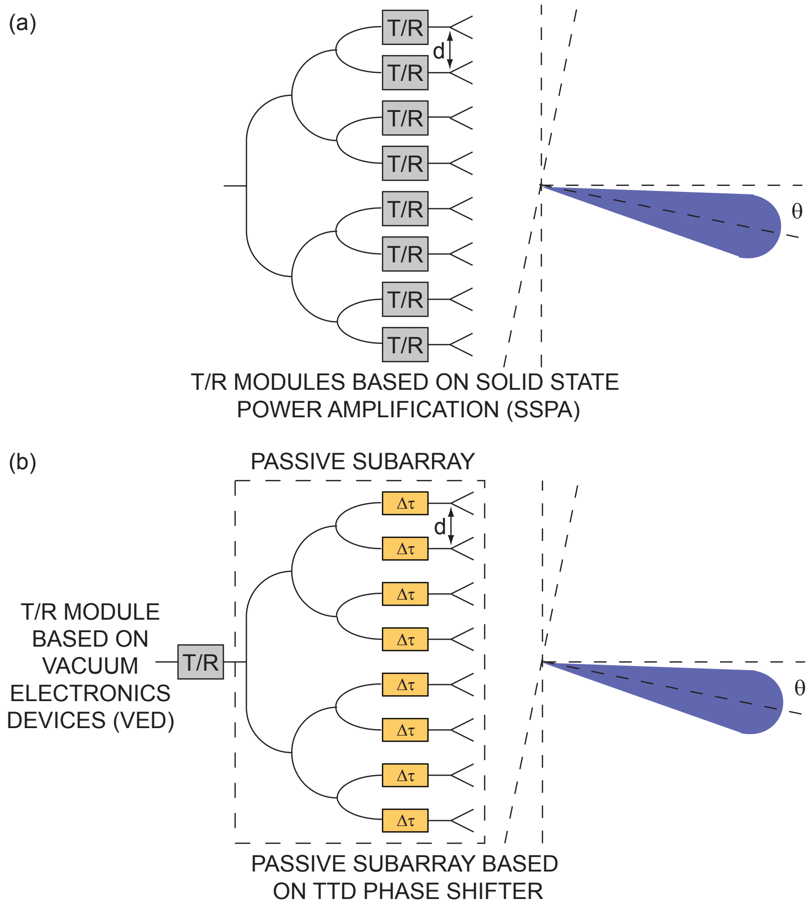

Figure 3: RF power amplification: (a) An active electronically scanned array (AESA), and (b) a passive electronically scanned array (PESA).

Electronically Scanned Arrays

Design trade-offs are necessary in the selection of:

- Aperture: real beam or synthetic aperture (SAR)
- Antenna: connected or folded dipole, microstrip, tapered slot, or waveguide antenna
- Beamforming: digital (DBF), IF, optical, RF
- Feed network: constrained (corporate, series) or space-fed (lens array, reflect array). Extensions include monopulse feeds and calibration networks.
- Grid: periodic (hexagonal, rectangular, or triangular) or aperiodic (sparse)
- Manufacturing: 2-D arrays: brick, stick, tile [8] or tray, 3-D arrays: geodesic dome, multifaceted (pyramidal frusta)
- Polarization: vertical (taking advantage of Brewster angle for ground-based and naval platforms), polarimetric (all-weather, foilage penetration (FOPEN), SAR/ATR)
- RF power amplification: active (SSPA) [9], passive subarrays, passive (VED)
- Scanning: frequency-, space-, or time-orthogonal waveform-coherent pencil beams, or multiple input multiple output (MIMO) waveform-orthogonal wide beams

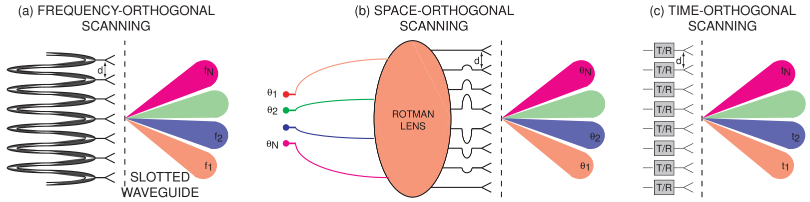

Figure 3: Electronically scanned array architectures: (a) frequency-orthogonal scanning with a slotted waveguide, (b) spatially-orthogonal scanning with a Rotman lens, (c) time-orthogonal scanning with RF (TTD) phase shifters.

Introduction: References

[1] G. W. Stimson, *Introduction to Airborne Radar, 2nd Ed.* SciTech Publishing, 1998.

[2] P. Lacomme, J.-P. Hardange, J.-C. Marchais, and E. Normant, *Air and Spaceborne Radar Systems: An Introduction*. IEE, 2001.

[3] M. I. Skolnik, *Introduction to Radar Systems, 3rd Ed.* McGraw-Hill, 2005.

[4] D. Parker and D. C. Zimmermann, "Phased arrays - Part I: Theory and architectures," *IEEE Trans. Microwave Theory Tech.*, vol. 50, no. 3, pp. 678–687, March 2002.

[5] ——, "Phased arrays - Part II: Implementations, applications, and future trends," *IEEE Trans. Microwave Theory Tech.*, vol. 50, no. 3, pp. 688–698, March 2002.

[6] R. J. Mailloux, *Phased Array Antenna Handbook*. Artech House, 2005.

[7] E. Brookner, "Phased array radars: Past, astounding breakthroughs and future trends," *Microwave Journal*, vol. 51, no. 1, p. 30, January 2008.

[8] A. M. Puzella, J. M. Crowder, P. S. Dupuis, M. C. Fallica, J. B. Francis, and J. A. Licciardello, "Tile sub-array and related circuits and techniques," U.S. Patent 7,348,932 B1, September 21, 2006.

[9] M. Smith, M. Sarcione, and R. Conilogue, "Pioneering phased array systems & technologies. active electronically steered antennas," *Technology Today (Highlighting Raytheon's Technology)*, vol. 3, no. 1, pp. 19–23, 2004.

RF MEMS Technology

MEMS Disambiguation

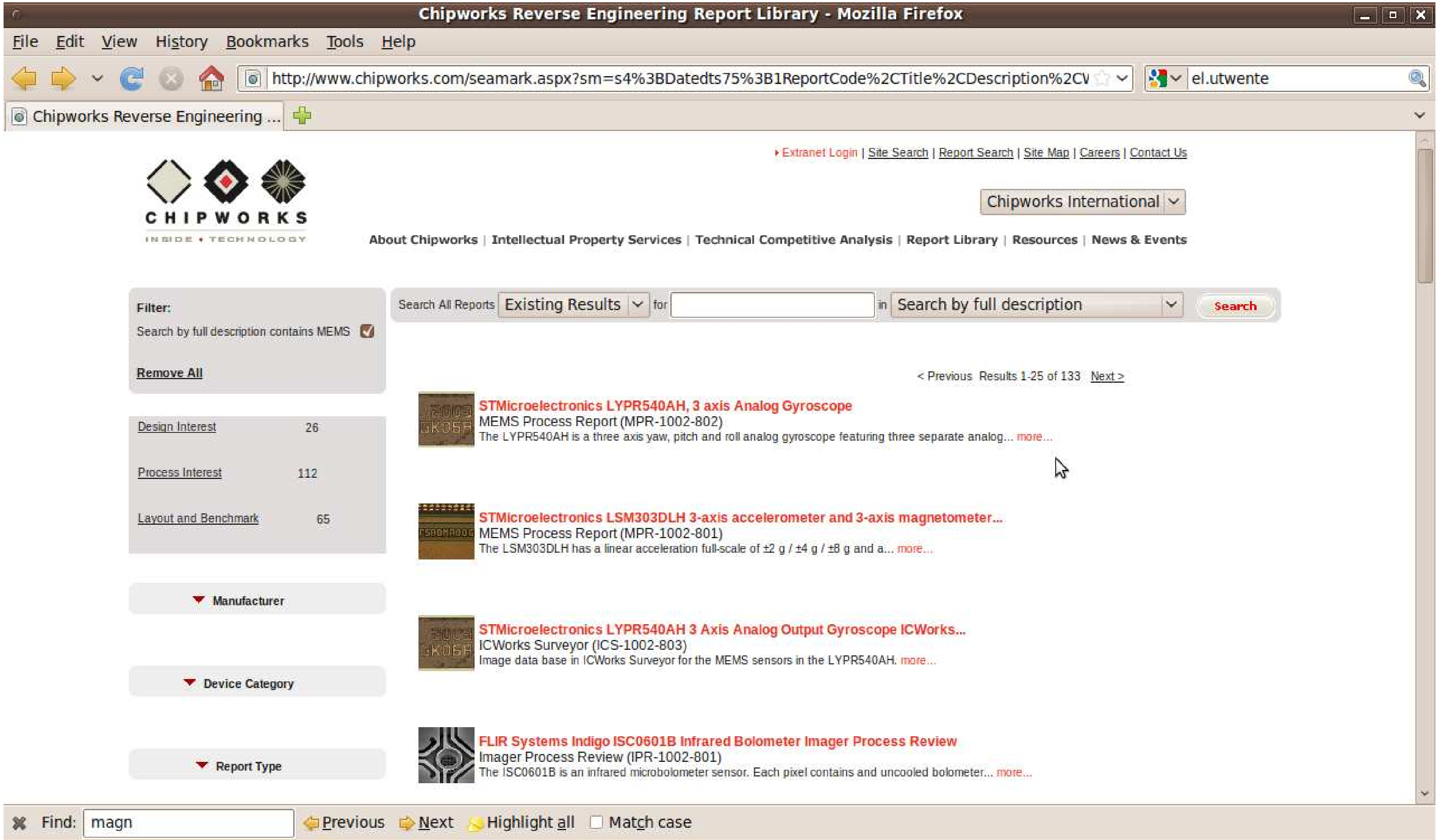

Figure 4: Chipworks.com search results for MEMS

MEMS Disambiguation: Actuators, Harvesters and Sensors

- **Definition**: Micro-electromechanical system (MEMS) = bulk or surface-micromachined device
- **General advantages**: cost, dynamic range (resolution), integration (on-chip or in-package integration with a mixed-signal IC for ADC, calibration, electronic power conditioning (charge-pumping, DC-DC conversion), digital serial interface (I_2C, SPI), power consumption (cooling), sensitivity, size.
- **Classification** [1–3]:
  - MEMS actuators:
    - Inkjet printheads
    - Micro-mirrors (digital light processors (DLP), pico-projectors)
  - MEMS chemical sensors:
    - BioMEMS: lab-on-a-chip, micro total analysis system (μTAS) (advantages: fast biomedical analysis)
    - MEMS multicapillary gas chromatographs, gas spectrometers (advantages: portable, shock and vibration resistant)
    - MEMS nanoreactors for hydrogen storage (applications: fuel cells)

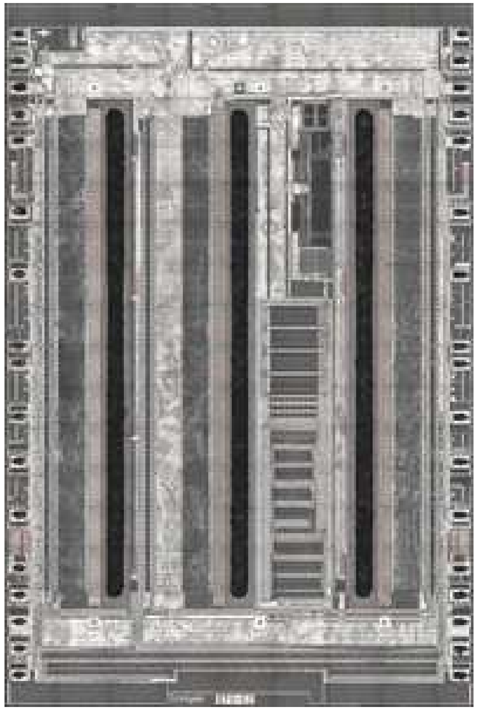

Figure 5: Source: Lexmark 18C0033 Color Inkjet Printhead Process Review (MEMS) Process Review (PPR-0607-802) [4]

MEMS Disambiguation: Actuators, Harvesters and Sensors

- **Classification (continued)**:
  - MEMS pressure sensors (applications: barometric altitude sensors, flow sensors, tire pressure monitoring system (TPMS)):
    - MEMS microphone (capacitive) arrays are a replacement for electret condenser microphones (ECM) and sonar hydrophones (advantages: directionality, echo and noise suppression)
  - MEMS Hall sensors measure magnetic field
  - MEMS motion scavengers and sensors (applications: airbag sensor, dead-reckoning localization, electronic compass, electronic stability control, energy harvesting, gesture recognition):
    - MEMS accelerometers (capacitive) measure acceleration (a_x, a_y, a_z) of translation
    - MEMS gyroscopes (capacitive) measure angular rate (roll, pitch and yaw) of rotation
    - MEMS inertial measurement units (IMU) measure all 6 degrees of freedom
  - MEMS temperature sensors:
    - MEMS infrared bolometer (advantage: uncooled)

According to Chipworks, the Motorola RAZR 2003 used the Knowles Acoustics SPM0103ND3 microphone [5, 6].

Figure 6: Source: Knowles Acoustics SPM0405HD4H, Microphone ASIC (AudioAsics A315KA3) Process Node Assessment (PNA-0907-901) [4]

MEMS Disambiguation: Actuators, Harvesters and Sensors

- **Classification (continued)**:
  - MEMS pressure sensors (applications: barometric altitude sensors, flow sensors, tire pressure monitoring system (TPMS)):
    - MEMS microphone (capacitive) arrays are a replacement for electret condenser microphones (ECM) and sonar hydrophones (advantages: directionality, echo and noise suppression)
  - MEMS Hall sensors measure magnetic field
  - MEMS motion scavengers and sensors (applications: airbag sensor, dead-reckoning localization, electronic compass, electronic stability control, energy harvesting, gesture recognition):
    - MEMS accelerometers (capacitive) measure acceleration (a_x, a_y, a_z) of translation
    - MEMS gyroscopes (capacitive) measure angular rate (roll, pitch and yaw) of rotation
    - MEMS inertial measurement units (IMU) measure all 6 degrees of freedom
  - MEMS temperature sensors:
    - MEMS infrared bolometer (advantage: uncooled)

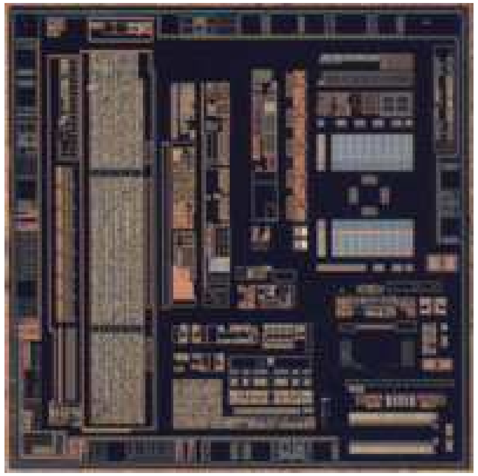

Figure 6: Source: AKM Semiconductor AK8973 Hall-Effect Magnetic Electronic Device Cicuit Analysis Report (CAR-1001-801) [4]

MEMS Disambiguation: Actuators, Harvesters and Sensors

- **Classification (continued)**:
  - MEMS pressure sensors (applications: barometric altitude sensors, flow sensors, tire pressure monitoring system (TPMS)):
    - MEMS microphone (capacitive) arrays are a replacement for electret condenser microphones (ECM) and sonar hydrophones (advantages: directionality, echo and noise suppression)
  - MEMS Hall sensors measure magnetic field
  - MEMS motion scavengers and sensors (applications: airbag sensor, dead-reckoning localization, electronic compass, electronic stability control, energy harvesting, gesture recognition):
    - MEMS accelerometers (capacitive) measure acceleration (a_x, a_y, a_z) of translation
    - MEMS gyroscopes (capacitive) measure angular rate (roll, pitch and yaw) of rotation
    - MEMS inertial measurement units (IMU) measure all 6 degrees of freedom
  - MEMS temperature sensors:
    - MEMS infrared bolometer (advantage: uncooled)

According to Chipworks, the Apple iPhone uses the ST LIS302D 3-axis accelerometer [7], whereas the Nintendo Wii uses the ADI ADXL330 3-axis iMEMS accelerometer [8] or the ST LIS3L02AE 3-axis accelerometer [7].

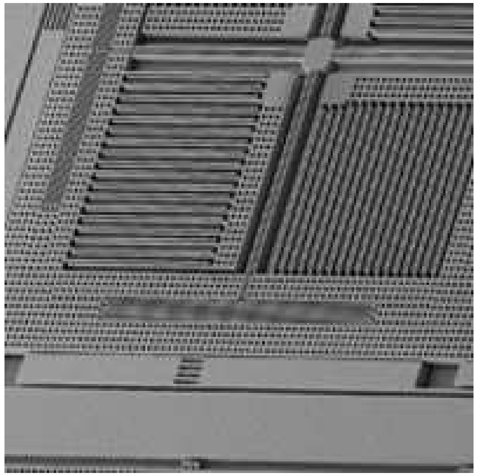

Figure 6: Source: ST Microelectronics LIS331DLH Three-Axis MEMS Accelerometer ICWorks Surveyor (ICS-0903-801) [4]

MEMS Disambiguation: Actuators, Harvesters and Sensors

- **Classification (continued)**:
  - MEMS pressure sensors (applications: barometric altitude sensors, flow sensors, tire pressure monitoring system (TPMS)):
    - MEMS microphone (capacitive) arrays are a replacement for electret condenser microphones (ECM) and sonar hydrophones (advantages: directionality, echo and noise suppression)
  - MEMS Hall sensors measure magnetic field
  - MEMS motion scavengers and sensors (applications: airbag sensor, dead-reckoning localization, electronic compass, electronic stability control, energy harvesting, gesture recognition):
    - MEMS accelerometers (capacitive) measure acceleration (a_x, a_y, a_z) of translation
    - MEMS gyroscopes (capacitive) measure angular rate (roll, pitch and yaw) of rotation
    - MEMS inertial measurement units (IMU) measure all 6 degrees of freedom
  - MEMS temperature sensors:
    - MEMS infrared bolometer (advantage: uncooled)

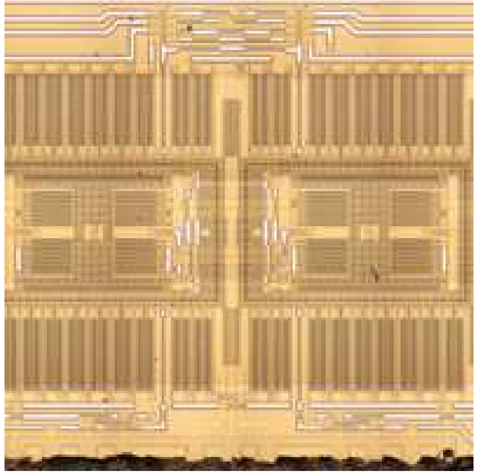

Figure 6: Source: ST Microelectronics LISY300AL Gyroscope MEMS Process Review (MPR-0809-801) [4]

MEMS Disambiguation: Actuators, Harvesters and Sensors

- **Classification (continued)**:
  - MEMS pressure sensors (applications: barometric altitude sensors, flow sensors, tire pressure monitoring system (TPMS)):
    - MEMS microphone (capacitive) arrays are a replacement for electret condenser microphones (ECM) and sonar hydrophones (advantages: directionality, echo and noise suppression)
  - MEMS Hall sensors measure magnetic field
  - MEMS motion scavengers and sensors (applications: airbag sensor, dead-reckoning localization, electronic compass, electronic stability control, energy harvesting, gesture recognition):
    - MEMS accelerometers (capacitive) measure acceleration (a_x, a_y, a_z) of translation
    - MEMS gyroscopes (capacitive) measure angular rate (roll, pitch and yaw) of rotation
    - MEMS inertial measurement units (IMU) measure all 6 degrees of freedom
  - MEMS temperature sensors:
    - MEMS infrared bolometer (advantage: uncooled)

MEMS Disambiguation: Actuators, Harvesters and Sensors

- **Classification (continued)**:
  - MEMS pressure sensors (applications: barometric altitude sensors, flow sensors, tire pressure monitoring system (TPMS)):
    - MEMS microphone (capacitive) arrays are a replacement for electret condenser microphones (ECM) and sonar hydrophones (advantages: directionality, echo and noise suppression)
  - MEMS Hall sensors measure magnetic field
  - MEMS motion scavengers and sensors (applications: airbag sensor, dead-reckoning localization, electronic compass, electronic stability control, energy harvesting, gesture recognition):
    - MEMS accelerometers (capacitive) measure acceleration (a_x, a_y, a_z) of translation
    - MEMS gyroscopes (capacitive) measure angular rate (roll, pitch and yaw) of rotation
    - MEMS inertial measurement units (IMU) measure all 6 degrees of freedom
  - MEMS temperature sensors:
    - MEMS infrared bolometer (advantage: uncooled)

Most temperature sensors are based on positive temperature coefficient (PTC) or negative temperature coefficient (NTC) materials. The temperature coefficient is the relative change of a physical property when the temperature is changed by 1 K.

Figure 6: Source: FLIR Systems Indigo ISC0601B Infrared Bolometer Imager Process Review (IPR-1002-801) [4]

- **Classification (continued)**:
  - Micro-optoelectromechanical systems (MOEMS) provide optical functionality:
    - Micro-mirrors (digital light processors (DLP), pico-projectors)
    - Interferometric modulator display (low-power displays with high brightness and contrast)
  - RF MEMS provide RF functionality:
    - RF MEMS resonators (applications: filters, oscillators) [9]
    - RF MEMS switches, switched capacitors, varactors (applications: attenuators, limiters, (TTD) phase shifters, T/R switches, tunable antennas, filters and matching networks) [10–16]
    - Thin film bulk acoustic resonator (FBAR) [a] (applications: filters)

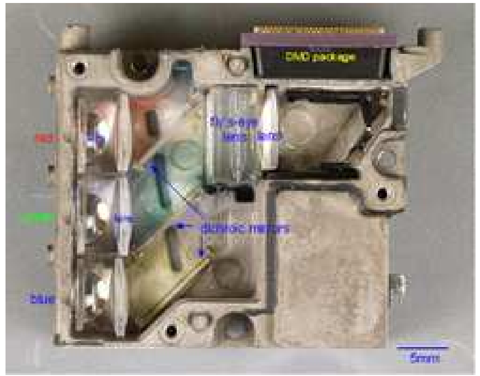

Figure 7: Source: Texas Instruments DLP (MEMS) Pico Projector from the Optoma PK-101 (EXR-0903-802) [4]

[a] An FBAR is a device consisting of a piezoelectric material sandwiched between two electrodes and acoustically isolated from the surrounding medium. FBAR devices using piezoelectric films with thicknesses ranging from several micrometres down to tenth of micrometres resonate in the frequency range of roughly 100 MHz to 10 GHz. Aluminum nitride and Zinc oxide are two common piezoelectric materials used in FBARs.

MEMS Disambiguation: Capacitors, Resonators, and Switches

- **Classification (continued)**:
  - Micro-optoelectromechanical systems (MOEMS) provide optical functionality:
    - Micro-mirrors (digital light processors (DLP), pico-projectors)
    - Interferometric modulator display (low-power displays with high brightness and contrast)
  - RF MEMS provide RF functionality:
    - RF MEMS resonators (applications: filters, oscillators) [9]
    - RF MEMS switches, switched capacitors, varactors (applications: attenuators, limiters, (TTD) phase shifters, T/R switches, tunable antennas, filters and matching networks) [10–16]
    - Thin film bulk acoustic resonator (FBAR) [a] (applications: filters)

Figure 7: Source: Qualcomm Mirasol MEMS Display Process Flow Analysis (CWR-0811-802) [4]

[a] An FBAR is a device consisting of a piezoelectric material sandwiched between two electrodes and acoustically isolated from the surrounding medium. FBAR devices using piezoelectric films with thicknesses ranging from several micrometres down to tenth of micrometres resonate in the frequency range of roughly 100 MHz to 10 GHz. Aluminum nitride and Zinc oxide are two common piezoelectric materials used in FBARs.

MEMS Disambiguation: Capacitors, Resonators, and Switches

- **Classification (continued)**:
  - Micro-optoelectromechanical systems (MOEMS) provide optical functionality:
    - ▹ Micro-mirrors (digital light processors (DLP), pico-projectors)
    - ▹ Interferometric modulator display (low-power displays with high brightness and contrast)
  - RF MEMS provide RF functionality:
    - ▹ RF MEMS resonators (applications: filters, oscillators) [9]
    - ▹ RF MEMS switches, switched capacitors, varactors (applications: attenuators, limiters, (TTD) phase shifters, T/R switches, tunable antennas, filters and matching networks) [10–16]
    - ▹ Thin film bulk acoustic resonator (FBAR) [a] (applications: filters)

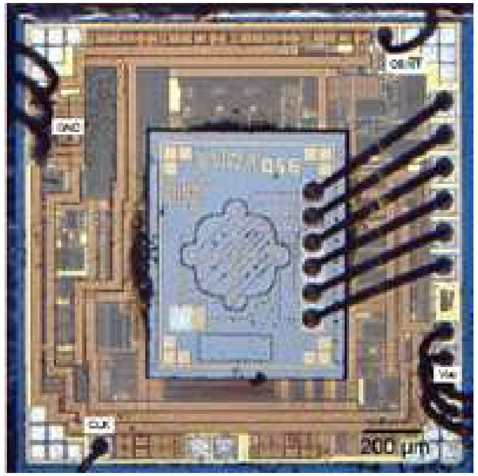

Figure 7: Source: SiTime SIT8002AC-13-18E50 One Time Programmable Oscillator Custom Process Node Assessment (PNA-0811-901) [4]

[a] An FBAR is a device consisting of a piezoelectric material sandwiched between two electrodes and acoustically isolated from the surrounding medium. FBAR devices using piezoelectric films with thicknesses ranging from several micrometres down to tenth of micrometres resonate in the frequency range of roughly 100 MHz to 10 GHz. Aluminum nitride and Zinc oxide are two common piezoelectric materials used in FBARs.

MEMS Disambiguation: Capacitors, Resonators, and Switches

- **Classification (continued)**:
  - Micro-optoelectromechanical systems (MOEMS) provide optical functionality:
    - Micro-mirrors (digital light processors (DLP), pico-projectors)
    - Interferometric modulator display (low-power displays with high brightness and contrast)
  - RF MEMS provide RF functionality:
    - RF MEMS resonators (applications: filters, oscillators) [9]
    - RF MEMS switches, switched capacitors, varactors (applications: attenuators, limiters, (TTD) phase shifters, T/R switches, tunable antennas, filters and matching networks) [10–16]
    - Thin film bulk acoustic resonator (FBAR) [a] (applications: filters)

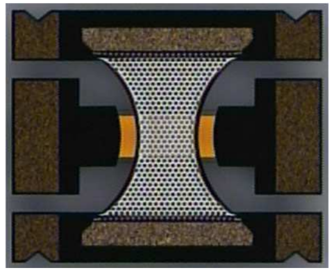

Figure 7: MEMtronics capacitive fixed-fixed beam RF MEMS switch [17]

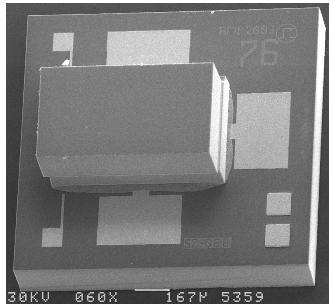

Figure 8: Radant MEMS RMSW220HP ohmic-contact cantilever RF MEMS switch [18]

[a] An FBAR is a device consisting of a piezoelectric material sandwiched between two electrodes and acoustically isolated from the surrounding medium. FBAR devices using piezoelectric films with thicknesses ranging from several micrometres down to tenth of micrometres resonate in the frequency range of roughly 100 MHz to 10 GHz. Aluminum nitride and Zinc oxide are two common piezoelectric materials used in FBARs.

MEMS Disambiguation: Capacitors, Resonators, and Switches

- **Classification (continued)**:
  - Micro-optoelectromechanical systems (MOEMS) provide optical functionality:
    - Micro-mirrors (digital light processors (DLP), pico-projectors)
    - Interferometric modulator display (low-power displays with high brightness and contrast)
  - RF MEMS provide RF functionality:
    - RF MEMS resonators (applications: filters, oscillators) [9]
    - RF MEMS switches, switched capacitors, varactors (applications: attenuators, limiters, (TTD) phase shifters, T/R switches, tunable antennas, filters and matching networks) [10–16]
    - Thin film bulk acoustic resonator (FBAR) [a] (applications: filters)

[a] An FBAR is a device consisting of a piezoelectric material sandwiched between two electrodes and acoustically isolated from the surrounding medium. FBAR devices using piezoelectric films with thicknesses ranging from several micrometres down to tenth of micrometres resonate in the frequency range of roughly 100 MHz to 10 GHz. Aluminum nitride and Zinc oxide are two common piezoelectric materials used in FBARs.

MEMS Disambiguation: References

[1] S. D. Senturia, *Microsystem Design*. Kluwer Academic Publishers, 2001.

[2] EE Times. [Online]. Available: http://www.eetimes.com

[3] MEMS Investor Journal. [Online]. Available: http://www.memsinvestorjournal.com

[4] Semiconductor reverse engineering and patent infringement analysis. Chipworks. [Online]. Available: http://www.chipworks.com

[5] Surface mount MEMS microphones. Knowles. [Online]. Available: http://www.knowles.com/search/products/m_surface_mount.jsp

[6] P. V. Loeppert, "Silicon capacitive microphone," U.S. Patent 6,847,090, January 8, 2002.

[7] Sensors and MEMS – motion sensors (MEMS) – accelerometers. ST Microelectronics. [Online]. Available: http://www.st.com/stonline/products/families/sensors/accelerometers.htm

[8] Analog Devices' inertial sensing technology. Analog Devices. [Online]. Available: http://www.analog.com/en/sensors/inertial-sensors/products/overview/over_Inertial_Sensing_Technology/fca.html

[9] C. T.-C. Nguyen, "MEMS technology for timing and frequency control," *IEEE Trans. Ultrason., Ferroelect., Freq. Contr.*, vol. 54, no. 2, pp. 251–270, February 2007.

[10] K. E. Petersen, "Micro-mechanical membrane switches on silicon," *IBM J. Res. & Dev.*, vol. 23, no. 4, pp. 376–385, July 1979.

[11] L. E. Larson, "Micro-machined switch and method of fabrication," U.S. Patent 5,121,089, November 1, 1990.

[12] P. M. Zavracky, S. Majumder, and N. E. McGruer, "Micromechanical switches fabricated using nickel surface micromachining," *J. Microelectromech. Syst.*, vol. 6, no. 1, pp. 3–9, March 1997.

[13] C. L. Goldsmith, B. M. Kanack, T.-H. Lin, B. R. Norvell, L. Y. Pang, B. Powers, Jr., C. Rhoads, and D. Seymour, "Micromechanical microwave switching," U.S. Patent 5,619,061, October 31, 1994.

[14] C. L. Goldsmith, Z. Yao, S. Eshelman, and D. Denniston, "Performance of low-loss RF MEMS capacitive switches," *IEEE Microwave Wireless Compon. Lett.*, vol. 8, no. 8, pp. 269–271, August 1998.

[15] J. B. Hacker, R. E. Mihailovich, M. Kim, and J. F. DeNatale, "A Ka-band 3-bit RF MEMS true-time-delay network," *IEEE Trans. Microwave Theory Tech.*, vol. 51, no. 1, part 1, pp. 305–308, January 2003.

[16] G. M. Rebeiz, *RF MEMS, Theory, Design and Technology*. John Wiley & Sons, 2003.

[17] MEMtronics website. [Online]. Available: http://www.memtronics.com

[18] Radant MEMS RMSW220HP Datasheet. [Online]. Available: http://www.radantmems.com

RF MEMS Switch, Switched Capacitor and Varactor Commercialization

- Business case examples:
  - Tunable antennas, tunable bandpass filters with high linearity, and tunable matching networks for cognitive, multiband, and software defined radio (SDR) [1, 2].
  - Ultra wideband (UWB) passive electronically scanned arrays for:
    - Airborne radars, such as FOPEN radar and SAR/ATR, which require low cross-polarization, low power consumption, and wideband ESAs, but do not require long-range search and track capability [3].
    - Passive identification (identification friend or foe (IFF), radio frequency identification (RFID)) requires low-power retrodirective arrays [4].
    - Wireless communication: Increasing the bandwidth or the signal-to-noise ratio (SNR), through spatial diversity, increases the Shannon channel capacity [5].

Active-g_m/C and active-RC CMOS filters lack linearity [6]. In addition, CMOS transistor scaling is accompanied by a supply voltage (linearity) reduction in order to maintain acceptable lifetime and power consumption of digital circuitry [7]. FBAR filters lack tunability.

RF MEMS Switch, Switched Capacitor and Varactor Commercialization

- Business case examples:
  - Tunable antennas, tunable bandpass filters with high linearity, and tunable matching networks for cognitive, multiband, and software defined radio (SDR) [1, 2].
  - Ultra wideband (UWB) passive electronically scanned arrays for:
    - ▷ Airborne radars, such as FOPEN radar and SAR/ATR, which require low cross-polarization, low power consumption, and wideband ESAs, but do not require long-range search and track capability [3].
    - ▷ Passive identification (identification friend or foe (IFF), radio frequency identification (RFID)) requires low-power retrodirective arrays [4].
    - ▷ Wireless communication: Increasing the bandwidth or the signal-to-noise ratio (SNR), through spatial diversity, increases the Shannon channel capacity [5].

RF MEMS Switch, Switched Capacitor and Varactor Commercialization

- Business case examples:
  - Tunable antennas, tunable bandpass filters with high linearity, and tunable matching networks for cognitive, multiband, and software defined radio (SDR) [1,2].
  - Ultra wideband (UWB) passive electronically scanned arrays for:
    - Airborne radars, such as FOPEN radar and SAR/ATR, which require low cross-polarization, low power consumption, and wideband ESAs, but do not require long-range search and track capability [3].
    - Passive identification (identification friend or foe (IFF), radio frequency identification (RFID)) requires low-power retrodirective arrays [4].
    - Wireless communication: Increasing the bandwidth or the signal-to-noise ratio (SNR), through spatial diversity, increases the Shannon channel capacity [5].

RF MEMS Switch, Switched Capacitor and Varactor Commercialization

- Business case examples:
  - Tunable antennas, tunable bandpass filters with high linearity, and tunable matching networks for cognitive, multiband, and software defined radio (SDR) [1, 2].
  - Ultra wideband (UWB) passive electronically scanned arrays for:
    - Airborne radars, such as FOPEN radar and SAR/ATR, which require low cross-polarization, low power consumption, and wideband ESAs, but do not require long-range search and track capability [3].
    - Passive identification (identification friend or foe (IFF), radio frequency identification (RFID)) requires low-power retrodirective arrays [4].
    - Wireless communication: Increasing the bandwidth or the signal-to-noise ratio (SNR), through spatial diversity, increases the Shannon channel capacity [5].

Shannon theorem [8] – The channel capacity, C, which is the theoretical upper bound on the bit rate, which can be transmitted with a given average signal power S through an analog communication channel subject to additive white Gaussian noise (AWGN) of power N, is:

$$C = BW \log_2 \left(1 + \frac{S}{N}\right) \tag{1}$$

where:

- C is the channel capacity in bits per second.
- BW is the (passband) bandwidth of the channel in hertz.
- S is the total received signal (modulation) power over the bandwidth, measured in watt.
- N is the total noise or interference power over the bandwidth, measured in watt.
- S/N is the signal-to-noise ratio (SNR) or the carrier-to-noise ratio (CNR) of the communication signal to the Gaussian noise interference expressed as a linear power ratio.

RF MEMS Switch, Switched Capacitor and Varactor Commercialization

Whereas capacitive MEMS accelerometers, gyroscopes and microphones have been successfully commercialized, RF MEMS switches, switched capacitors and varactors have not, which is due to contact physics related reliability issues and due to the availability of alternative RF technologies.

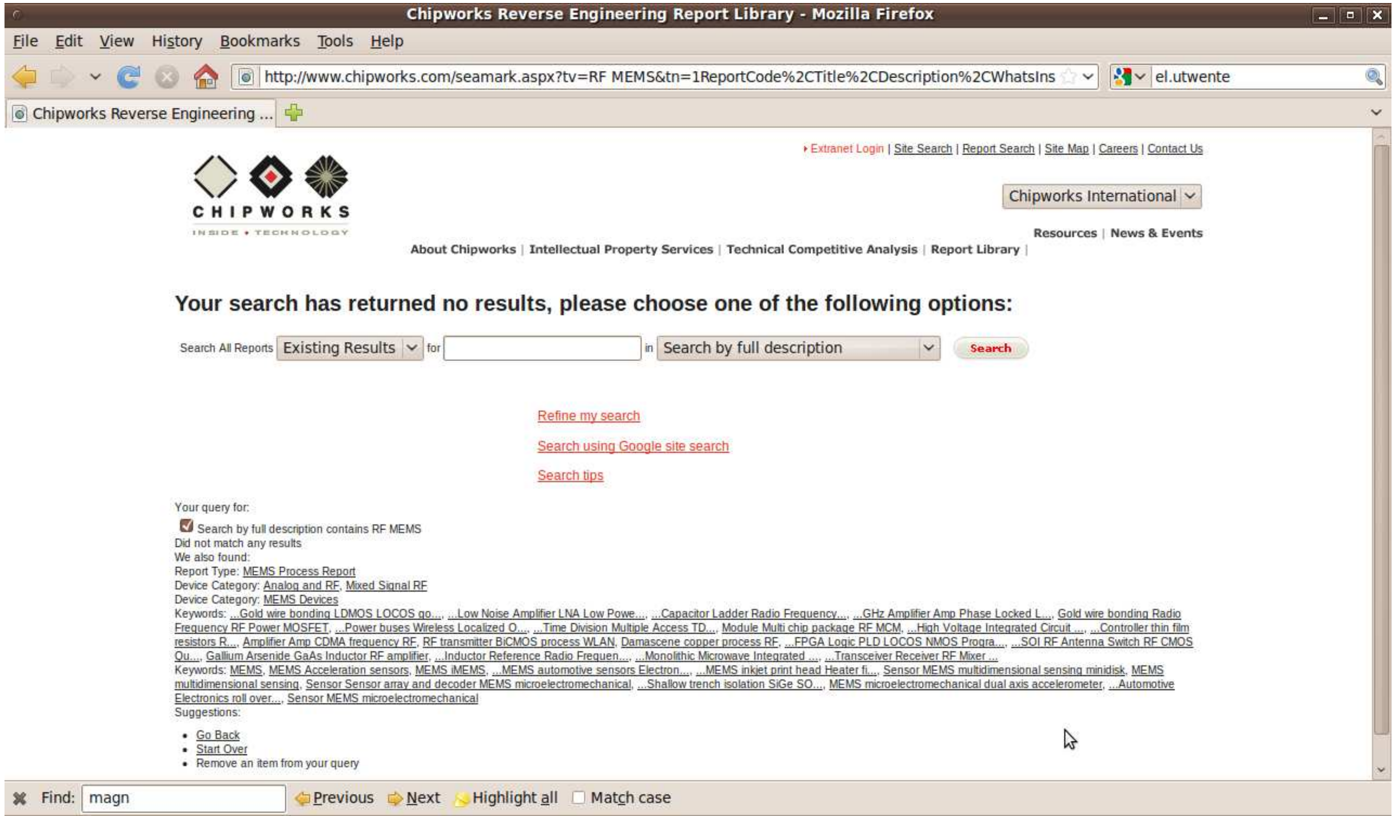

Figure 7: Chipworks.com search results for RF MEMS

RF MEMS Switch, Switched Capacitor and Varactor Commercialization

- RF MEMS switch, switched capacitor and varactor market size:

  > RF MEMS switches have led a short, interesting life so far. A lot of hope was heaped on these components, but six years after the first commercial announcements were made in 2003, there are still no significant revenues, and the field has already claimed a number of victims. The most well-known casualty is Magfusion; more recently, Teravicta, Simpler Networks, and Siverta have fallen by the wayside as well. Such fallout does not even take into account the RF MEMS switch programs that have closed down at companies like Infineon, ST, Motorola, Alcatel-Lucent and more recently, RFMD.
  >
  > Despite this gloomy picture, MEMS switches continue to fascinate the industry, and like salmon springing upstream against the odds, there are always companies launching new RF MEMS switch development programs or products. Examples include Omron, Maxim, and new start-up companies like MultusMEMS.
  >
  > In 2013, the RF MEMS market is expected to be in the range of $160 million. (Source: MEMS Market Brief, June 2009, by J. Bouchaud, iSuppli, Germany)

- RF MEMS switch, switched capacitor and varactor product developments:
  - Passive electronically scanned lens array (Source: World's First Demonstration of MEMS-Based X-Band Radar, Radant MEMS, April 6, 2006) [9]
  - Active electronically scanned lens array (Source: Raytheon Technologies Promise to Improve Radar Affordability, Raytheon, July 17, 2008) [10]

- RF MEMS switch, switched capacitor and varactor foundries, suppliers and subsystem integrators (courtesy of J. Bouchaud, iSuppli, Germany):
  - American:
    - ▷ Large companies: ADI, IBM, Jazz, Raytheon
    - ▷ New ventures: Advanced MicroSensors, MEMtronics, Radant MEMS, XCOM Wireless, WiSpry
  - Asian:
    - ▷ Large companies: Advantest (JPN), Panasonic (JPN), Fujitsu (JPN), Toshiba (JPN), Mitsubishi (JPN), NTT DoCoMo (JPN), Omron (JPN)
    - ▷ New ventures: APM (TWN), China Resources Semiconductor (CHN), MEMS Solutions (SGP)
  - European:
    - ▷ Large companies: BAE Systems (GBR), EPCOS (DEU) acquired by TDK (JPN), Thales Research & Technology (FRA), EADS Innovation Works (DEU), Rafael (ISR)
    - ▷ New ventures: BAOLAB (ESP), DelfMEMS (FRA), FBK-Irst (ITA), MEMSCAP (FRA), MultusMEMS (SWE), Protron Mikrotechnik (DEU), Tronics Microsystems (FRA)

RF MEMS Switch, Switched Capacitor and Varactor Commercialization: References

[1] J. Mitola, III and G. Q. Maguire, Jr, "Cognitive radio: making software radios more personal," *IEEE Personal Commun. Mag.*, vol. 6, no. 4, pp. 13–18, August 1999.

[2] J. L. Hilbert, "RF MEMS for wireless communications," *IEEE Commun. Mag.*, vol. 46, no. 8, pp. 68–74, August 2008.

[3] K. Van Caekenberghe, "RF MEMS on the radar," *IEEE Microwave Magazine*, vol. 10, no. 6, pp. 99–116, October 2009.

[4] R. Y. Miyamoto and T. Itoh, "Retrodirective arrays for wireless communications," *IEEE Microwave Magazine*, vol. 3, no. 1, pp. 71–79, Mar. 2002.

[5] S. Cherry, "Edholm's law of bandwidth," *IEEE Spectr.*, vol. 41, no. 7, pp. 58–60, July 2004.

[6] K. R. Laker and W. M. C. Sansen, *Design of Analog Integrated Circuits and Systems*. McGraw-Hill, 1994.

[7] A.-J. Annema, B. Nauta, R. van Langevelde, and H. Tuinhout, "Analog circuits in ultra-deep-submicron CMOS," *IEEE J. Solid-State Circuits*, vol. 40, no. 1, pp. 132–143, Jan. 2005.

[8] Wikipedia. [Online]. Available: http://en.wikipedia.org

[9] Radant MEMS website. [Online]. Available: http://www.radantmems.com

[10] Raytheon technologies promise to improve radar affordability. [Online]. Available: http://investor.raytheon.com/phoenix.zhtml?c=84193\&p=irol-newsArticle\&ID=1176149

RF MEMS Technology

- **RF Technologies**: III-V compound semiconductor (AIN, GaAs, GaN [1], InP, InSb), ferrite, ferroelectric, RF MEMS, silicon-based semiconductor (LDMOS, RF CMOS, SiC and SiGe), and vacuum microelectronics technology offer a distinct trade-off between cost, frequency, gain, large-scale integration, lifetime, linearity, noise figure, packaging, power handling, power consumption, reliability, ruggedness, size, supply voltage, switching time and weight.
- Electrostatically-actuated **RF MEMS**:
  - **Advantages**:
    - Bandwidth: intrinsically wideband due to electrostatic biasing and absence of parasitics
    - Cost: fabrication process requires min. 3 masks [2].
    - Low insertion loss (high Q factor) and high isolation
    - High linearity and high power handling
    - No power consumption
  - **Disadvantages**:
    - Reliability
    - Switching time [3, 4]

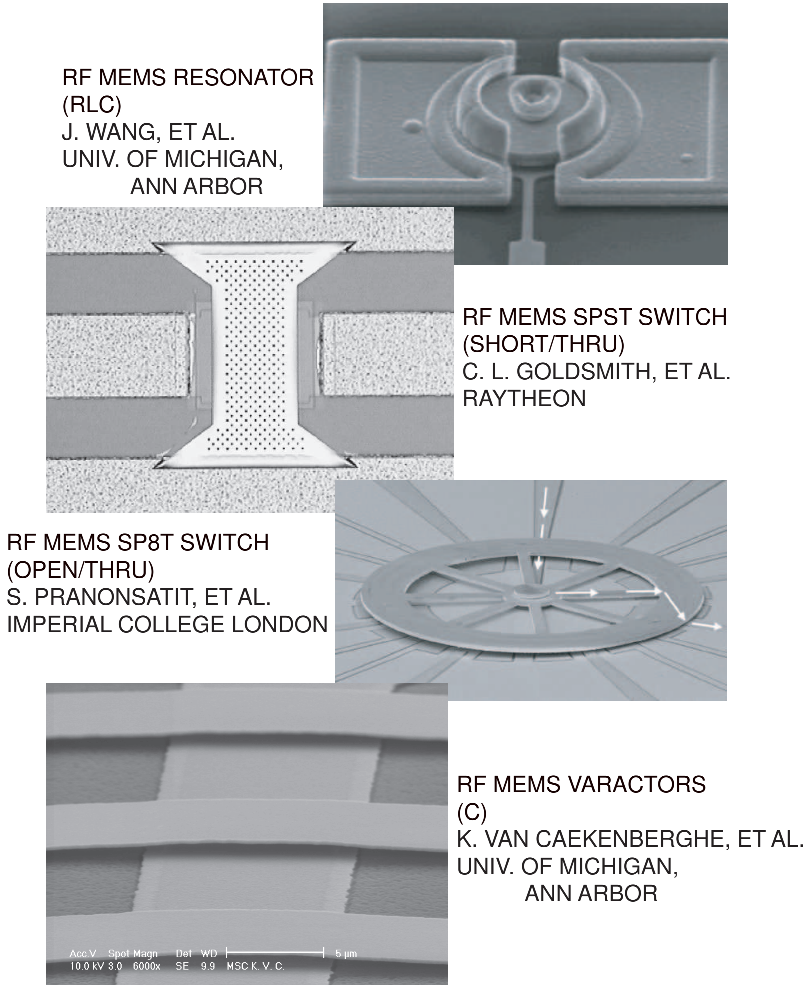

Figure 8: (a) RF MEMS resonator, (b) RF MEMS SPST switch, (c) RF MEMS SPNT switch, and (d) RF MEMS varactors

RF MEMS Technology: References

[1] N. Kolias, "RF systems - the benefits of gallium nitride technology," *Technology Today (Highlighting Raytheon's Technology)*, no. 2, pp. 27–28, 2007.

[2] A. Stehle, C. Siegel, V. Ziegler, B. Schönlinner, U. Prechtel, H. Seidel, and U. Schmid, "High-power handling capability of low complexity RF MEMS switch in Ku-band," *Electronics Letters*, vol. 43, no. 24, pp. 1367–1368, Nov. 2007.

[3] D. Mercier, K. Van Caekenberghe, and G. M. Rebeiz, "Miniature RF MEMS switched capacitors," in *IEEE MTT-S International Microwave Symposium Digest*, June 2005.

[4] B. Lacroix, A. Pothier, A. Crunteanu, C. Cibert, F. Dumas-Bouchiat, C. Champeaux, A. Catherinot, and P. Blondy, "Sub-microsecond RF MEMS switched capacitors," *IEEE Trans. Microwave Theory Tech.*, vol. 55, no. 6, pp. 1314–1321, June 2007.

Electromechanical model: mass-spring system [1]

- Mass:

$$m = 0.4\, \rho\, l\, w\, t$$

- Spring constant (capacitive fixed-fixed beam):

$$k = 32\, E\, w \left(\frac{t}{l}\right)^3 \left(\frac{27}{49}\right) + 8\, \sigma\, (1-\nu)\, w\, \frac{t}{l} \left(\frac{3}{5}\right)$$

- Electrostatic force:

$$F_e = -\frac{1}{2} \frac{\epsilon_0\, A\, V_s^2}{g^2}$$

- Pull-in voltage (capacitive fixed-fixed beam):

$$V_p = \sqrt{\frac{8\, k (g_0 + t_d/\epsilon_d)^3}{27\, \epsilon_0\, A}}$$

- Hold-down voltage (capacitive fixed-fixed beam):

$$V_h = \sqrt{\frac{2\, k\, g_0\, (t_d/\epsilon_d)^2}{\epsilon_0\, \epsilon_d\, A}}$$

- Switching time (pull-in time):

$$t_s = 3.67 \frac{V_p}{V_s \sqrt{k/m}} \sim \sqrt{\frac{\rho}{E}} \text{ for } V_s = V_p$$

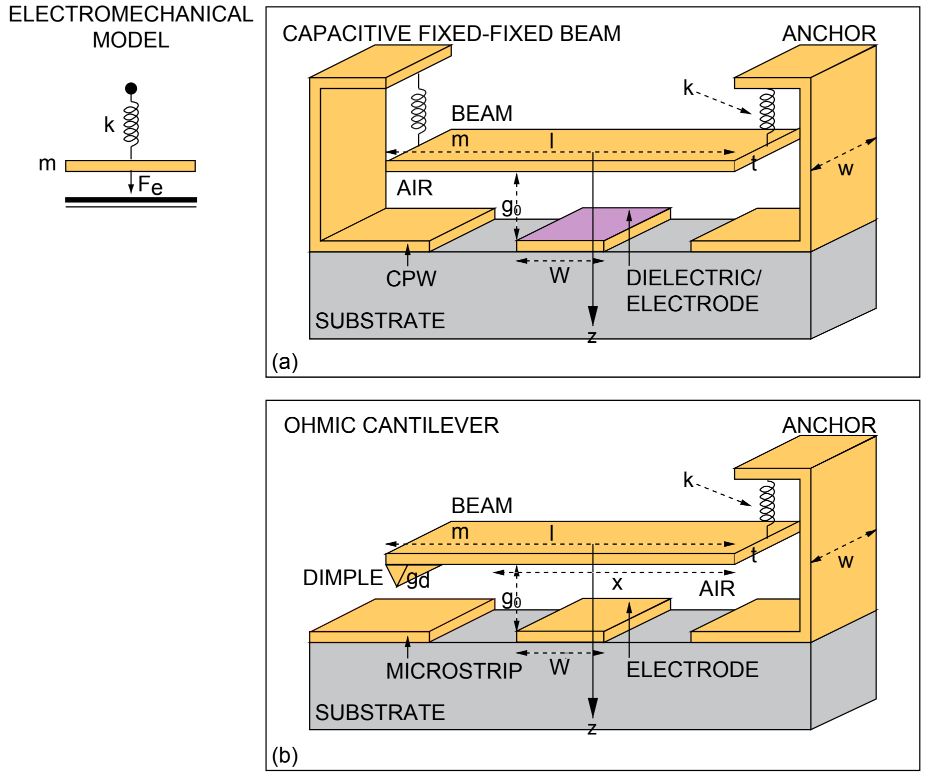

Figure 9: (a) a capacitive fixed-fixed beam RF MEMS switch, connected in shunt to a CPW line, (b) an ohmic cantilever RF MEMS switch, connected in series to a microstrip line.

RF MEMS Modeling

Electromechanical model: mass-spring system [1]

- Mass:

$$m = 0.4\,\rho\,l\,w\,t$$

- Spring constant (ohmic cantilever):

$$k = 2\,E\,w\left(\frac{t}{l}\right)^3 \frac{1-(x/l)}{3-4\,(x/l)^3+(x/l)^4}$$

- Electrostatic force:

$$F_e = -\frac{1}{2}\,\frac{\epsilon_0\,A\,V_s^2}{g^2}$$

- Pull-in voltage (ohmic cantilever):

$$V_p = \sqrt{\frac{8\,k\,g_0^3}{27\,\epsilon_0\,A}}$$

- Hold-down voltage (ohmic cantilever):

$$V_h = \sqrt{\frac{2\,k\,(g_0-g_d)\,g_d^2}{\epsilon_0\,A}}$$

- Switching time (pull-in time):

$$t_s = 3.67\,\frac{V_p}{V_s\,\sqrt{k/m}} \sim \sqrt{\frac{\rho}{E}}\ \text{for } V_s = V_p$$

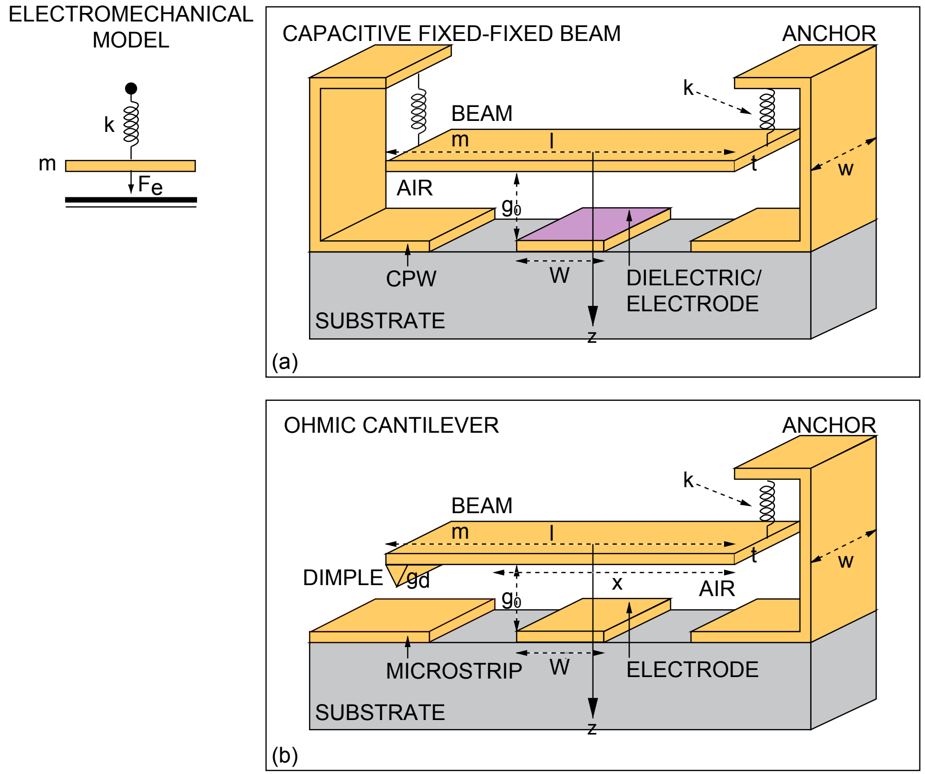

Figure 9: (a) a capacitive fixed-fixed beam RF MEMS switch, connected in shunt to a CPW line, (b) an ohmic cantilever RF MEMS switch, connected in series to a microstrip line.

In reality, RF MEMS beams are not flat but track the underlying topology and are bowed due to residual stress.

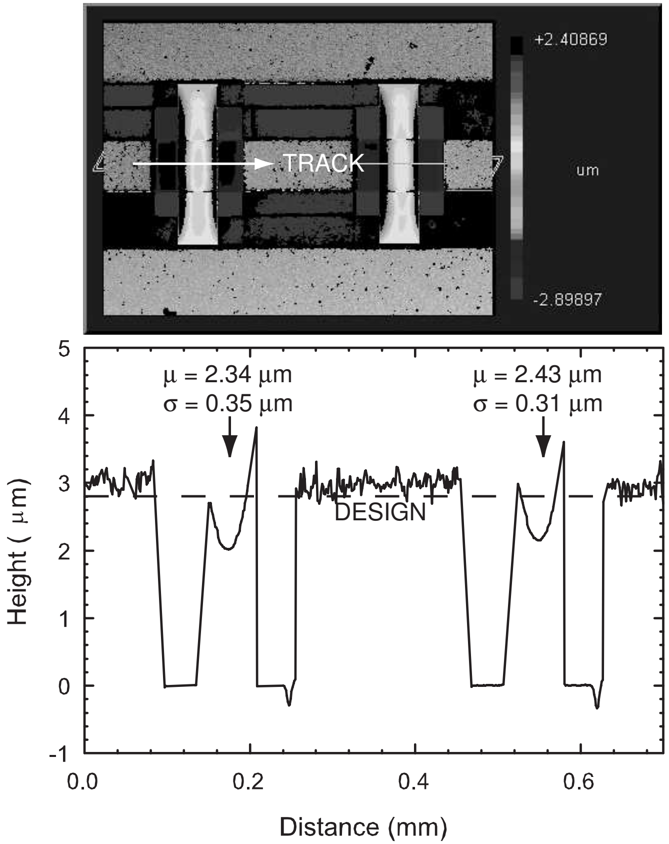

Figure 10: Optical interferometry imagery (top) and surface profile (bottom) of capacitive fixed-fixed beam RF MEMS components fabricated using the conventional fabrication process [2, 3]. The mean and standard deviation of the transverse beam profile are shown.

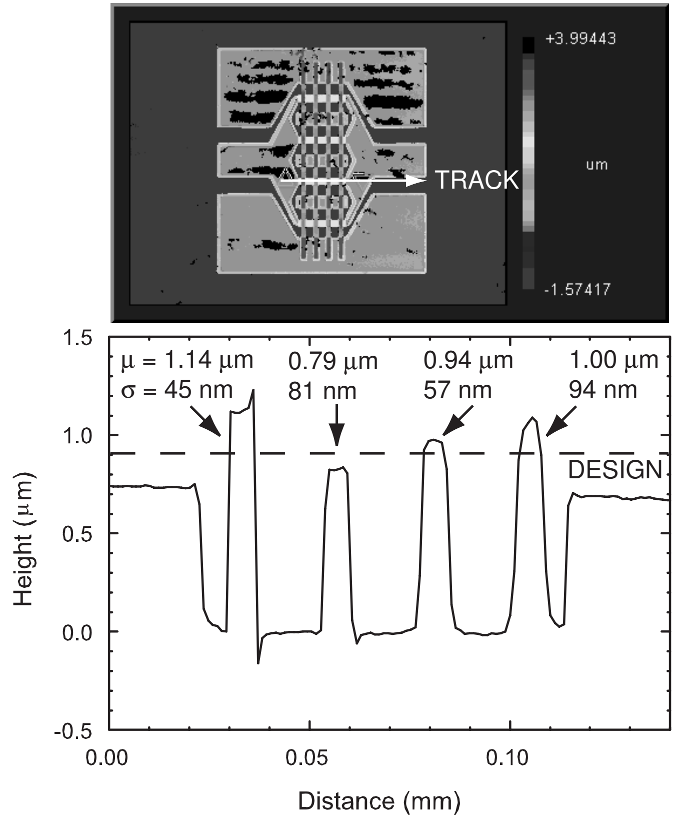

Figure 11: Optical interferometry imagery (top) and surface profile (bottom) of capacitive fixed-fixed beam RF MEMS components fabricated using the self-aligned fabrication process [4]. The mean and standard deviation of the transverse beam profile are shown.

RF MEMS Modeling

Small signal RF model for S-parameter simulation: C_u/C_d [1]

- Up-state capacitance:

$$C_u = 1.4 \frac{\epsilon_0 \, A}{g_0 + t_d / \epsilon_d}$$

- Quality factor:

$$Q = \frac{1}{\omega \, R \, C_u}$$

- Down-state capacitance (capacitive fixed-fixed beam):

$$C_d = 0.65 \frac{\epsilon_0 \, \epsilon_d \, A}{t_d}$$

Large signal RF model for harmonic balance simulation (IP3, P1dB): memcapacitor (nonlinear capacitor with hysteresis in the C-V curve) [1, 5]

- Up-state capacitance:

$$C_u = 1.4 \frac{\epsilon_0 \, A}{g(j\,\omega) + t_d / \epsilon_d}$$

- Electrostatic force:

$$F_e(j\,\omega) = -\frac{1}{2} \, \frac{C_u(j\,\omega) \, v_{RMS}^2(j\,\omega)}{g(j\,\omega)}$$

- Second law of Newton (frequency domain):

$$g(j\,\omega) = g_0 + \frac{F_e(j\,\omega)}{k + j\,\omega\,b - \omega^2\,m}$$

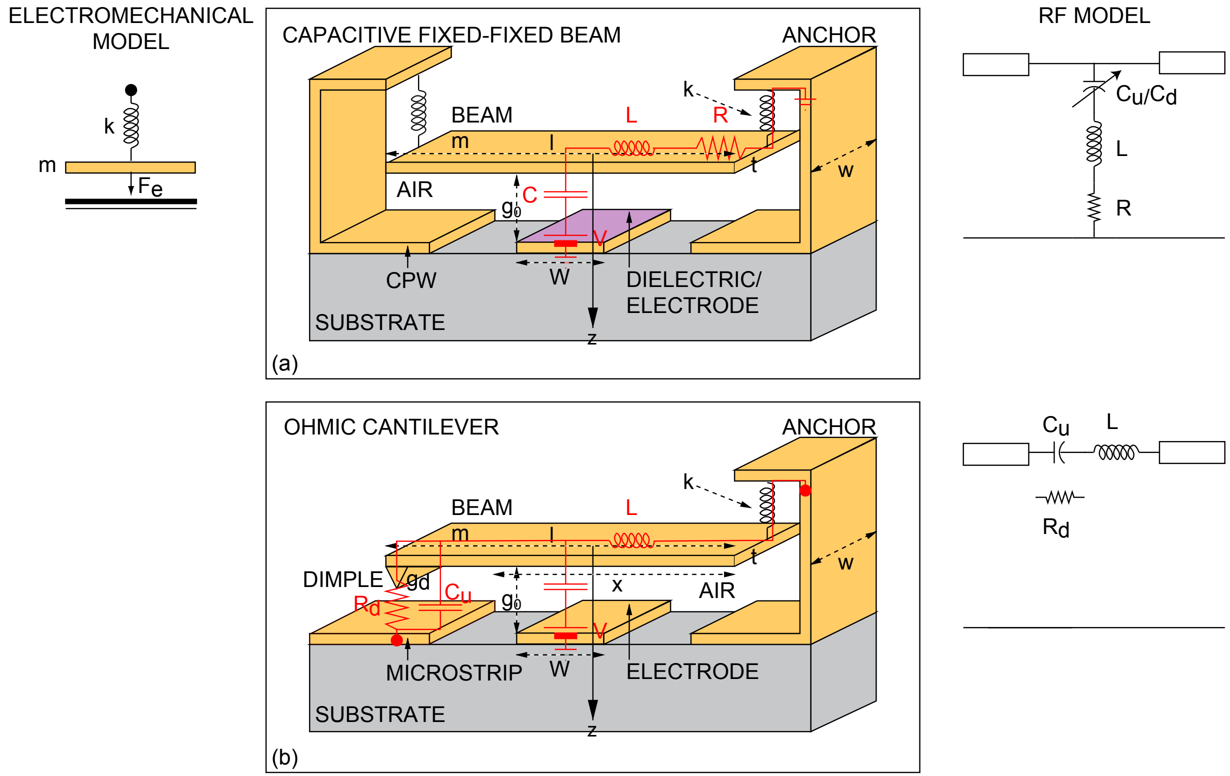

Figure 12: (a) a capacitive fixed-fixed beam RF MEMS switch, connected in shunt to a CPW line, (b) an ohmic cantilever RF MEMS switch, connected in series to a microstrip line.

Small signal RF model for S-parameter simulation: C_u/R_d [1]

- Up-state capacitance:

$$C_u = 1.4 \frac{\epsilon_0 A}{g_0 + t_d/\epsilon_d}$$

- Quality factor:

$$Q = \frac{1}{\omega R C_u}$$

- Down-state resistance (ohmic cantilever):

$$R_d$$

Large signal RF model for harmonic balance simulation (IP3, P1dB): memcapacitor (nonlinear capacitor with hysteresis in the C-V curve) [1, 5]

- Up-state capacitance:

$$C_u = 1.4 \frac{\epsilon_0 A}{g(j\omega) + t_d/\epsilon_d}$$

- Electrostatic force:

$$F_e(j\omega) = -\frac{1}{2} \frac{C_u(j\omega)\, v_{RMS}^2(j\omega)}{g(j\omega)}$$

- Second law of Newton (frequency domain):

$$g(j\omega) = g_0 + \frac{F_e(j\omega)}{k + j\omega b - \omega^2 m}$$

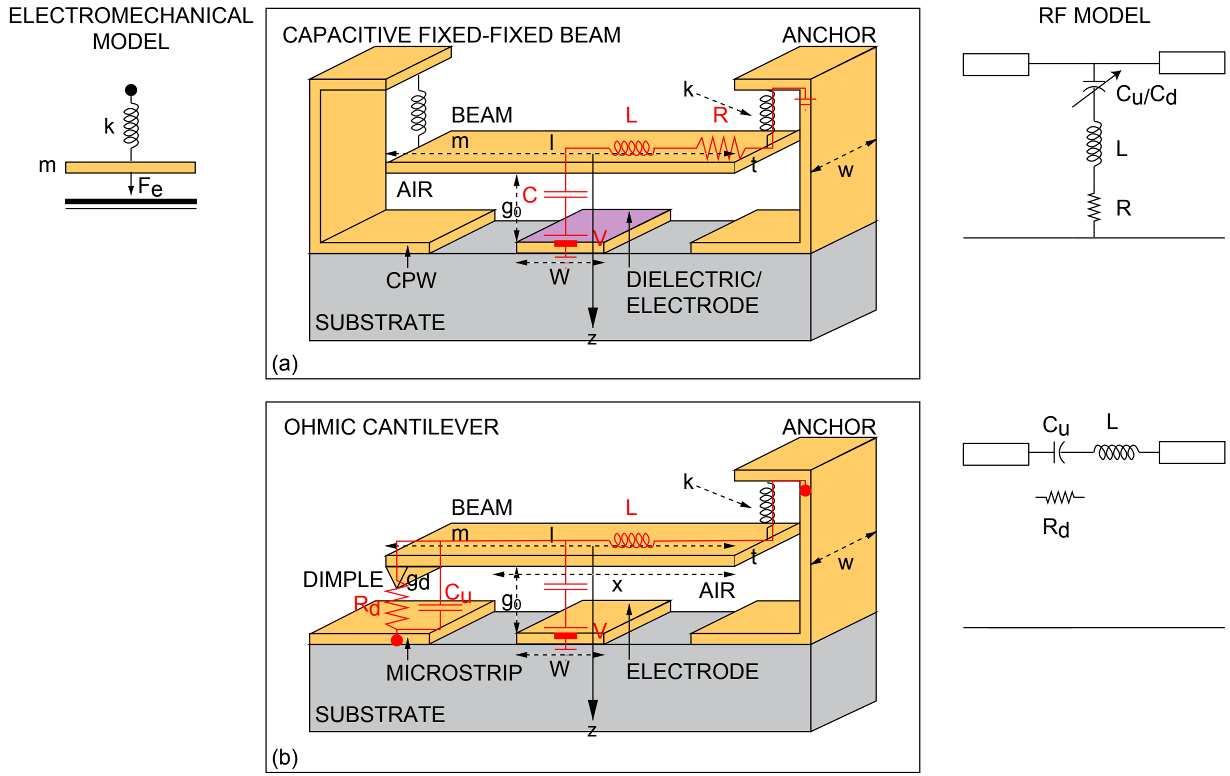

Figure 12: (a) a capacitive fixed-fixed beam RF MEMS switch, connected in shunt to a CPW line, (b) an ohmic cantilever RF MEMS switch, connected in series to a microstrip line.

Table I: Comparison of fabrication processes for capacitive fixed-fixed beam RF MEMS Components (unmeasured or unpublished quantities are denoted with -)

Reference	Goldsmith, et al. [6–9], 1994-1998	Barker, et al. [2, 3], 1998-2000	Goldsmith, et al. [10], 2002	Lacroix, et al. [11], 2007	Van Caekenberghe, et al. [4], 2008
Component	switch	varactor	switch	switched capacitor	varactor
Foundry	Raytheon	Univ. of Michigan	MEMtronics	XLIM, France	Univ. of Michigan
Design characteristics					
Air gap, g_0	4 μm	2 μm	4 μm	0.3 μm	0.4 μm
Beam dimensions ($l \times w \times t$)	300 x 120 x 0.5 μm^3	300 x 80 x 0.8 μm^3	300 x 120 x 0.5 μm^3	40 x 10 x 0.35 μm^3	30 x 12 x 0.3 μm^3
Beam holes	yes	no	yes	no	no
Beam material[a]	Al	Au	Al	Al	Au
Dielectric material	Si_3N_4 (ϵ_r = 6-9)	Si_3N_4 (ϵ_r = 6-9)	Air	Al_2O_3 (ϵ_r = 9.1)	Si_3N_4 (ϵ_r = 6-9)
Dielectric thickness, t_d	-	200 nm	-	400 nm	200 nm
Electrode width, W	120 μm	100 μm	120 μm	-	12 μm
Metal thickness	4 μm	3 μm	4 μm	3 μm	0.9 μm
Number of masks	5	5	5	7	3
Figures of Merit					
Capacitance ratio, C_r	70-100	1.25-1.3	10-30	2.3	1.15
Power handling					
Cold-switched	5 W	0.5 W	-	-	200 mW
Hot-switched	2 W	-	0.5 W	-	-
Q factor	1300 @ 10 GHz	30 @ 10 GHz	-	20 @ 20 GHz	14.5 @ 20 GHz
Reliability (cycles)	10 B	-	$>$ 100 B	14 B	-
R_s	0.2-0.25 Ω	-	0.2-0.25 Ω	7 Ω @ 20 GHz	3.1 Ω @ 20 GHz
Switching time, t_s	$<$ 20 μs	-	$<$ 20 μs	0.15 - 0.4 μs	-

[a] Aluminium has a Young's modulus, E, of 70 GPa, a Poisson ratio, ν, of 0.35, and a mass density, ρ, of 2.7 g/cm^3. Gold has a Young's modulus, E, of 78 GPa, a Poisson ratio, ν, of 0.44, and a mass density, ρ, of 19.3 g/cm^3.

RF MEMS Modeling: References

[1] G. M. Rebeiz, *RF MEMS, Theory, Design and Technology*. John Wiley & Sons, 2003.

[2] N. S. Barker and G. M. Rebeiz, "Distributed MEMS true-time delay phase shifters and wideband switches," *IEEE Trans. Microwave Theory Tech.*, vol. 46, no. 11, pp. 1881–1890, November 1998.

[3] ——, "Optimization of distributed MEMS transmission-line phase shifters - U-band and W-band designs," *IEEE Trans. Microwave Theory Tech.*, vol. 48, no. 11, pp. 1957–1966, November 2000.

[4] K. Van Caekenberghe and K. Sarabandi, "A self-aligned fabrication process for capacitive fixed-fixed beam RF MEMS components," *J. Microelectromech. Syst.*, vol. 17, no. 3, pp. 747–754, June 2008.

[5] M. D. Ventra, Y. V. Pershin, and L. O. Chua, "Circuit elements with memory: Memristors, memcapacitors, and meminductors," *Proc. IEEE*, vol. 97, no. 10, pp. 1717–1724, Oct. 2009.

[6] C. L. Goldsmith, B. M. Kanack, T.-H. Lin, B. R. Norvell, L. Y. Pang, B. Powers, Jr., C. Rhoads, and D. Seymour, "Micromechanical microwave switching," U.S. Patent 5,619,061, October 31, 1994.

[7] C. L. Goldsmith, Z. Yao, S. Eshelman, and D. Denniston, "Performance of low-loss RF MEMS capacitive switches," *IEEE Microwave Wireless Compon. Lett.*, vol. 8, no. 8, pp. 269–271, August 1998.

[8] Z. J. Yao, S. Chen, S. Eshelman, D. Denniston, and C. Goldsmith, "Micromachined low-loss microwave switches," *J. Microelectromech. Syst.*, vol. 8, no. 2, pp. 129–134, June 1999.

[9] S. Chen, T. V. Baughn, Z. J. Yao, and C. L. Goldsmith, "A new in situ residual stress measurement method for a MEMS thin fixed-fixed beam structure," *J. Microelectromech. Syst.*, vol. 11, no. 4, pp. 309–316, August 2002.

[10] C. L. Goldsmith, "Proximity micro-electromechanical system," U.S. Patent 6,608,268, August 19, 2003.

[11] B. Lacroix, A. Pothier, A. Crunteanu, C. Cibert, F. Dumas-Bouchiat, C. Champeaux, A. Catherinot, and P. Blondy, "Sub-microsecond RF MEMS switched capacitors," *IEEE Trans. Microwave Theory Tech.*, vol. 55, no. 6, pp. 1314–1321, June 2007.

RF MEMS Biasing

- RF MEMS components are biased electrostatically using a bipolar non-return to zero (NRZ) drive voltage in order to avoid dielectric charging.
- **Advantages** of electrostatic biasing:
  - No current flow, no biasing induced electromigration
  - No power consumption
  - Wideband, high resistivity bias lines can be used instead of RF chokes

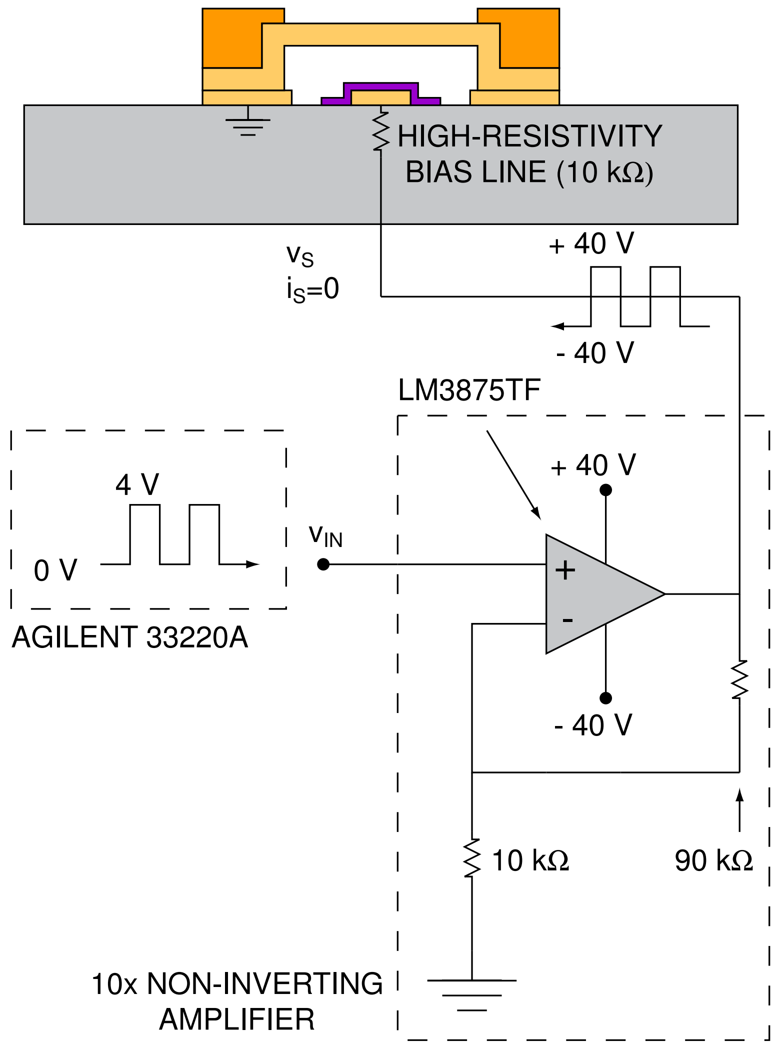

Figure 13: Electrostatic biasing of a capacitive fixed-fixed beam RF MEMS switch, switched capacitor or varactor.

RF MEMS Fabrication

- RF MEMS components are fabricated using bulk or surface micromachining techniques [1–5], directly on the microwave substrate, or substrate transferred to the microwave substrate.
  - Deposition of the electrode layer
  - Deposition of the dielectric layer
  - Deposition of the sacrificial spacer
  - Deposition of the seed layer, and subsequent electroplating
  - Definition and release of the beams, drying of the wafer using a critical point dryer, to avoid beam stiction while evaporating polar solvents (water) between the dielectric and the beam.

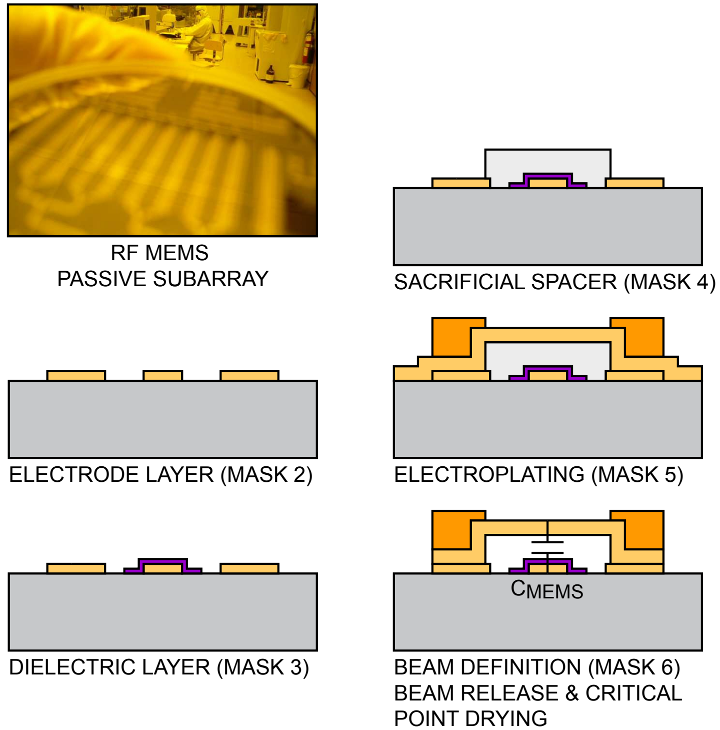

Figure 14: Surface micromachining of an RF MEMS component directly on the microwave substrate

RF MEMS Fabrication

- Heterogeneous integration of
  - RF MEMS and III-V compound semiconductors [6, 7], which will enable single-chip T/R modules.
  - RF MEMS and (Bi)CMOS, which will enable *integrated* highly linear tunable filters.
    - MEMS first (in the CMOS front-end)
      - Examples: Analog Devices SOIMEMS [8], SiTime MEMS-FIRST [9]
      - Advantages: access to mono-crystalline silicon, high-temperature process feasible
      - Disadvantages: transistor density is reduced, lower Q factor
    - MEMS interleaved
      - Examples: Analog Devices iMEMS [8]
    - MEMS last (in the CMOS back-end)
      - Examples: BAOLAB Microsystems [10], WiSpry [11, 12]
      - Advantages: transistor density is maintained, higher Q factor
      - Disadvantages: limited J_{RMS} and V_{RMS} handling, metal creep and residual stress, of Al interconnects

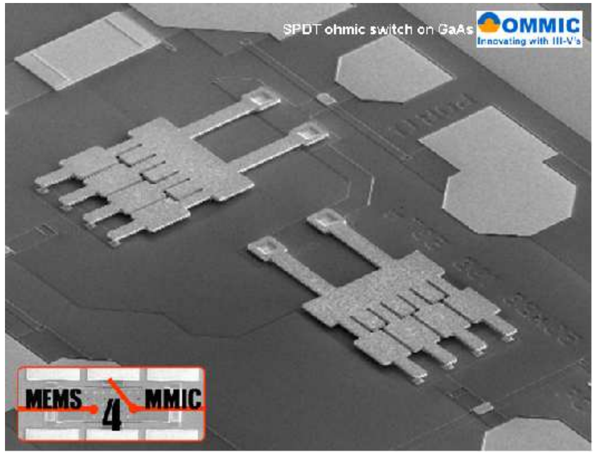

Figure 15: Singe pole double throw (SPDT) switch based on ohmic cantilever RF MEMS switches, fabricated on a GaAs substrate (courtesy of R. Baggen, IMST, Germany) [7]

RF MEMS Fabrication: References

[1] K. R. Williams and R. S. Muller, "Etch rates for micromachining processing," *J. Microelectromech. Syst.*, vol. 5, no. 4, pp. 256–269, December 1996.

[2] J. M. Bustillo, R. T. Howe, and R. S. Muller, "Surface micromachining for microelectromechanical systems," *Proc. IEEE*, vol. 86, no. 8, pp. 1552–1574, August 1998.

[3] M. J. Madou, *Fundamentals of Microfabrication: The Science of Miniaturization, 2nd Ed.* CRC Press, March 2002.

[4] G. M. Rebeiz, *RF MEMS, Theory, Design and Technology*. John Wiley & Sons, 2003.

[5] K. R. Williams, K. Gupta, and M. Wasilik, "Etch rates for micromachining processing - Part II," *J. Microelectromech. Syst.*, vol. 12, no. 6, pp. 761–778, December 2003.

[6] D. Hyman, A. Schmitz, B. Warneke, T. Y. Hsu, J. Lam, J. Brown, J. Schaffner, A. Walston, R. Y. Loo, G. L. Tangonan, M. Mehregany, and J. Lee, "GaAs-compatible surface-micromachined RF MEMS switches," *Electronics Letters*, vol. 35, no. 3, pp. 224–226, Feb. 1999.

[7] Enabling MEMS-MMIC technology for cost-effective multifunctional RF system integration. [Online]. Available: ftp://ftp.cordis.europa.eu/pub/fp7/ict/docs/micro-nanosystems/20080630-rf-mems-cluster-workshop-report_en.pdf

[8] Analog Devices' inertial sensing technology. Analog Devices. [Online]. Available: http://www.analog.com/en/sensors/inertial-sensors/products/overview/over_Inertial_Sensing_Technology/fca.html

[9] MEMS-based silicon timing solutions. SiTime. [Online]. Available: http://www.sitime.com

[10] BAOLAB Microsystems. [Online]. Available: http://www.baolab.com/technology.htm

[11] Radio frequency (RF) programmable silicon solutions. WiSpry. [Online]. Available: http://www.wispry.com

[12] J. L. Hilbert, "RF MEMS for wireless communications," *IEEE Commun. Mag.*, vol. 46, no. 8, pp. 68–74, August 2008.

RF MEMS Packaging

- **Function**: RF MEMS components are fragile and require hermetic cavity sealing through wafer level packaging (WLP) or single chip packaging (SCP).
  - WLP is applied *before* wafer dicing, and is based on thin film capping (PECVD nitride, PECVD oxide, or electroplated metal thin film capping), or based on wafer bonding (anodic, metal diffusion, metal eutectic, glass frit [1], polymer adhesive, and silicon fusion wafer bonding).
    - ▷ Anodic and silicon fusion bonding do not require an intermediate layer, but do not tolerate surface roughness.
    - ▷ WLP techniques using a conductive intermediate layer (conductive split ring) restrict the bandwidth and isolation of the RF MEMS component.
    - ▷ The most common WLP techniques are based on anodic and glass frit wafer bonding.
  - SCP is applied *after* wafer dicing. The dies are attached to prefabricated liquid crystal polymer (LCP) [2] injection molded packages or low temperature co-fired ceramic (LTCC) packages [3].

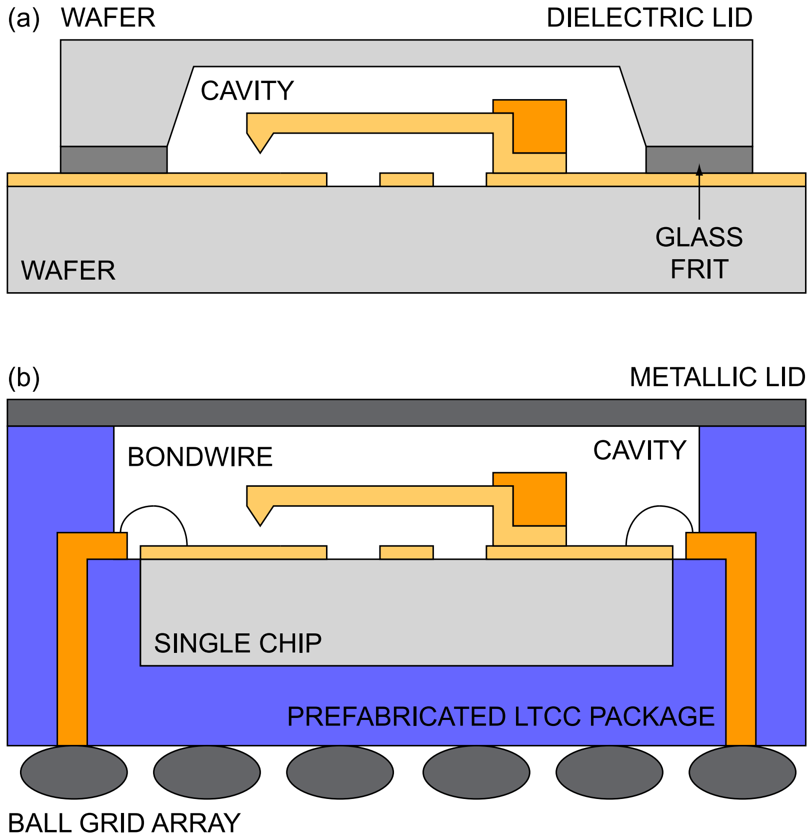

Figure 16: (a) Wafer-level packaging. (b) Single chip packaging of an ohmic cantilever RF MEMS switch.

RF MEMS Packaging

- **Figures of merit**:
  - Chip size
  - Cleanliness: RF MEMS resonators must be packaged in a clean environment because even small amounts of surface contamination can significantly change the resonator frequency.
  - Cost
  - Fabrication process maximum temperature, and (in)-tolerance to alignment errors and surface roughness
  - Hermeticity
  - Insertion loss
  - Thermo-mechanical properties (mechanical strength, thermal conductivity, maximum temperature)

- **Design trade-offs**:
  - Cavity filling: vacuum, nitrogen gas, apolar solvent (oil) for cooling (applications: hot-switching) or damping
  - Die attachment technique (RF MEMS chip attachment in a prefabricated package): chip-stack, flip-chip, wire bonding
  - Feedthroughs: lateral feedthroughs are susceptible to capacitive coupling to the metallic bond ring and/or lid, whereas vertical feedthroughs are not. Vertical feedthroughs based on through silicon vias (TSV) offer 3D integration opportunities.
  - Lid: absorbing or metallic
  - Pin and wiring: differential or single-ended, density. *Differential* interconnects offer higher isolation levels.
  - Surface mounting technique (SMT) (package attachment on RF printed circuit board (PCB)): ball grid array (BGA), flip-chip, lead frame, wire bonding with organic (globtop) over-molding

Packaging: References

[1] Radant MEMS RMSW220HP Datasheet. [Online]. Available: http://www.radantmems.com

[2] N. Kingsley, “Liquid crystal polymer: Enabling next generation conformal and multilayer electronics,” *Microwave Journal*, vol. 51, no. 5, p. 188, May 2008.

[3] R. Y. Jacobson, T. K. Gupta, I. John S. Fisher, and A. Curbean, “Fabrication of LTCC T/R modules with multiple cavities and an integrated ceramic ring frame,” U.S. Patent 7,416,630 B2, November 24, 2003.

RF MEMS Power Handling

- Definitions [1]:
  - **Cold-switching** is defined as switching in the *absence* of RF power, and is applied in attenuators and (TTD) phase shifters. Cold-switched power handling is limited by self-actuation.
  - **Hot-switching** is defined as switching in the *presence* of RF power, and is applied in limiters, tunable matching networks and T/R switches. Hot-switched power handling is limited by hold-down.
  - **Self-actuation** occurs when the root-mean-square (RMS) RF voltage, V_{RMS}, across the RF MEMS beam in the *up-state* and the electrode, exceeds the pull-in voltage, V_p.
  - **Hold-down** occurs when the V_{RMS} across the RF MEMS beam in the *down-state* and the electrode, exceeds the hold-down voltage, V_h.

- Remark:
  - The breakdown power handling is set by the maximum allowable RMS of the RF current density through the beam, J_{RMS}, in the light of electromigration[1], and the maximum allowable V_{RMS} in the light of dielectric breakdown.

- Solutions:
  - *Differential* circuits have 3 dB more power handling than their single-ended counterparts.
  - J_{RMS} and V_{RMS} are related through the characteristic impedance of the transmission line, $Z = V_{RMS}/I_{RMS}$.

[1] Electromigration is the mass transport caused by a high direct current density [2], which rips loose ions from the conductor lattice. Electromigration is a function of J_{RMS} and the exposure time.

RF MEMS Power Handling: References

[1] B. Pillans, J. Kleber, C. Goldsmith, and M. Eberly, "RF power handling of capacitive RF MEMS devices," in *IEEE MTT-S International Microwave Symposium Digest*, June 2002.

[2] B. D. Jensen, K. Saitou, J. L. Volakis, and K. Kurabayashi, "Fully integrated electrothermal multidomain modeling of RF MEMS switches," *IEEE Microwave Wireless Compon. Lett.*, vol. 13, no. 9, pp. 364–366, September 2003.

- **Capacitive fixed-fixed beam**:
  - Beam stiction due to polar solvents (humidity) and dielectric charging [1–3]
  - Dielectric charging also shifts the C-V curves [4, 5]. However, defect reduction has reduced charge trapping in SiO_2 gate oxide of MOSFET transitors.
- **Ohmic cantilever**:
  - Contact interface degradation due to microwelding leads to higher insertion loss, especially if the ohmic cantilever RF MEMS switch is hot-switched.

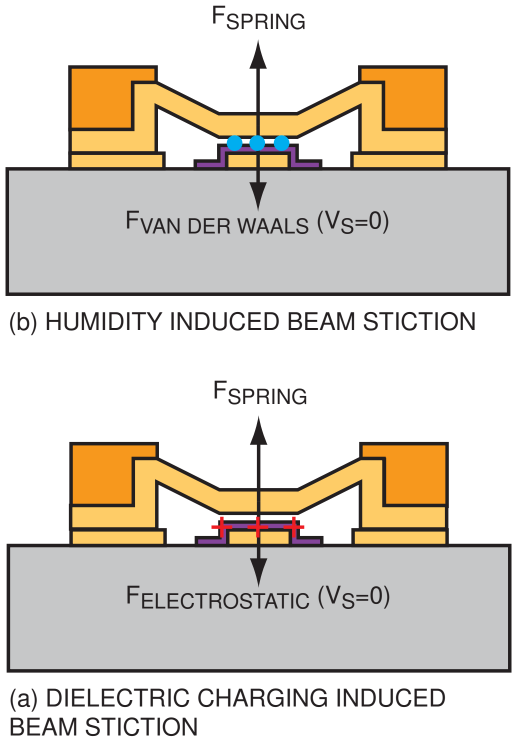

Figure 17: (a) Dielectric charging induced beam stiction. (b) Humidity induced beam stiction.

- **Solution**: Carbon nanotube (CNT) and ultrananocrystalline diamond (UNCD) thin films solve hard contact related reliability issues. In particular, UNCD [6–11] has following extra-ordinary properties:
  - **Electrical**: Diamond is a large bandgap semiconductor ($E_g = 5.5$ eV)[a]. Depending on the doping level, it can be used as an insulator with low leakage current (dielectric), or as a conductor (electrode).
  - **Thermo-mechanical**: UNCD thin films have a very high Young's modulus ($E = 980$ GPa) compared with materials currently used in RF MEMS components[b], improving the reliability (high contact force) and the switching time (high E/ρ, with the mass density, ρ, equal to 3.5 g/cm^3[c]). Microwave plasma-enhanced chemical vapor deposition (MPE-CVD) can deposit UNCD thin films at temperatures $\leq 400°$C. The thermal conductivity, κ, of UNCD is 12-15 W/(m.K)[d].
  - **Tribological**: UNCD thin films are energy-saving ultra-low friction and wear coatings. UNCD is hydrophobic and has very high resistance to adhesion between two surfaces in physical contact, avoiding beam stiction.

[a] The bandgap of CNT varies between 0 and 2 eV; it can be used as a metal or as a semiconductor.
[b] The Young's modulus, E, of CNT is 1000-5000 GPa, E of Kevlar is 150-250 GPa, and E of stainless steel is 200 GPa [12]
[c] The mass density, ρ, of CNT is 0.037 g/cm^3 [12].
[d] The thermal conductivity, κ, of CNT is 3500 W/(m.K), whereas κ of copper is 385 W/(m.K) [12].

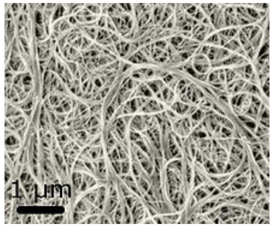

Figure 18: SEM imagery of carbon nanotube (CNT) bundles [12].

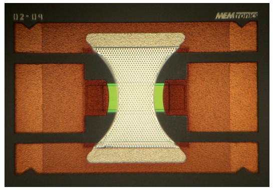

Figure 19: The MEMtronics capacitive fixed-fixed beam RF MEMS switch with Advanced Diamond Technologies UNCD Aqua 25 low-trap dielectric achieved over one billion cycles in dry air [13].

RF MEMS Reliability

- **Solution**: Carbon nanotube (CNT) and ultrananocrystalline diamond (UNCD) thin films solve hard contact related reliability issues. In particular, UNCD [6–11] has following extra-ordinary properties:
  - **Electrical**: Diamond is a large bandgap semiconductor ($E_g = 5.5$ eV)[a]. Depending on the doping level, it can be used as an insulator with low leakage current (dielectric), or as a conductor (electrode).
  - **Thermo-mechanical**: UNCD thin films have a very high Young's modulus ($E = 980$ GPa) compared with materials currently used in RF MEMS components[b], improving the reliability (high contact force) and the switching time (high E/ρ, with the mass density, ρ, equal to 3.5 g/cm^3[c]). Microwave plasma-enhanced chemical vapor deposition (MPE-CVD) can deposit UNCD thin films at temperatures $\leq 400°$C. The thermal conductivity, κ, of UNCD is 12-15 W/(m.K)[d].
  - **Tribological**: UNCD thin films are energy-saving ultra-low friction and wear coatings. UNCD is hydrophobic and has very high resistance to adhesion between two surfaces in physical contact, avoiding beam stiction.

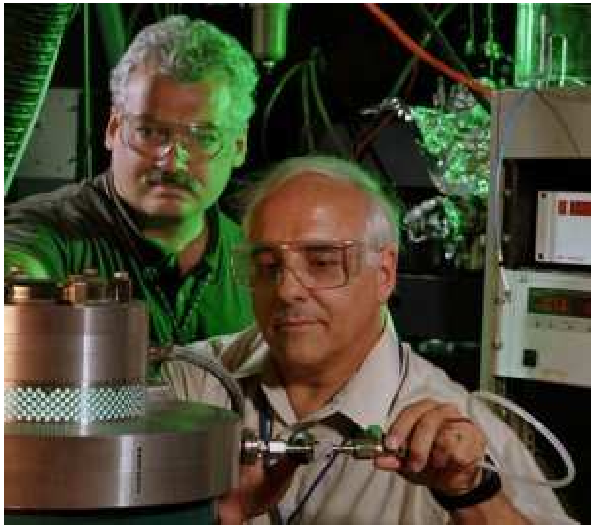

Figure 18: Microwave plasma enhanced chemical vapor deposition (MPE-CVD) of ultrananocrystalline diamond (UNCD), inventors John Carlisle and Orlando Auciello of Argonne National Laboratory, Argonne, IL [14]

[a] The bandgap of CNT varies between 0 and 2 eV; it can be used as a metal or as a semiconductor.
[b] The Young's modulus, E, of CNT is 1000-5000 GPa, E of Kevlar is 150-250 GPa, and E of stainless steel is 200 GPa [12]
[c] The mass density, ρ, of CNT is 0.037 g/cm^3 [12].
[d] The thermal conductivity, κ, of CNT is 3500 W/(m.K), whereas κ of copper is 385 W/(m.K) [12].

- **Solution**: Carbon nanotube (CNT) and ultrananocrystalline diamond (UNCD) thin films solve hard contact related reliability issues. In particular, UNCD [6–11] has following extra-ordinary properties:
  - **Electrical**: Diamond is a large bandgap semiconductor ($E_g = 5.5$ eV)[a]. Depending on the doping level, it can be used as an insulator with low leakage current (dielectric), or as a conductor (electrode).
  - **Thermo-mechanical**: UNCD thin films have a very high Young's modulus ($E = 980$ GPa) compared with materials currently used in RF MEMS components[b], improving the reliability (high contact force) and the switching time (high E/ρ, with the mass density, ρ, equal to 3.5 g/cm^3[c]). Microwave plasma-enhanced chemical vapor deposition (MPE-CVD) can deposit UNCD thin films at temperatures $\leq 400°$C. The thermal conductivity, κ, of UNCD is 12-15 W/(m.K)[d].
  - **Tribological**: UNCD thin films are energy-saving ultra-low friction and wear coatings. UNCD is hydrophobic and has very high resistance to adhesion between two surfaces in physical contact, avoiding beam stiction.

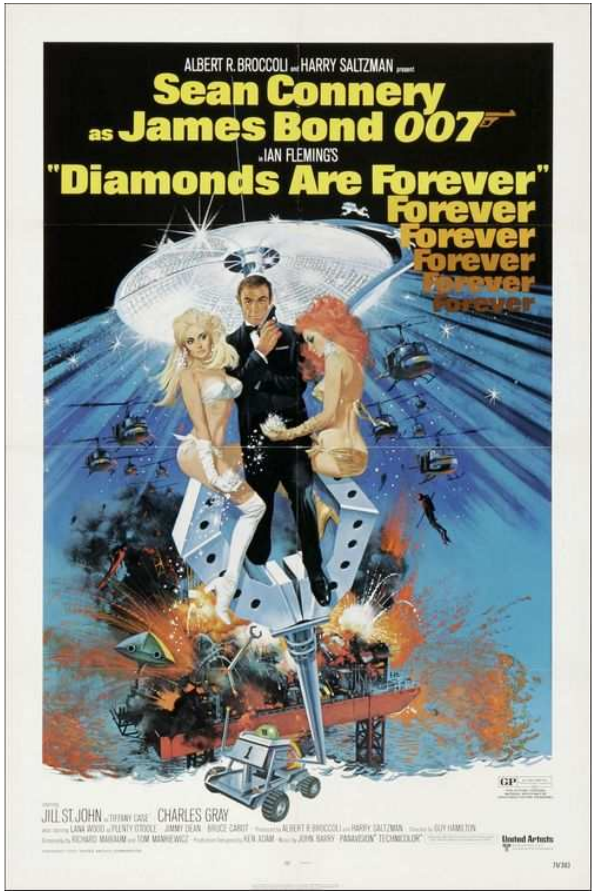

Figure 18: Diamonds are forever (1971)

[a] The bandgap of CNT varies between 0 and 2 eV; it can be used as a metal or as a semiconductor.

[b] The Young's modulus, E, of CNT is 1000-5000 GPa, E of Kevlar is 150-250 GPa, and E of stainless steel is 200 GPa [12]

[c] The mass density, ρ, of CNT is 0.037 g/cm^3 [12].

[d] The thermal conductivity, κ, of CNT is 3500 W/(m.K), whereas κ of copper is 385 W/(m.K) [12].

RF MEMS Reliability: References

[1] J. F. Kucko, J. C. Petrosky, J. R. Reid, and Yung Kee Yeo, “Non-charge related mechanism affecting capacitive MEMS switch lifetime,” *IEEE Microwave Wireless Compon. Lett.*, vol. 16, no. 3, pp. 140–142, March 2006.

[2] C. Goldsmith, J. Maciel, and J. McKillop, “Demonstrating reliability,” *IEEE Microwave Magazine*, vol. 8, no. 6, pp. 56–60, December 2007.

[3] H. S. Newman, J. L. Ebel, D. Judy, and J. Maciel, “Lifetime measurements on a high-reliability RF MEMS contact switch,” *IEEE Microwave Wireless Compon. Lett.*, vol. 18, no. 2, pp. 100–102, February 2008.

[4] J. R. Reid and R. T. Webster, “Measurements of charging in capacitive microelectromechanical switches,” *Electronics Letters*, vol. 38, no. 24, pp. 1544–1545, November 2002.

[5] J. R. Reid, R. T. Webster, and L. A. Starman, “Noncontact measurement of charge induced voltage shift in capacitive MEM-switches,” *IEEE Microwave Wireless Compon. Lett.*, vol. 13, no. 9, pp. 367–369, September 2003.

[6] D. M. Gruen, A. R. Krauss, A. Erdemir, C. Bindal, and C. D. Zuiker, “Smooth diamond films as low friction long wear surfaces,” U.S. Patent 5,989,511, March 22, 1996.

[7] D. M. Gruen, T. G. Mccauley, D. Zhou, and A. R. Krauss, “Tailoring nanocrystalline diamond film properties,” U.S. Patent 6,592,839, February 23, 1999.

[8] A. R. Krauss, D. M. Gruen, M. J. Pellin, and O. Auciello, “Ultrananocrystalline diamond cantilever wide dynamic range acceleration/vibration/pressure sensor,” U.S. Patent 6,422,077, April 06, 2000.

[9] D. M. Gruen, H.-G. Busman, E.-M. Meyer, O. Auciello, and A. R. Krauss, “Patterning of nanocrystalline diamond films for diamond microstructures useful in MEMS and other devices,” U.S. Patent 6,811,612, November 08, 2002.

[10] D. M. Gruen, A. R. Krauss, O. Auciello, and J. A. Carlisle, “N-type doping of nanocrystalline diamond films with nitrogen and electrodes made therefrom,” U.S. Patent 6,793,849, December 12, 2003.

[11] O. Auciello, S. Pacheco, A. V. Sumant, C. Gudeman, S. Sampath, A. Datta, R. W. Carpick, V. P. Adiga, P. Zurcher, Z. Ma, H.-C. Yuan, J. A. Carlisle, B. Kabius, J. Hiller, and S. Srinivasan, “Are diamonds a MEMS’ best friend?” *IEEE Microwave Magazine*, vol. 8, no. 6, pp. 61–75, December 2007.

[12] Wikipedia. [Online]. Available: http://en.wikipedia.org

[13] Advanced Diamond Technologies. [Online]. Available: http://www.www.thindiamond.com

[14] Argonne National Laboratory. Ultrananocrystalline Diamond (UNCD). [Online]. Available: http://www.anl.gov/techtransfer/Available_Technologies/Chemistry/uncd_flc.html

Components

Antenna Elements for Wide-Angle Electronically Scanned Arrays

- **Function**: Antennas transform guided waves into space waves.

Table II: Comparison of Antenna Elements for Wide-Angle Electronically Scanned Arrays.

	microstrip Touchard, et al. [1], 2009	waveguide & ind. iris Keizer, et al. [2], 1991	tapered slot Holter, et al. [3, 4], 2000	bunny ear Lee, et al. [5–7], 2003	connected dipole Neto, et al. [8], 2009	connected Huygens source
Design characteristics						
Broadside or endfire[a]	broadside unidirectional	endfire	endfire	broadside	broadside bidirectional	broadside bidirectional
Feed, Z_{IN}	microstrip, 50 Ω	waveguide, $Z_{TE_{10}}$	stripline,[b] 50 Ω	slotline, 50π Ω	CPS, 120π Ω	CPS, 120π Ω
Feed mode[c]	single-ended	TE_{10}	single-ended[b]	*differential*	*differential*	*differential*
Manufacturing	tile, laminate	brick, waveguide	brick	brick	brick	tile, laminate
Mutual coupling usage[d]	no, metal fence & cavity backing	yes, WAIM	no, metal fence	no	yes, connected	yes, connected
Polarization[e]	single-polarized	single-polarized	dual-polarized	dual-polarized	single-polarized	dual-polarized

[a] Front to back ratio: The front to back ratio of bidirectional broadside radiators can be improved using cavity or reflector (ground (GND) plane) backing, or dielectric lens, resonator or superstrate front-ends, at the expense of bandwidth, group velocity dispersion (GVD) and phase center stability.

[b] Feed mode: The intrinsic feed mode of the tapered slot antenna is a slot mode. A hockey stick balun is used in [3] to transition the *differential* slotline mode to a single-ended stripline mode.

[c] Bandwidth: *Wideband antenna elements have differential feeds*. Differentially-fed antenna elements might suffer from common mode radiation and resonances.

[d] Mutual coupling usage: best friend (wide angle impedance matching (WAIM) layers induce leaky surface waves to reduce the scan loss), or worst enemy (cavity backing, metal fence, or pseudo-differential feeding prevent substrate mode and surface wave propagation and scan blindness due to edge radiation)

[e] Cross polarization level: The minimum achievable Ludwig-3 cross polarization level (θ=45°,ϕ=45°) of an array of single-polarized and dual-polarized electrical dipoles is -17 dB and -20 dB respectively. *An array of connected Huygens sources is perfectly polarized over an infinite bandwidth and at all scanning angles.*

Antenna Elements for Wide-Angle Electronically Scanned Arrays

Table II: Comparison of Antenna Elements for Wide-Angle Electronically Scanned Arrays (continued).

	microstrip Touchard, et al. [1], 2009	waveguide & ind. iris Keizer, et al. [2], 1991	tapered slot Holter, et al. [3, 4], 2000	bunny ear Lee, et al. [5–7], 2003	connected dipole Neto, et al. [8], 2009	connected Huygens source
Figures of merit (VSWR $<$ 2)						
Active gain	$\approx 0.9\pi$ @ f_c	$\approx 0.9\pi$ @ f_c	$\approx 0.9\pi$ @ f_c	[-8, 6] dBi	$\approx 0.9\pi$ @ f_c	$< \pi$ @ f_c [a]
Active RL (VSWR)	10 dB	9.5 dB (2:1)	9.5 dB (2:1)	15 dB	10 dB	∞
Bandwidth	2.7-3.3 GHz (20%)	30%	1-5.9 GHz (5.9:1) [b,c]	1-5 GHz (5:1) [c]	6-9 GHz (40%) [c]	∞
Cross polarization [e]	$>$ -17 dB	-	?	-15 dB	$>$ -17 dB	0
Field of view	$\pm$ 60°	$\pm$ 60°	$\pm$ 50°	$\pm$ 45°	$\pm$ 45°	$\pm$ 70°
Phase center stability	instable, Yagi-Uda [f]	instable, WAIM	instable [a]	stable [a]	stable [a]	stable
RCS	-	-	-	-	-	0
Scan loss, $(\cos\theta)^n$	-	n=1.1 (E)	n=1.3 (E)	n=1.2 (E)	n=1.3 (E)	n=1 (E)
	-	n=1.1 (H)	n=1.3 (H)	n=1.2 (H)	n=1.3 (H)	n=1 (H)
Thickness, from GND plane	-	N/A	$\lambda_{min}/4$	$\lambda_{min}/4$	$\lambda_{min}/4$	N/A, no GND plane

[f] Yagi-Uda directors (multi-stacked patches for example) with varying resonant length increase the bandwidth and the gain, but the GVD, the phase center instability, and the scan loss as well.

Antenna Elements for Wide-Angle Electronically Scanned Arrays

Figure 19: Connecting antenna elements in a revolutionary way could allow UWB antenna arrays with 100:1 bandwidth, capable of replacing as many as five conventional antennas, inventors James Maloney (left) and Paul Friederich (right) of Georgia Tech Research Institute, Atlanta, GA [9].

Antenna Elements for Wide-Angle Electronically Scanned Arrays: References

[1] S. Touchard and O. Maas, "Low loss multifunction building block panel for S-band radar," *International Radar Conference Digest, Bordeaux, France*, Oct. 12–16 2009.

[2] W. Keizer, A. P. de Hek, and A. Smolders, "Theoretical and experimental performance of a wideband wide-scan-angle rectangular waveguide phased array [for radar application]," *IEEE AP-S International Symposium Digest, London, Ontario, Canada*, vol. 3, pp. 1724–1727, June 24–28 1991.

[3] H. Holter, T.-H. Chio, and D. H. Schaubert, "Experimental results of 144-element dual-polarized endfire tapered-slot phased arrays," *IEEE Trans. Antennas Propagat.*, vol. 48, no. 11, pp. 1707–1718, Nov. 2000.

[4] D. H. Schaubert, W. Elsallal, S. Kasturi, A. O. Boryssenko, M. N. Vouvakis, and G. Paraschos, "Wide bandwidth arrays of Vivaldi antennas," in *Digest of the IET Seminar on Wideband, Multiband Antennas and Arrays for Defence or Civil Applications, London, UK*, Mar. 13–13, 2008, pp. 1–20.

[5] J. J. Lee and S. Livingston, "Wide-band bunny-ear radiating element," in *IEEE AP-S International Symposium Digest, Ann Arbor, MI*, June 1993, pp. 1604–1607.

[6] J. J. Lee and S. W. Livingston, "Wide band dipole radiating element with a slot line feed having a Klopfenstein impedance taper," U.S. Patent 5,428,364, May 20, 1993.

[7] J. J. Lee, S. Livingston, and R. Koenig, "A low-profile wide-band (5:1) dual-pol array," *IEEE Antennas Wireless Propagat. Lett.*, vol. 2, pp. 46–49, December 2003.

[8] A. Neto, D. Cavallo, G. Gerini, and G. Toso, "Scanning performances of wideband connected arrays in the presence of a backing reflector," *IEEE Trans. Antennas Propagat.*, vol. 57, no. 10, Part 2, pp. 3092–3102, October 2009.

[9] 100-to-1 Bandwidth: New Planar Design Allows Fabrication of Ultra Wideband Phased Array Antennas. Georgia Tech Research Institute. [Online]. Available: http://www.gtri.gatech.edu/casestudy/100-1-bandwidth

Attenuators

- **Function**: Attenuators provide (non)-uniform symmetric amplitude weighting to control the side lobe level of an RF beamforming ESA.

Table III: Comparison of State-of-the-Art Attenuators.

	MMIC	RFIC	RF MEMS
Reference	MIMIX XA1000BD [1], 2009	Min, et al. [2], 2007	-
RF technology	0.5 μm GaAs pHEMT	0.12 μm SiGe BiCMOS	-
Foundry	WIN	IBM	-
Design characteristics			
Bus	parallel	parallel	-
Design	switched constant-k network	loaded-line	-
Differential or single-ended	single-ended	single-ended	-
Frequency	DC-18 GHz	10-50 GHz	-
Packaging requirement	none	none	-
Metal thickness	4.5 μm	3.1 μm	-
Substrate	100 μm GaAs	9.25 μm SiO_2	-
	$\epsilon_r = 12.9$, tan $\delta = 0.001$	$\epsilon_r = 4.2$, tan $\delta = 0.001$	-
Supply voltage	-7.5/0/3.3 V	0/1.5 V	-
Transmission line	microstrip	11/12/11 μm GCPW	-
Figures of merit			
Attenuation range	28 dB	11 dB	-
Bandwidth	18 GHz	40 GHz	-
Insertion loss	5.5 dB @ 10 GHz	2.1 dB @ 35 GHz	-
	1.1 dB/bit @ 10 GHz	0.57 dB/bit @ 35 GHz	-
Linearity (IP1dB)	24 dBm	5 dBm	-
Noise figure	5.5 dB @ 10 GHz	2.1 dB @ 35 GHz	-
Number of bits, P	5	3.7	-
Power consumption[a]	67.5 mW	0 mW	-
Power handling (cold-switched)	30 dBm	13-14 dBm	-
RMS amplitude error, $\mathrm{S_{A_{ATT}}}$	$<$ 0.5 dB	$<$ 0.25 dB	-
RMS phase error, $\mathrm{S_{P_{ATT}}}$	$< 10^{\circ}$	$< 3^{\circ}$	-
Size	2.376×0.858 mm^2	200×750 μm^2	-
Switching time	$<$ 45 ns	$<$ 1 ns	-

[a] Switched network attenuators are passive and reciprocal and do not consume power if implemented using common gate HEMT, MESFET, nMOS transistor stages or RF MEMS switches. Power consumption is due to the bias circuitry.

Attenuators: References

[1] MIMIX XA1000-BD 5-bit digital attenuator. [Online]. Available: http://www.mimixbroadband.com/defense.asp

[2] B.-W. Min and G. M. Rebeiz, "A 1050 GHz CMOS distributed step attenuator with low loss and low phase imbalance," *IEEE J. Solid-State Circuits*, vol. 42, no. 11, pp. 2547–2554, November 2007.

Limiters

- **Function**: Limiters prevent high power levels from damaging non-robust microwave circuitry [1–3].

Table IV: Comparison of State-of-the-Art Single-Ended (Distributed) Loaded-Line Limiters

	GaAs p-i-n diode	RF MEMS[a]	μVED
Reference	TGL2201 [4, 5], 2002	-	Phommahaxay, et al. [6], 2006
RF technology	GaAs VPIN	-	spark gaps
Foundry	Triquint	-	ESIEE, France
Design characteristics			
AC-coupled or DC-coupled	AC-coupled	-	AC-coupled
Design[b]	reflective	-	reflective
	loaded-line	-	distributed loaded-line
Metal thickness	3 μm	-	-
Packaging	-	-	hermetic, N_2
Substrate	100 μm GaAs	-	500 μm silicon
	$\epsilon_r = 12.9$, tan $\delta = 0.001$	-	$\epsilon_r = 11.7$, tan $\delta = 0.006$
	$\kappa = 0.55$ W/(cm.K)	-	$\kappa = 1.56$ W/(cm.K)
Supply voltage or current	N/A	-	N/A
Transmission line	microstrip	-	CPW
Figures of merit			
Bandwidth	3-25 GHz	-	6-18 GHz
Insertion loss	$<$ 0.5 dB, X-band	-	$<$ 2 dB/cm
Flat leakage[c]	$<$ 18 dBm	-	350 W (P_{IN} = 2 kW)
Linearity	-	-	-
Power handling			
Breakdown	-	-	$>$ 2 kW
Hot-switched	$>$ 5 W (CW)	-	-
Size	1.1 x 1.1 mm^2	-	-
Temperature, max.	320° C	-	-
Response & recovery time [7]	-	-	100 ns
Spike leakage level [7]	-	-	-

[a] Self-actuation could be exploited to design RF MEMS limiters. Upon self-actuation, an RF MEMS shunt-switch-based limiter short-circuits and reflects the incident RF wave. RF MEMS shunt switches can be prebiased in order to assure self-actuation at a required incident power level.

[b] Absorptive loaded-line limiters allow low RCS, but require thermal dissipation management.

[c] Flat leakage is the output power level during limiting.

Limiters: References

[1] R. V. Garver, *Microwave Diode Control Devices*. Artech House, 1976.

[2] B. A. Kopp, C. R. Moore, and R. V. Coffman, "Transmit/receive module packaging: electrical design issues," *Johns Hopkins APL Technical Digest*, vol. 20, no. 1, pp. 70–80, January 1999.

[3] M. van Heijningen, J. P. B. Janssen, and F. E. van Vliet, "Robust AlGaN/GaN MMIC receiver components," *Frequenz*, no. 3-4, pp. 47–50, 2009.

[4] Triquint TGL2201 Wideband Dual Stage VPIN Limiter. [Online]. Available: http://www.triquint.com

[5] D. G. Smith, D. D. Heston, J. Heston, B. Heimer, and K. Decker, "Designing reliable high-power limiter circuits with GaAs PIN diodes," in *IEEE MTT-S International Microwave Symposium Digest , Seattle, WA*, June 2–7, 2002, pp. 1245–1247.

[6] A. Phommahaxay, G. Lissorgues, C. Vasseure, L. Rousseau, T. Bourouina, and P. Nicole, "Towards a fully passive Ku-band power limiter using RF MEMS technologies and vacuum microelectronics," *European Microwave Conference*, pp. 1288–1291, September 2006.

[7] R. J. Tan, A. L. Ward, R. V. Garver, and H. Brisker, "PIN diode limiter spike leakage, recovery time, and damage," in *IEEE MTT-S International Microwave Symposium Digest , New York, NY*, May 25–27, 1988, pp. 1245–1247.

(True-Time-Delay) Phase Shifters

- **Function**: TTD phase shifters provide (TTD) phase shift to steer the beam of an RF beamforming ESA.
- Design trade-offs are necessary in the selection of:
  - Biasing: current-controlled, voltage-controlled (electrodynamic (current flow), electrostatic (no current flow))
  - Design: (distributed) loaded-line [1–4], reflect-type [5], switched LC network (high-pass, low-pass) [6], switched-line [7–10], vector modulator
  - Differential (CPS, slotline) or single-ended (CPW, microstrip) transmission line
  - Phase shift versus time delay
  - Quantization: analog or digital (4b, 5b)
  - RF power amplification: active (unilateral) or passive (reciprocal)

(True-Time-Delay) Phase Shifters

- **Function**: TTD phase shifters provide (TTD) phase shift to steer the beam of an RF beamforming ESA.
- Design trade-offs are necessary in the selection of:
  - Biasing: current-controlled, voltage-controlled (electrodynamic (current flow), electrostatic (no current flow))
  - Design: (distributed) loaded-line [1–4], reflect-type [5], switched LC network (high-pass, low-pass) [6], switched-line [7–10], vector modulator
  - Differential (CPS, slotline) or single-ended (CPW, microstrip) transmission line
  - Phase shift versus time delay
  - Quantization: analog or digital (4b, 5b)
  - RF power amplification: active (unilateral) or passive (reciprocal)

(True-Time-Delay) Phase Shifters

- **Function**: TTD phase shifters provide (TTD) phase shift to steer the beam of an RF beamforming ESA.
- Design trade-offs are necessary in the selection of:
  - Biasing: current-controlled, voltage-controlled (electrodynamic (current flow), electrostatic (no current flow))
  - Design: (distributed) loaded-line [1–4], reflect-type [5], switched LC network (high-pass, low-pass) [6], switched-line [7–10], vector modulator
  - Differential (CPS, slotline) or single-ended (CPW, microstrip) transmission line
  - Phase shift versus time delay
  - Quantization: analog or digital (4b, 5b)
  - RF power amplification: active (unilateral) or passive (reciprocal)

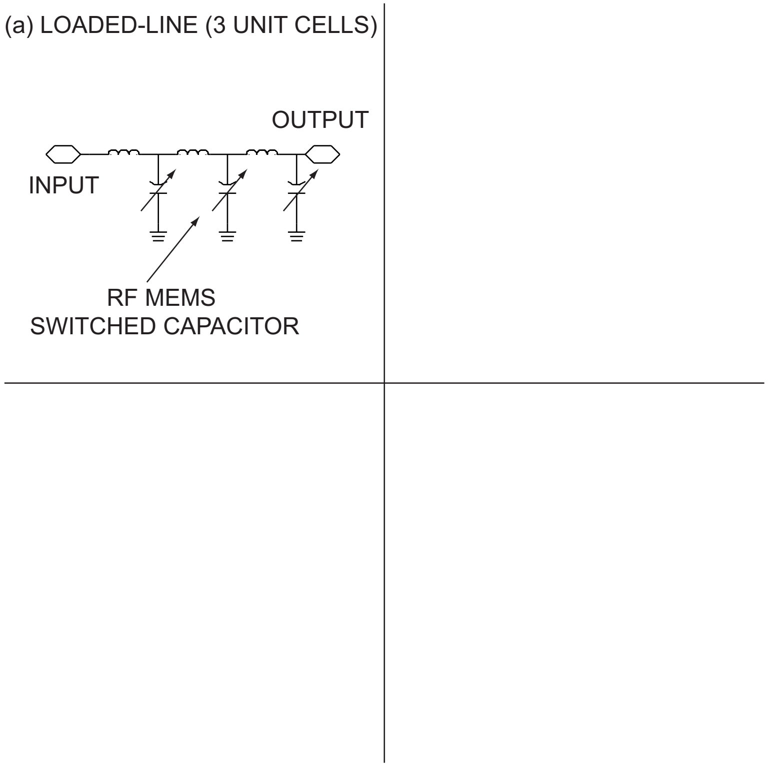

(True-Time-Delay) Phase Shifters

- **Function**: TTD phase shifters provide (TTD) phase shift to steer the beam of an RF beamforming ESA.
- Design trade-offs are necessary in the selection of:
  - Biasing: current-controlled, voltage-controlled (electrodynamic (current flow), electrostatic (no current flow))
  - Design: (distributed) loaded-line [1–4], reflect-type [5], switched LC network (high-pass, low-pass) [6], switched-line [7–10], vector modulator
  - Differential (CPS, slotline) or single-ended (CPW, microstrip) transmission line
  - Phase shift versus time delay
  - Quantization: analog or digital (4b, 5b)
  - RF power amplification: active (unilateral) or passive (reciprocal)

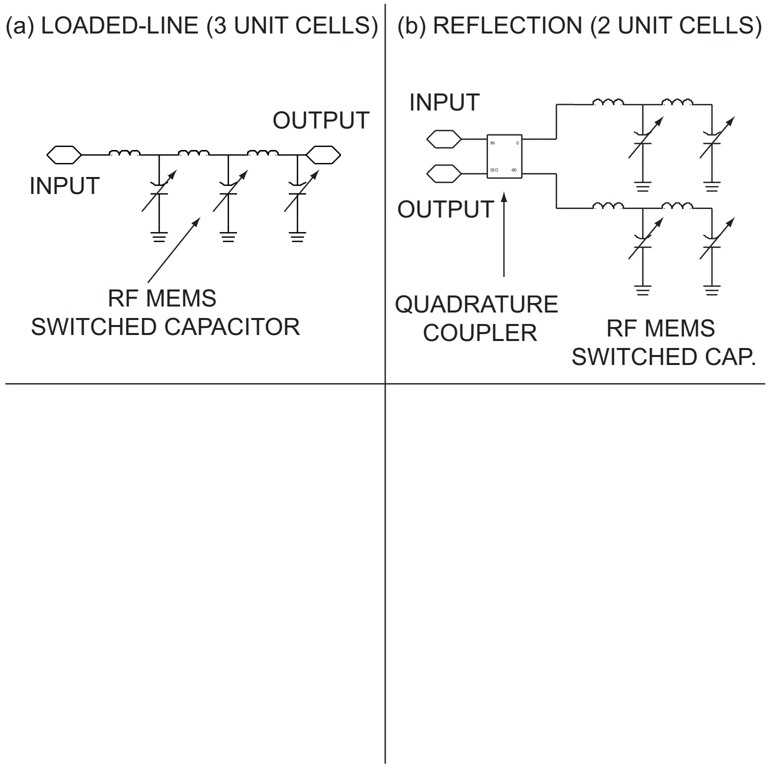

(True-Time-Delay) Phase Shifters

- **Function**: TTD phase shifters provide (TTD) phase shift to steer the beam of an RF beamforming ESA.
- Design trade-offs are necessary in the selection of:
  - Biasing: current-controlled, voltage-controlled (electrodynamic (current flow), electrostatic (no current flow))
  - Design: (distributed) loaded-line [1–4], reflect-type [5], switched LC network (high-pass, low-pass) [6], switched-line [7–10], vector modulator
  - Differential (CPS, slotline) or single-ended (CPW, microstrip) transmission line
  - Phase shift versus time delay
  - Quantization: analog or digital (4b, 5b)
  - RF power amplification: active (unilateral) or passive (reciprocal)

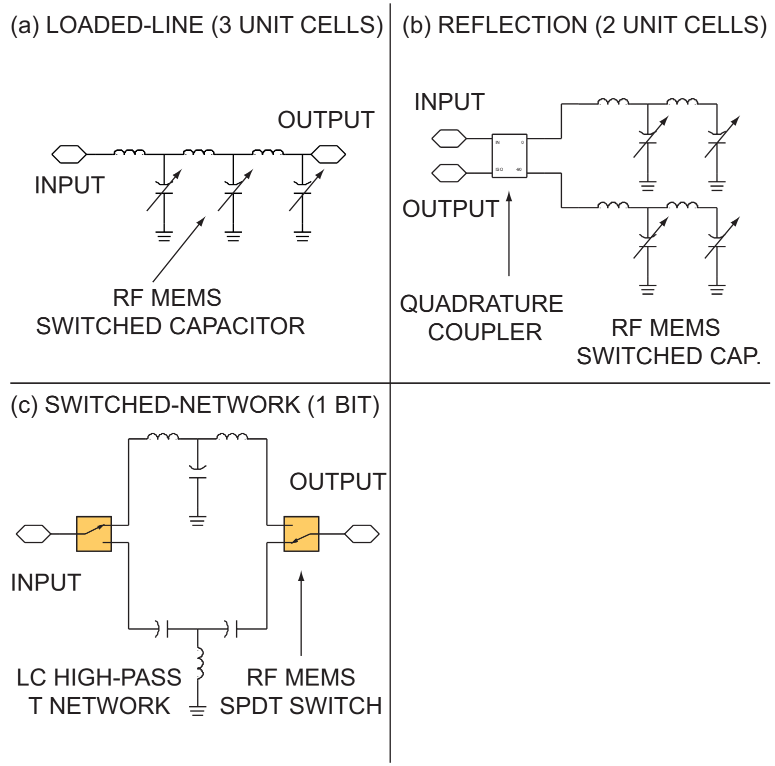

(True-Time-Delay) Phase Shifters

- **Function**: TTD phase shifters provide (TTD) phase shift to steer the beam of an RF beamforming ESA.
- Design trade-offs are necessary in the selection of:
  - Biasing: current-controlled, voltage-controlled (electrodynamic (current flow), electrostatic (no current flow))
  - Design: (distributed) loaded-line [1–4], reflect-type [5], switched LC network (high-pass, low-pass) [6], switched-line [7–10], vector modulator
  - Differential (CPS, slotline) or single-ended (CPW, microstrip) transmission line
  - Phase shift versus time delay
  - Quantization: analog or digital (4b, 5b)
  - RF power amplification: active (unilateral) or passive (reciprocal)

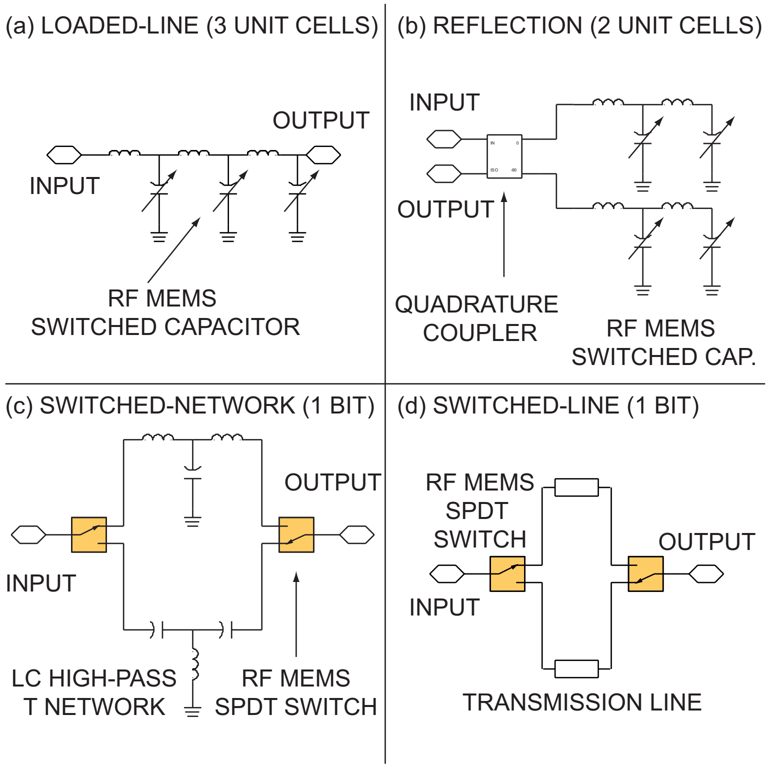

(True-Time-Delay) Phase Shifters

- **Function**: TTD phase shifters provide (TTD) phase shift to steer the beam of an RF beamforming ESA.
- Design trade-offs are necessary in the selection of:
  - Biasing: current-controlled, voltage-controlled (electrodynamic (current flow), electrostatic (no current flow))
  - Design: (distributed) loaded-line [1–4], reflect-type [5], switched LC network (high-pass, low-pass) [6], switched-line [7–10], vector modulator
  - Differential (CPS, slotline) or single-ended (CPW, microstrip) transmission line
  - Phase shift versus time delay
  - Quantization: analog or digital (4b, 5b)
  - RF power amplification: active (unilateral) or passive (reciprocal)

(True-Time-Delay) Phase Shifters

- **Function**: TTD phase shifters provide (TTD) phase shift to steer the beam of an RF beamforming ESA.
- Design trade-offs are necessary in the selection of:
  - Biasing: current-controlled, voltage-controlled (electrodynamic (current flow), electrostatic (no current flow))
  - Design: (distributed) loaded-line [1–4], reflect-type [5], switched LC network (high-pass, low-pass) [6], switched-line [7–10], vector modulator
  - Differential (CPS, slotline) or single-ended (CPW, microstrip) transmission line
  - Phase shift versus time delay
  - Quantization: analog or digital (4b, 5b)
  - RF power amplification: active (unilateral) or passive (reciprocal)
- Phase shifting
  - Bandwidth:

    $$BW_{max} < 0.886\, B_b \frac{c}{L\, \sin \theta_{max}}$$

  - Frequency squinting:

    $$\theta - \theta_0 = \arcsin\left(\frac{-\beta}{k\, d}\right) - \arcsin\left(\frac{-\beta}{k_0\, d}\right)$$

- TTD phase shifting
  - TTD beam steering:

    $$\theta = \arcsin\left(\frac{c}{d}\, \Delta\tau\right)$$

(True-Time-Delay) Phase Shifters

- **Function**: TTD phase shifters provide (TTD) phase shift to steer the beam of an RF beamforming ESA.

- Design trade-offs are necessary in the selection of:
  - Biasing: current-controlled, voltage-controlled (electrodynamic (current flow), electrostatic (no current flow))
  - Design: (distributed) loaded-line [1–4], reflect-type [5], switched LC network (high-pass, low-pass) [6], switched-line [7–10], vector modulator
  - Differential (CPS, slotline) or single-ended (CPW, microstrip) transmission line
  - Phase shift versus time delay
  - Quantization: analog or digital (4b, 5b)
  - RF power amplification: active (unilateral) or passive (reciprocal)

- Phase shifting
  - Bandwidth:

    $BW_{max} < 0.886\, B_b \frac{c}{L \sin\theta_{max}}$

  - Frequency squinting:

    $\theta - \theta_0 = \arcsin\left(\frac{-\beta}{k\, d}\right) - \arcsin\left(\frac{-\beta}{k_0\, d}\right)$

- TTD phase shifting
  - TTD beam steering:

    $\theta = \arcsin\left(\frac{c}{d}\,\Delta\tau\right)$

(True-Time-Delay) Phase Shifters

- **Function**: TTD phase shifters provide (TTD) phase shift to steer the beam of an RF beamforming ESA.

- Design trade-offs are necessary in the selection of:
  - Biasing: current-controlled, voltage-controlled (electrodynamic (current flow), electrostatic (no current flow))
  - Design: (distributed) loaded-line [1–4], reflect-type [5], switched LC network (high-pass, low-pass) [6], switched-line [7–10], vector modulator
  - Differential (CPS, slotline) or single-ended (CPW, microstrip) transmission line
  - Phase shift versus time delay
  - Quantization: analog or digital (4b, 5b)
  - RF power amplification: active (unilateral) or passive (reciprocal)

- Phase shifting
  - Bandwidth:

    $BW_{max} < 0.886\, B_b \frac{c}{L\, \sin \theta_{max}}$
  - Frequency squinting:

    $\theta - \theta_0 = \arcsin\left(\frac{-\beta}{k\, d}\right) - \arcsin\left(\frac{-\beta}{k_0\, d}\right)$

- TTD phase shifting
  - TTD beam steering:

    $\theta = \arcsin\left(\frac{c}{d}\, \Delta\tau\right)$

(True-Time-Delay) Phase Shifters

- **Function**: TTD phase shifters provide (TTD) phase shift to steer the beam of an RF beamforming ESA.
- Design trade-offs are necessary in the selection of:
  - Biasing: current-controlled, voltage-controlled (electrodynamic (current flow), electrostatic (no current flow))
  - Design: (distributed) loaded-line [1–4], reflect-type [5], switched LC network (high-pass, low-pass) [6], switched-line [7–10], vector modulator
  - Differential (CPS, slotline) or single-ended (CPW, microstrip) transmission line
  - Phase shift versus time delay
  - Quantization: analog or digital (4b, 5b)
  - RF power amplification: active (unilateral) or passive (reciprocal)
- Number of *effective* bits:

$$\tilde{P} = \frac{1}{2}\,\log_2 \pi^2 - \log_2 3\,(S^2_{P_{ATT}} + S^2_{P_{PS}} + \frac{1}{3}\,\frac{\pi^2}{2^{2P}})$$

(True-Time-Delay) Phase Shifters

- **Function**: TTD phase shifters provide (TTD) phase shift to steer the beam of an RF beamforming ESA.
- Design trade-offs are necessary in the selection of:
  - Biasing: current-controlled, voltage-controlled (electrodynamic (current flow), electrostatic (no current flow))
  - Design: (distributed) loaded-line [1–4], reflect-type [5], switched LC network (high-pass, low-pass) [6], switched-line [7–10], vector modulator
  - Differential (CPS, slotline) or single-ended (CPW, microstrip) transmission line
  - Phase shift versus time delay
  - Quantization: analog or digital (4b, 5b)
  - RF power amplification: active (unilateral) or passive (reciprocal)

(True-Time-Delay) Phase Shifters

Table V: Comparison of State-of-the-Art Switched LC Network (High-Pass/Low-Pass) Phase Shifters.

	MMIC		RFIC	RF MEMS
Reference	Bahl, et al. [11], 2008	MIMIX XS1000BS [12], 2008	Min, et al. [13], 2008	Morton, et al. [6], 2008
RF technology	0.4 μm GaAs MESFET	0.5 μm GaAs pHEMT	0.12 μm SiGe BiCMOS	240 μm capacitive cantilever switch
Foundry	M/A-COM	WIN	IBM	Georgia Tech
Design characteristics				
Bus	parallel	parallel	parallel	parallel
Differential or single-ended[a]	single-ended	single-ended	*differential*	single-ended
Frequency	10-16 GHz	7-13 GHz	31-38 GHz	8-12 GHz
Packaging requirement	none	none	none	hermetic[b]
Metal thickness	4.5 μm	3.1 μm	4 μm	1.5 μm
Substrate	125 μm GaAs	100 μm GaAs	9.25 μm SiO_2	10 μm SiO_2
	$\epsilon_r = 12.9$, tan $\delta = 0.001$	$\epsilon_r = 12.9$, tan $\delta = 0.001$	$\epsilon_r = 4.2$, tan $\delta = 0.001$	$\epsilon_r = 4.2$, tan $\delta = 0.001$
Supply voltage	-5/0/5 V	-7.5/0 V	0/1.5 V	-22/0/22 V
Transmission line	microstrip	microstrip	11/12/11 μm GCPW	microstrip
Figures of merit				
Bandwidth	6 GHz	6 GHz	7 GHz	4 GHz
Insertion loss	5 dB	6.2 dB	13 dB	4.5 dB (8 dB packaged)
	1.25 dB/b	1.03 dB/b	3.25 dB/b	0.9 dB/b (1.6 dB/b packaged)
Linearity (IP1dB)	29-30 dBm	25 dBm	10 dBm	$>$ 30 dBm
Noise figure	5 dB	6.2 dB	13 dB	4.5 dB (8 dB packaged)
Number of bits, P	4	6	4	5
Power consumption[c]	20 mW	$<$ 100 mW	0 mW	0 mW
Power handling (cold-switched)	-	30 dBm	-	30 dBm
RMS amplitude error, $S_{A_{PS}}$	0.3 dB	0.9 dB	2 dB	1.29 dB
RMS phase error, $S_{P_{PS}}$	4°	2.5°	11°	10°
Size	2.6 mm^2	3×2.1 mm^2	530×220 μm^2	7.1×1.3 mm^2
Switching time	$<$ 20 ns	$<$ 45 ns	- ns	13 μs

[a] *Differential* phase shifters have no second-order intermodulation products, and are low noise and wideband.

[b] The package is an in-situ thin-film cap.

[c] Switched LC network phase shifters are passive and reciprocal and do not consume power if implemented using common gate HEMT, MESFET, nMOS transistor stages or RF MEMS switches. Power consumption is due to the bias circuitry.

(True-Time-Delay) Phase Shifters: References

[1] N. S. Barker and G. M. Rebeiz, "Optimization of distributed MEMS transmission-line phase shifters - U-band and W-band designs," *IEEE Trans. Microwave Theory Tech.*, vol. 48, no. 11, pp. 1957–1966, November 2000.

[2] J. Perruisseau-Carrier, R. Fritschi, P. Crespo-Valero, and A. K. Skrivervik, "Modeling of periodic distributed MEMS application to the design of variable true-time delay lines," *IEEE Trans. Microwave Theory Tech.*, vol. 54, no. 1, pp. 383–392, January 2006.

[3] B. Lakshminarayanan and T. M. Weller, "Optimization and implementation of impedance-matched true-time-delay phase shifters on quartz substrate," *IEEE Trans. Microwave Theory Tech.*, vol. 55, no. 2, part 1, pp. 335–342, February 2007.

[4] K. Van Caekenberghe and T. Vähä-Heikkilä, "An analog RF MEMS slotline true-time-delay phase shifter," *IEEE Trans. Microwave Theory Tech.*, vol. 56, no. 9, pp. 2151–2159, September 2008.

[5] B. Pillans, S. Eshelman, A. Malczewski, J. Ehmke, and C. Goldsmith, "Ka-band RF MEMS phase shifters," *IEEE Microwave Wireless Compon. Lett.*, vol. 9, no. 12, pp. 520–522, December 1999.

[6] M. A. Morton and J. Papapolymerou, "A packaged MEMS-based 5-bit X-band high-pass/low-pass phase shifter," *IEEE Trans. Microwave Theory Tech.*, vol. 56, no. 9, pp. 2025–2031, September 2008.

[7] J. B. Hacker, R. E. Mihailovich, M. Kim, and J. F. DeNatale, "A Ka-band 3-bit RF MEMS true-time-delay network," *IEEE Trans. Microwave Theory Tech.*, vol. 51, no. 1, part 1, pp. 305–308, January 2003.

[8] C. D. Nordquist, C. W. Dyck, G. M. Kraus, I. C. Reines, C. L. Goldsmith, W. D. Cowan, T. A. Plut, F. Austin, P. S. Finnegan, M. H. Ballance, and C. T. Sullivan, "A DC to 10 GHz 6-bit RF MEMS time delay circuit," *IEEE Microwave Wireless Compon. Lett.*, vol. 16, no. 5, pp. 305–307, May 2006.

[9] J. Muldavin, C. Bozler, S. Rabe, and C. Keast, "Fully packaged 4-bit 100 ps RF MEMS time delay," in *IEEE MTT-S International Microwave Symposium Digest, Honolulu, HI*, June 3–8, 2007, pp. 493–496.

[10] A. Stehle, G. Georgiev, V. Ziegler, B. Schönlinner, U. Prechtel, H. Seidel, and U. Schmid, "RF MEMS switch and phase shifter optimized for W-band," *European Microwave Conference, Amsterdam, The Netherlands*, pp. 104–107, October 2008.

[11] I. J. Bahl and M. Dayton, "A Ku-band 4-bit compact octave bandwidth GaAs MMIC phase shifter," *Microwave Journal*, vol. 51, no. 6, pp. 30–42, June 2008.

[12] MIMIX XS1000-BD 6-bit digital phase shifter. [Online]. Available: http://www.mimixbroadband.com/defense.asp

[13] B. Min and G. M. Rebeiz, "Single-ended and differential Ka-band BiCMOS phased array front-ends," *IEEE J. Solid-State Circuits*, vol. 43, no. 10, pp. 2239–2250, October 2008.

Transmit/Receive Switches (Duplexers)

- **Function**: T/R switches are single pole double throw (SPDT) switches, which can be used instead of large and narrow-band ferrite circulators to time-share the antenna between the transmitter and receiver of a T/R module [1, 2].

Table VI: Comparison of State-of-the-Art Circulators and Wideband SPDT Switches.

	Ferrite circulator	MMIC SPDT	RF MEMS SPDT	
Reference	RDKC [3], 2008	Südow, et al. [4], 2008	Kong et al. [5, 6], 1999	RMSW220HP [7], 2009
RF technology	ferrite	0.25 μm AlGaN/GaN HEMT	ohmic lateral deflection fixed-fixed beam	ohmic cantilever
Foundry/vendor	Raditek	Chalmers	Northrop Grumman Space Technology	Radant MEMS
Design characteristics				
Differential or single-ended	single-ended	single-ended	single-ended	single-ended
Frequency	9-10.5 GHz	2-18 GHz	DC-50 GHz	DC-40 GHz
Packaging requirement	metal package	none	hermetic	hermetic[a]
Substrate	-	2 μm GaN & 95 μm SiC	100 μm GaAs	250 μm high-resistivity Si
	-	$\epsilon_r = 5.35$ & $\epsilon_r = 6.5$	$\epsilon_r = 12.8$, tan $\delta = 0.001$	$\epsilon_r = 11.9$, tan $\delta = 0.001$
Supply voltage	-	-20/0 V	0/70 V	$\pm$100/0 V
Transmission line	microstrip	microstrip	CPW	microstrip
Figures of merit				
Bandwidth	1.5 GHz	16 GHz	50 GHz	40 GHz
Power handling				
Cold-switched	25 W	$>$ 5 W	-	16 W
Hot-switched	-	-	-	20 dBm
Insertion loss	0.5 dB	2 dB @ 10 GHz	$<$ 0.2 dB @ 10 GHz	$<$ 0.45 dB @ 10 GHz[a]
Isolation	20 dB	$>$ 30 dB @ 10 GHz	$>$ 33 dB @ 10 GHz	$>$ 19 dB @ 10 GHz[a]
Lifetime	-	-	-	$> 10^9$ cycles, 40 dBm, cold-switched
	-	-	-	$> 10^9$ cycles, -10 dBm, hot-switched
Linearity (IP1dB)	-	37 dBm @ 10 GHz	-	$>$ 55 dBm @ 900 MHz
Noise figure	0.5 dB	2 dB @ 10 GHz	$<$ 0.2 dB @ 10 GHz	$<$ 0.45 dB @ 10 GHz[a]
Power consumption	0 mW	$<$ 0.1 mW	-	$<$ 2 μW
Size	$17 \times 10.2 \times 5.65$ mm^3	1.4×0.8 mm^2	-	$1.44 \times 1.4 \times 0.65$mm^3 [a]
Switching time	full-duplex	$<$ 300 ns	$<$ 2 μs	$<$ 10 μs

[a] incl. glass frit sealed wafer-level package

Transmit/Receive Switches (Duplexers): References

[1] R. Z. Jones and B. A. Kopp, "Duplexer consideration for X-band T/R modules," *Microwave Journal*, vol. 43, no. 5, pp. 348–352, May 2000.

[2] L. G. Maloratsky, "Transceiver duplexer design considerations," *Microwave Journal*, vol. 51, no. 10, p. 68, October 2008.

[3] Raditek RDKC Circulator Datasheet. [Online]. Available: http://www.raditek.com

[4] M. Südow, M. Fagerlind, M. Thorsell, K. Andersson, N. Billström, P.-Å. Nilsson, and N. Rorsman, "An AlGaN/GaN HEMT-based microstrip MMIC process for advanced transceiver design," *IEEE Trans. Microwave Theory Tech.*, vol. 56, no. 8, pp. 1827–1833, August 2008.

[5] A. M. Kong, R. B. Stokes, J. P. Trieu, R. U. Bhorania, and M. D. Lammert, "Planar airbridge RF terminal MEMS switch," U.S. Patent 6,218,911, July 13, 1999.

[6] R. B. Stokes and A. M. Kong, "MEMS millimeter wave switches," U.S. Patent 6,873,223, December 16, 2002.

[7] Radant MEMS RMSW220HP Datasheet. [Online]. Available: http://www.radantmems.com

Tunable Matching Networks

- **Function**: Tunable matching networks can be used instead of narrow-band and large ferrite isolators (or 4-port ferrite circulators) to transform the optimal load impedance of the power amplifier to a changing antenna impedance. The antenna impedance changes while changing carrier frequency or while scanning.

Table VII: Comparison of State-of-the-Art Tunable Matching Networks

	Ferroelectric	RFIC	RF MEMS		
Reference	Chen, et al. [1], 2004	Buisman, et al. [2], 2005	Qiao, et al. [3,4], 2006	Vähä-Heikkilä, et al. [5], 2007	van Bezooijen, et al. [6], 2008
RF technology	BST varactors, C_r=3	SOI pn diode	300 μm cap. fix. fix. beam	280 μm cap. fix. fix. beam	500 μm cap. fix. fix. beam
Foundry	UCSB	DIMES, TU Delft	Raytheon	VTT, Finland	NXP
Design characteristics					
AC- or DC-coupled	AC-coupled	DC-coupled	AC-coupled	DC-coupled	AC-coupled
Analog or digital	analog	analog	analog / 4 b digital	13 b	5 b
Design [7]	shunt/series C	two-section LC network	loaded-line	triple-stub	series LC network
Diff. or single-ended	single-ended	single-ended	single-ended	single-ended	single-ended
Feedback	no	no	yes	no	yes
Metal thickness	-	4 μm	4 μm	3 μm	5 μm
Packaging	-	-	In-Au WLP	-	hermetic, AuSn solder
Substrate	sapphire	silicon on glass	GaAs	fused silica	silicon
	$\epsilon_r = 9.30$	$\epsilon_r = 6.2$	$\epsilon_r = 13.1$	$\epsilon_r = 3.78$	$\epsilon_r = 11.7$
	$\tan\delta = 0.0002$	$\tan\delta = 0.0009$	$\tan\delta = 0.0004$	$\tan\delta = 0.0002$	$\tan\delta = 0.006$
	$\kappa = 23.1$ W/(cm.K)	$\kappa = 0.93$ W/(cm.K)	$\kappa = 0.55$ W/(cm.K)	$\kappa = 1.40$-2.00 W/(cm.K)	$\kappa = 1.56$ W/(cm.K)
Supply voltage	$<$ 14 V	$<$ 15 V	$<$ 40 V	$<$ 20 V	60 / 30 V
Transmission line	microstrip	CPW	microstrip	CPW	CPW
Figures of merit					
Bandwidth	420-500 MHz	1.6-2.4 GHz	2-18 GHz	6-20 GHz	1-3 GHz
Power handling					
Breakdown	30 V	$>$ 30 dBm	-	-	$>$ 45 V, $>$ 46 dBm
Cold-switched	-	-	37 dBm	23 dBm	45 V, 46 dBm
Hot-switched	-	-	33 dBm	-	12 V, 35 dBm
Insertion loss	0.3 dB	0.4-3.5 dB	-	2 dB	-
Linearity[a]	ACPR1 $>$ 50 dBc	IIP3 $>$ 42 dBm	-	IIP3 $>$ 60 dBm	THD $<$ -85 dBc @ 35 dBm
	$P_{IN} = 27$ dBm	$\Delta f = 20$ MHz	-	$\Delta f = 1$ MHz	-
Size	0.7 x 0.8 mm^2	1.975 x 4.2 mm^2	-	7.3 x 7.3 mm^2	6 x 8 mm^2
Switching time	-	-	-	-	50 μs
Tuning range	3.8:1-1.7:1 (VSWR)	(0.2:82,-24:24) Ω	-	see [5]	(50,-25:25:75) Ω

[a] The linearity also depends on the impedance transformation ratio.

Tunable Matching Networks: References

[1] L. Chen, R. Forse, D. Chase, and R. A. York, "Analog tunable matching network using integrated thin-film BST capacitors," in *IEEE MTT-S International Microwave Symposium Digest , Fort Worth, TX*, June 6–11, 2004, pp. 261–264.

[2] K. Buisman, L. C. N. de Vreede, L. E. Larson, M. Spirito, A. Akhnoukh, Y. Lin, X. Liu, and L. K. Nanver, "Low-distortion, low-loss varactor-based adaptive matching networks, implemented in a silicon-on-glass technology," in *IEEE Radio Frequency Integrated Circuits Symposium Digest , Long Beach, CA*, June 12–14, 2005, pp. 389–392.

[3] D. Qiao, R. Molfino, S. M. Lardizabal, B. Pillans, P. M. Asbeck, and G. Jerinic, "An intelligently controlled RF power amplifier with a reconfigurable MEMS-varactor tuner," *IEEE Trans. Microwave Theory Tech.*, vol. 53, no. 3, pp. 1089–1095, March 2005.

[4] K. J. Herrick, G. Jerinic, R. P. Molfino, S. M. Lardizabal, and B. Pillans, "S-Ku band intelligent amplifier microsystem," *Proceedings of the SPIE*, vol. 6232, May 2006.

[5] T. Vähä-Heikkilä, K. Van Caekenberghe, J. Varis, J. Tuovinen, and G. M. Rebeiz, "RF MEMS impedance tuners for 6-24 GHz applications," *Wiley Interscience International Journal of RF and Microwave Computer-Aided Engineering*, vol. 17, no. 3, pp. 265–278, May 2007.

[6] A. van Bezooijen, M. A. de Jongh, C. Chanlo, L. C. H. Ruijs, F. van Straten, R. Mahmoudi, and A. H. M. van Roermund, "A GSM/EDGE/WCDMA adaptive series-LC matching network using RF-MEMS switches," *IEEE J. Solid-State Circuits*, vol. 43, no. 10, pp. 2259–2268, Oct. 2008.

[7] D. M. Pozar, *Microwave Engineering, 2nd Ed.* John Wiley & Sons, 1998.

RF Beamforming AESA Subsystems

UWB RF MEMS T/R Modules for Pulse-Doppler Radars

- **Functions**: T/R modules set the transmit power in Tx mode, the noise figure (NF) in Rx mode, and time share the antenna between transmitter and receiver. RF beamforming T/R modules provide amplitude and (TTD) phase shift control [1–11].

- **Advantages**:
  - Bandwidth: TTD-capable[a]
  - Power consumption, heat dissipation
  - RMS amplitude and phase error: lower than for a common leg MMIC implementation

- **Disadvantages**:
  - Hot-switched power handling: lower than for a ferrite circulator
  - Response & recovery time: higher than for a p-i-n diode limiter
  - Switching time: higher than for an MMIC implementation

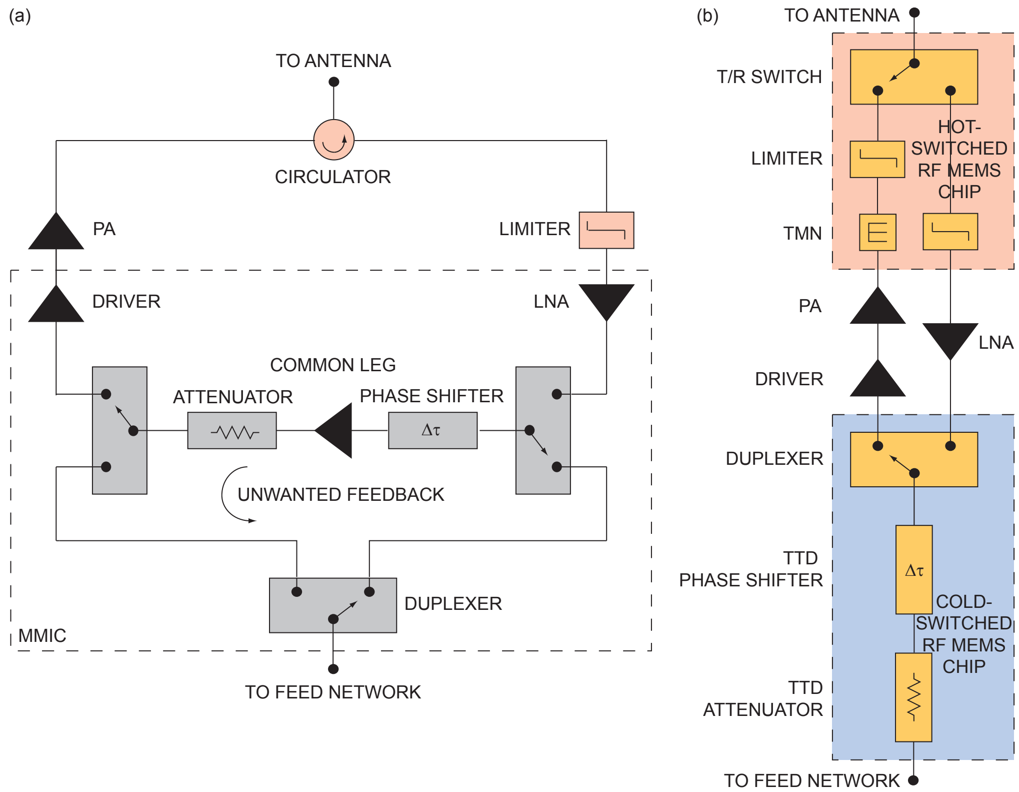

Figure 20: (a) block diagrams of T/R modules for RF beamforming AESA based pulse-Doppler radars: MMIC implementation based on active (black) and passive (gray) components, (b) RF MEMS (yellow) implementation.

[a]Contrary to wideband T/R switches, wideband circulators do not exist.

T/R Modules for Pulse-Doppler Radars: References

[1] M. J. Schindler, S. L. Chu, T. E. Kazior, A. M. Bertrand, and K. M. Simon, “A single chip 2-20 GHz T/R module,” in *IEEE MTT-S International Microwave Symposium Digest , Dallas, TX*, May 8–10, 1990, pp. 117–120.

[2] J. J. Komiak and A. K. Agrawal, “Design and performance of octave S/C band MMIC T/R modules for multi-function phased arrays,” *IEEE Trans. Microwave Theory Tech.*, vol. 39, no. 12, pp. 1955–1963, Dec. 1991.

[3] A. K. Agrawal, R. Clark, and J. J. Komiak, “T/R module architecture tradeoffs for phased array antennas,” in *IEEE MTT-S International Microwave Symposium Digest , San Francisco, CA*, Oct. 20–23, 1996, pp. 995–998.

[4] J. W. Cassen, S. A. Parks, E. L. Rich, III, G. N. Bonadies, G. L. Ferrell, J. S. Fisher, III, J. W. Gipprich, J. D. Gornto, D. J. Heffernan, D. A. Herlihy, A. J. Piloto, P. K. Richard, D. W. Strack, and S. K. Suko, “Dual channel microwave transmit/receive module for an active aperture of a radar system,” U.S. Patent 6,114,986, September 23, 1998.

[5] J. Bennett, K. Lewinski, P. Shearing, B. Velsher, J. van Houten, and A. Tiesinga, “Quadpack X-band T/R module for active phased array radar,” in *GaAs Conference, Amsterdam, The Netherlands*, Oct. 5–6, 1998, pp. 63–67.

[6] B. A. Kopp, C. R. Moore, and R. V. Coffman, “Transmit/receive module packaging: electrical design issues,” *Johns Hopkins APL Technical Digest*, vol. 20, no. 1, pp. 70–80, January 1999.

[7] B. A. Kopp, M. Borkowski, and G. Jerinic, “Transmit/receive modules,” *IEEE Trans. Microwave Theory Tech.*, vol. 50, no. 3, pp. 827–834, March 2002.

[8] H.-P. Feldle, H. Leier, W. Menzel, and M. Schreiner, “Amplitude and phase-controlled antennas-subsystem,” U.S. Patent 6,876,323 B2, January 09, 2003.

[9] Y. Mancuso, P. Gremillet, and P. Lacomme, “T/R-modules technological and technical trends for phased array antennas,” in *IEEE MTT-S International Microwave Symposium Digest, San Francisco, CA*, June 11–16, 2006, pp. 614–617.

[10] M. van Heijningen, A. de Boer, J. A. Hoogland, M. van Wanum, A. P. de Hek, F. E. van Vliet, and H. Brouzes, “Multi function and high power amplifier chipset for X-band phased array frontends,” in *1st European Microwave Integrated Circuits Conference, Manchester, UK*, Sept. 10–13, 2006, pp. 237–240.

[11] B.-W. Min, M. Chang, and G. M. Rebeiz, “SiGe T/R modules for Ka-band phased arrays,” in *IEEE Compound Semiconductor Integrated Circuit Symposium, Portland, OR*, Oct. 14–17, 2006, pp. 1–4.

RF Beamforming Passive Subarrays

RF MEMS Subarrays

- **Function**: Adding 2-D electronic scanning to 1-D RF beamforming AESA
- **Advantages**:
  - Cost: lower compared to AESA solution
- **Disadvantages**:
  - EIRP $\times$ G_r/T: lower compared to AESA solution

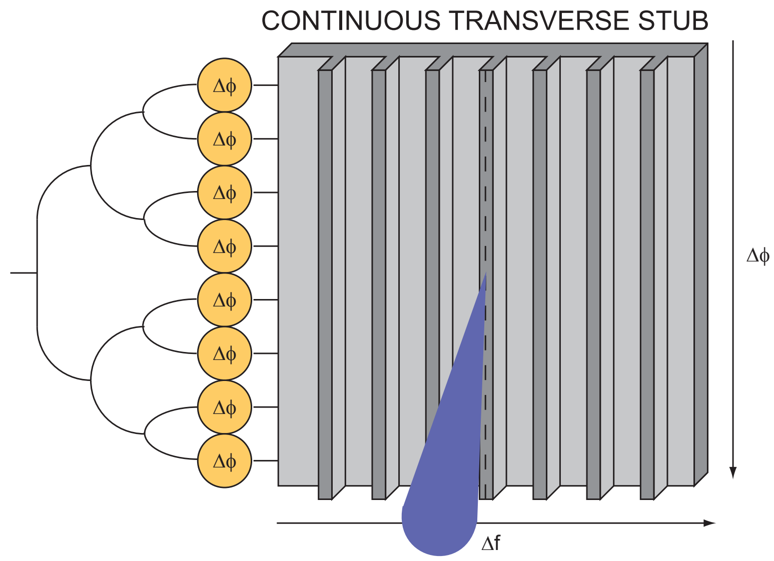

Figure 21: Stick-assembled continuous transverse stub fed by a passive subarray [1].

Subarrays: References

[1] C. Quan, J. J. Lee, B. M. Pierce, and R. C. Allison, “Wideband 2-D electronically scanned array with compact CTS feed and MEMS phase shifters,” U.S. Patent 6,822,615, February 25, 2003.

RF Beamforming PESA Subsystems

UWB Brick Assembled RF MEMS Lens Arrays

- **Principle of Operation**: A lens array captures an unbounded wave, (TTD) phase shifts and reradiates the guided wave [1–4].
- **Advantages**:
  - Bandwidth: TTD-capable
  - Beam pointing error (3b $< \tilde{P} <$ 4b)
  - Monopulse-capable
  - No feed blockage, protrusion (Cassegrain)
  - Polarimetric
- **Disadvantages**:
  - Beam steering controller on the outside
  - Size and weight (brick assembly)
  - Spill-over loss (Tx) and noise (Rx)
- **Examples**:
  - RADANT [3], Raytheon [5]

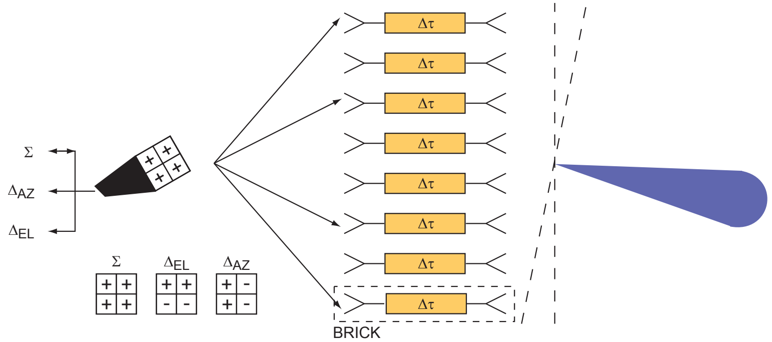

Figure 22: An UWB lens array is illuminated by a four-quadrant monopulse horn.

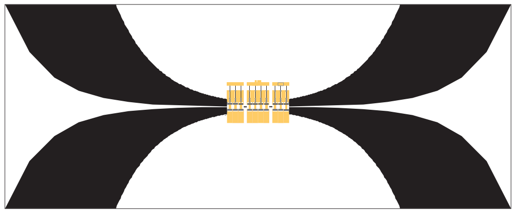

Figure 23: A *differential* UWB lens array brick (DETSA – slotline RF MEMS TTD phase shifter – DETSA)

Brick Assembled p-i-n Diode & RF MEMS Lens Array Patents

US005598172A

United States Patent [19] — **Chekroun**

[11] **Patent Number: 5,598,172**
[45] **Date of Patent: Jan. 28, 1997**

[54] **DUAL-POLARIZATION MICROWAVE LENS AND ITS APPLICATION TO A PHASED-ARRAY ANTENNA**

[75] Inventor: **Claude Chekroun**, Gif sur Yvette, France

[73] Assignee: **Thomson - CSF Radant**, Les Ulis, France

[21] Appl. No.: **799,785**

[22] Filed: **Nov. 5, 1991**

[30] **Foreign Application Priority Data**

Nov. 6, 1990 [FR] France 90 13708

[51] **Int. Cl.**^{6} **H01Q 19/06**; H01Q 15/02
[52] **U.S. Cl.** **343/754**; 343/756; 343/909
[58] **Field of Search** .... 343/754, 756, 343/909, 911 R, 913

[56] **References Cited**

U.S. PATENT DOCUMENTS

3,569,974	3/1971	McLeod, Jr.	343/754
4,212,014	7/1980	Chekroun	343/754
4,320,404	3/1982	Chekroun	343/754
4,344,077	8/1982	Chekroun et al.	343/754
4,447,815	5/1984	Chekroun et al.	343/754
4,975,712	12/1990	Chen	343/754
5,001,495	3/1991	Chekroun	343/754
5,081,465	1/1992	Collignon	343/754

Primary Examiner—Gregory C. Issing
Attorney, Agent, or Firm—Pollock, Vande Sande & Priddy

[57] **ABSTRACT**

A microwave lens of the type described in the French patent No. 2,469,808 is adapted to operate with two crossed polarizations. To this end, each of the phase-shifting channels of the lens is subdivided into two subchannels, each of them being assigned to one of said polarizations. Each subchannel includes, in addition to phase-shifting panels, means for rotating by 90° the polarization of the incident wave and impedance matching means.

12 Claims, 8 Drawing Sheets

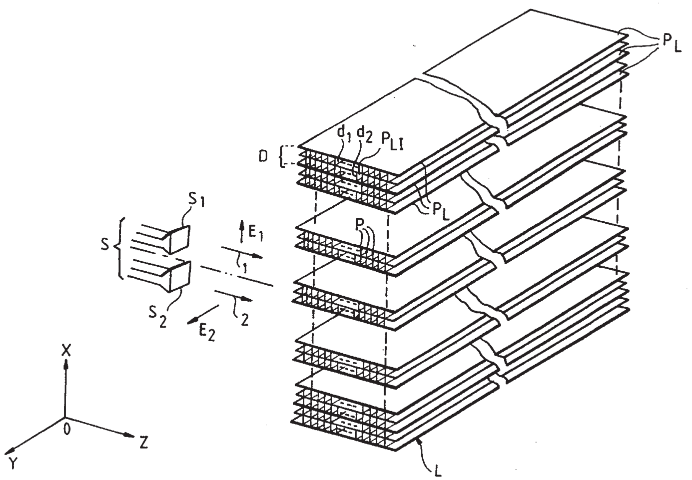

US006822615B2

(12) **United States Patent** — **Quan et al.**

(10) **Patent No.: US 6,822,615 B2**
(45) **Date of Patent: Nov. 23, 2004**

(54) **WIDEBAND 2-D ELECTRONICALLY SCANNED ARRAY WITH COMPACT CTS FEED AND MEMS PHASE SHIFTERS**

(75) Inventors: **Clifton Quan**, Arcadia, CA (US); **Jar J. Lee**, Irvine, CA (US); **Brian M. Pierce**, Moreno Valley, CA (US); **Robert C. Allison**, Rancho Palos Verdes, CA (US)

(73) Assignee: **Raytheon Company**, Waltham, MA (US)

(*) Notice: Subject to any disclaimer, the term of this patent is extended or adjusted under 35 U.S.C. 154(b) by 64 days.

(21) Appl. No.: **10/373,936**

(22) Filed: **Feb. 25, 2003**

(65) **Prior Publication Data**

US 2004/0164915 A1 Aug. 26, 2004

(51) **Int. Cl.**^{7} **H01Q 3/00**
(52) **U.S. Cl.** **343/754**; 342/376
(58) **Field of Search** 343/753, 754; 342/368, 369, 372, 376

(56) **References Cited**

U.S. PATENT DOCUMENTS

6,160,519 A	*	12/2000	Hemmi	343/754
6,421,021 B1	*	7/2002	Rupp et al.	343/753
6,677,899 B1	*	1/2004	Lee et al.	342/376

* cited by examiner

Primary Examiner—Michael C. Wimer
(74) *Attorney, Agent, or Firm*—Leonard A. Alkov; Karl A. Vick

(57) **ABSTRACT**

A microelectromechanical system (MEMS) steerable electronically scanned lens array (ESA) antenna and method of frequency scanning are disclosed. The MEMS ESA antenna includes a wide band feedthrough lens and a continuous transverse stub (CTS) feed array. The wide band feedthrough lens includes first and second arrays of wide band radiating elements and an array of MEMS phase shifter modules disposed between the first and second arrays of radiating elements. The continuous transverse stub (CTS) feed array is disposed adjacent the first array of radiating elements for providing a planar wave front in the near field. The MEMS phase shifter modules steer a beam radiated from the CTS feed array in two dimensions.

14 Claims, 5 Drawing Sheets

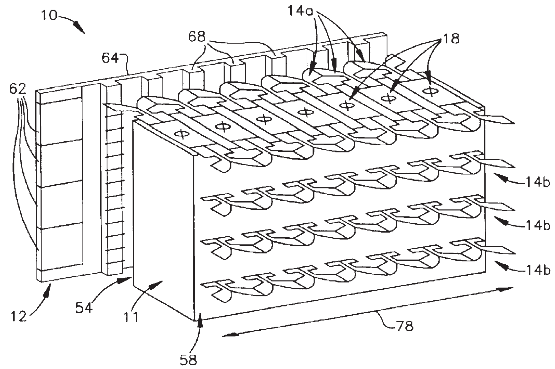

Lens Arrays: References

[1] C. Chekroun, "Microwave phase shifter and its application to electronic scanning," U.S. Patent 4,320,404, February 24, 1981.

[2] ——, "Dual-polarization microwave lens and its application to a phased-array antenna," U.S. Patent 5,598,172, November 05, 1991.

[3] J. J. Maciel, J. F. Slocum, J. K. Smith, and J. Turtle, "MEMS electronically steerable antennas for fire control radars," *IEEE Aerosp. Electron. Syst. Mag*, vol. 22, no. 11, pp. 17–20, November 2007.

[4] K. Van Caekenberghe and T. Vähä-Heikkilä, "An analog RF MEMS slotline true-time-delay phase shifter," *IEEE Trans. Microwave Theory Tech.*, vol. 56, no. 9, pp. 2151–2159, September 2008.

[5] Raytheon technologies promise to improve radar affordability. [Online]. Available: http://investor.raytheon.com/phoenix.zhtml?c=84193\&p=irol-newsArticle\&ID=1176149

Tile Assembled RF MEMS Reflect Arrays

- **Principle of operation**: A tunable impedance surface reflects an unbounded wave in a desired direction by tuning the surface impedance (reactance) of unit cells in order to obtain a linear reflection phase shift progression over the surface [1–6].
- **Advantages**:
  - Beam steering controller on the backside
  - EIRP $\times$ G_r/T: higher than for a brick-assembled lens or reflect array
  - Monopulse-capable
  - Size and weight (tile-assembly)
- **Disadvantages**:
  - Bandwidth: resonant
  - Beam pointing error (1b $< \tilde{P} <$ 2b)
  - Feed blocking, protrusion (Cassegrain)
  - (Single Polarized)
  - Spill-over loss (Tx) and noise (Rx)

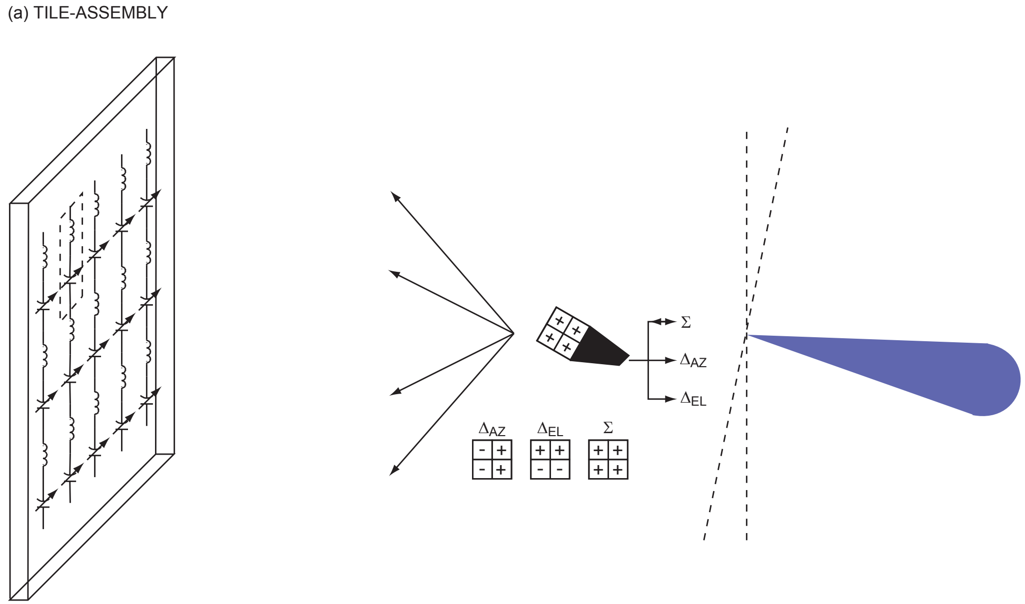

Figure 24: (a) tile-assembled resonant RF MEMS tunable impedance surface

Tile Assembled p-i-n Diode Reflect Array Patents

Sept. 27, 1966 A. DORNE ETAL 3,276,023

GRID ARRAY ANTENNA

Filed May 21, 1963 4 Sheets-Sheet 1

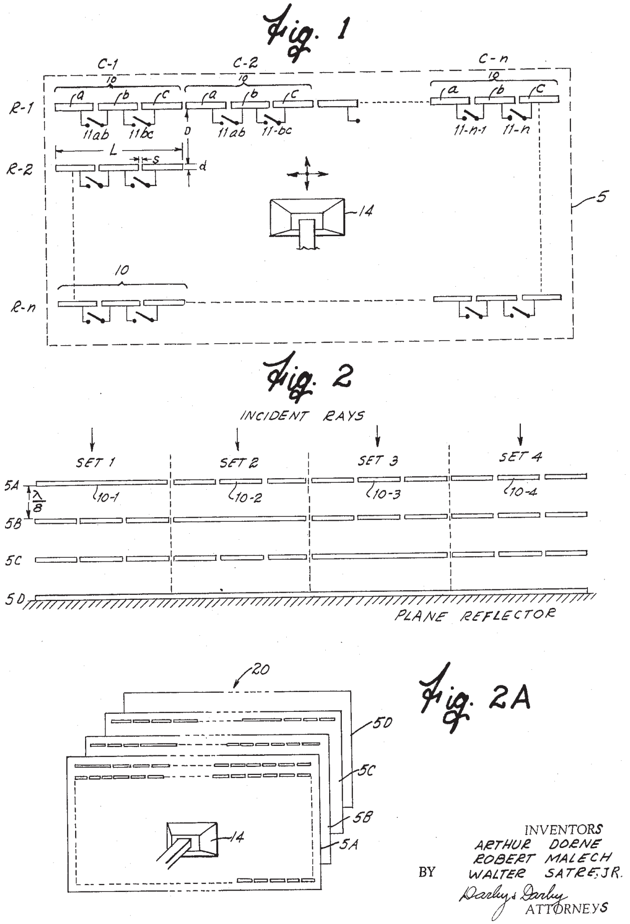

US007245269B2

(12) **United States Patent**
Sievenpiper et al.

(10) **Patent No.: US 7,245,269 B2**
(45) **Date of Patent: Jul. 17, 2007**

(54) **ADAPTIVE BEAM FORMING ANTENNA SYSTEM USING A TUNABLE IMPEDANCE SURFACE**

(75) Inventors: **Daniel F. Sievenpiper**, Santa Monica, CA (US); **James H. Schaffner**, Chatsworth, CA (US); **Gregory L. Tangonan**, Oxnard, CA (US)

(73) Assignee: **HRL Laboratories, LLC**, Malibu, CA (US)

(*) Notice: Subject to any disclaimer, the term of this patent is extended or adjusted under 35 U.S.C. 154(b) by 0 days.

(21) Appl. No.: **10/844,104**

(22) Filed: **May 11, 2004**

(65) **Prior Publication Data**

US 2004/0263408 A1 Dec. 30, 2004

Related U.S. Application Data

(60) Provisional application No. 60/470,029, filed on May 12, 2003.

(51) **Int. Cl.**
H01Q 15/02 (2006.01)
H01Q 15/24 (2006.01)
H01Q 1/38 (2006.01)

(52) **U.S. Cl.** .... **343/909**; 343/700 MS

(58) **Field of Classification Search** .... 343/700 MS, 343/745, 749, 756, 909, 910
See application file for complete search history.

(56) **References Cited**

U.S. PATENT DOCUMENTS

3,267,480	A	8/1966	Lerner	343/911
3,560,978	A	2/1971	Himmel et al.	343/106
3,810,183	A	5/1974	Krutsinger et al.	343/708
3,961,333	A	6/1976	Purinton	343/872
4,045,800	A	8/1977	Tang et al.	343/854
4,051,477	A	9/1977	Murphy et al.	343/700 MS
4,119,972	A	10/1978	Fletcher et al.	343/844
4,123,759	A	10/1978	Hines et al.	343/854
4,124,852	A	11/1978	Steudel	343/854
4,127,586	A	11/1978	Rody et al.	260/308 B
4,150,382	A	4/1979	King	343/754
4,173,759	A	11/1979	Bakhru	343/100
4,189,733	A	2/1980	Malm	343/100 SA
4,217,587	A	8/1980	Jacomini	343/100 SA

(Continued)

FOREIGN PATENT DOCUMENTS

DE 196 00 609 A1 4/1997

(Continued)

OTHER PUBLICATIONS

U.S. Appl. No. 10/944,032, Sep. 17, 2004, Sievenpiper.

(Continued)

Primary Examiner—Shih-Chao Chen
(74) *Attorney, Agent, or Firm*—Ladas & Parry

(57) **ABSTRACT**

A method of and apparatus for beam steering. A feed horn is arranged so that the feed horn illuminates a tunable impedance surface comprising a plurality of individually tunable resonator cells, each resonator element having a reactance tunable by a tuning element associated therewith. The tuning elements associated with the tunable impedance surface are adjusted so that the resonances of the individually tunable resonator cells are varied in a sequence and the resonances of the individually tunable resonator cells are set to values which improve transmission of information via the tunable impedance surface and the feed horn.

24 Claims, 9 Drawing Sheets

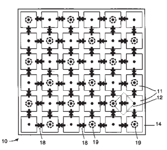

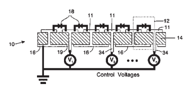

UWB Brick Assembled RF MEMS Reflect Arrays

- **Principle of operation**: Brick-assembled reflect arrays based on antennas and (TTD) phase shifters capture the unbounded wave, and (TTD) phase shift, reflect, (TTD) phase shift, and reradiate the guided wave [7–9].

- **Advantages**:
  - Bandwidth: TTD-capable
  - Beam pointing error (3b $< \tilde{P} <$ 4b)
  - Beam steering controller on the backside
  - Monopulse-capable
  - Polarimetric

- **Disadvantages**:
  - EIRP $\times$ G_r/T: Lower than for a tunable impedance surface, higher than for a lens
  - Feed blocking, protrusion (Cassegrain)
  - Size and weight (brick assembly)
  - Spill-over loss (Tx) and noise (Rx)

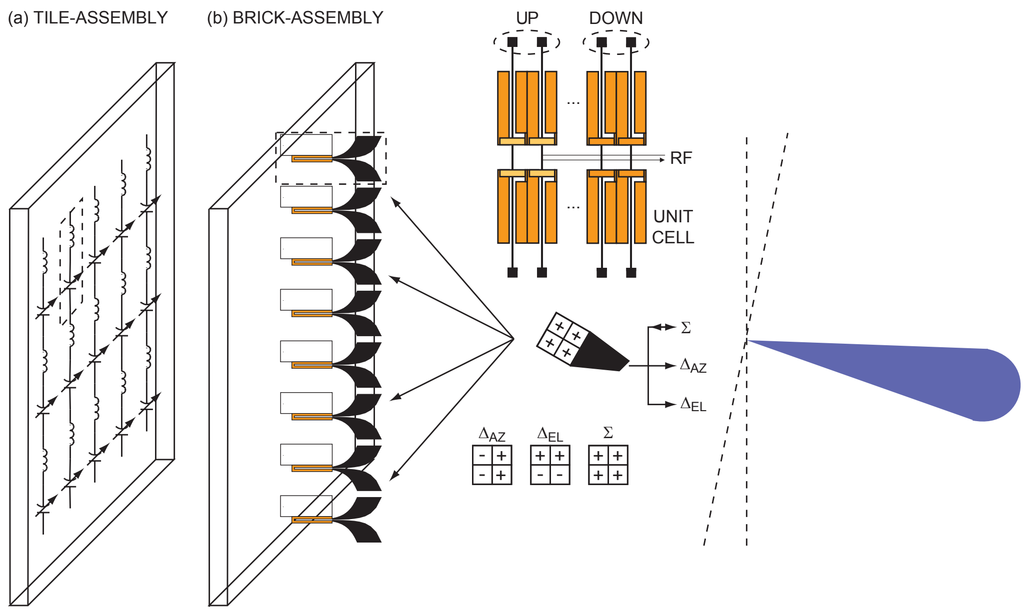

Figure 25: (a) tile-assembled resonant RF MEMS tunable impedance surface, (b) brick-assembled ultra wideband RF MEMS reflect array, (inset) *differential* RF MEMS slotline TTD reflection phase shifter.

UWB Brick Assembled RF MEMS Reflect Arrays

- **Principle of operation**: Brick-assembled reflect arrays based on antennas and (TTD) phase shifters capture the unbounded wave, and (TTD) phase shift, reflect, (TTD) phase shift, and reradiate the guided wave [7–9].
- **Advantages**:
  - Bandwidth: TTD-capable
  - Beam pointing error (3b $< \tilde{P} <$ 4b)
  - Beam steering controller on the backside
  - Monopulse-capable
  - Polarimetric
- **Disadvantages**:
  - EIRP $\times$ G_r/T: Lower than for a tunable impedance surface, higher than for a lens
  - Feed blocking, protrusion (Cassegrain)
  - Size and weight (brick assembly)
  - Spill-over loss (Tx) and noise (Rx)

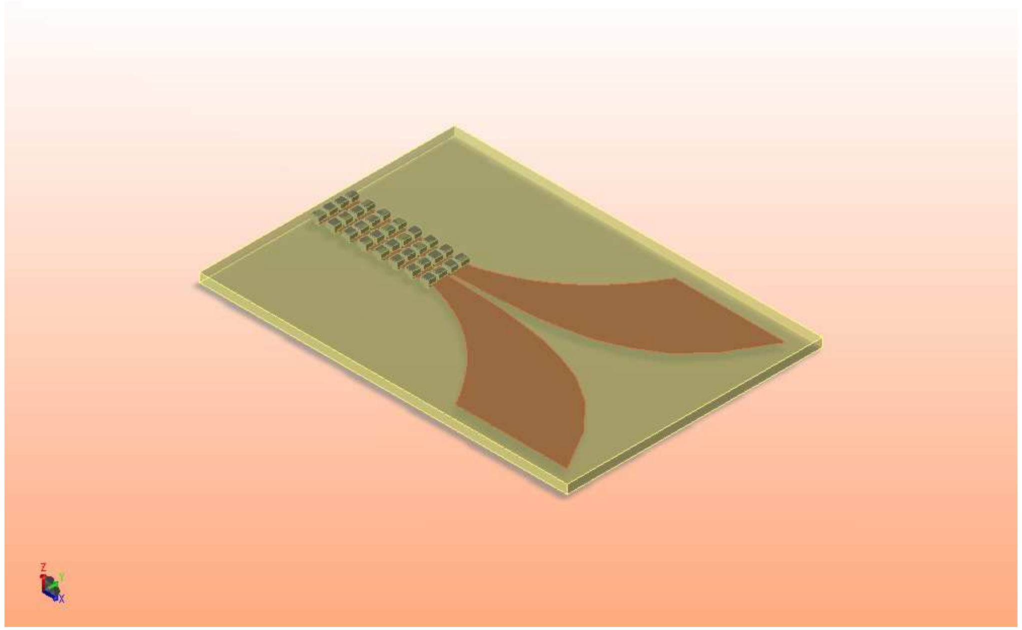

Figure 25: Artist impression of an RF MEMS reflect array brick with 3:1 bandwidth.

UWB Brick Assembled RF MEMS Reflect Arrays

- **Principle of operation**: Brick-assembled reflect arrays based on antennas and (TTD) phase shifters capture the unbounded wave, and (TTD) phase shift, reflect, (TTD) phase shift, and reradiate the guided wave [7–9].
- **Advantages**:
  - Bandwidth: TTD-capable
  - Beam pointing error (3b $< \tilde{P} <$ 4b)
  - Beam steering controller on the backside
  - Monopulse-capable
  - Polarimetric
- **Disadvantages**:
  - EIRP $\times$ G_r/T: Lower than for a tunable impedance surface, higher than for a lens
  - Feed blocking, protrusion (Cassegrain)
  - Size and weight (brick assembly)
  - Spill-over loss (Tx) and noise (Rx)

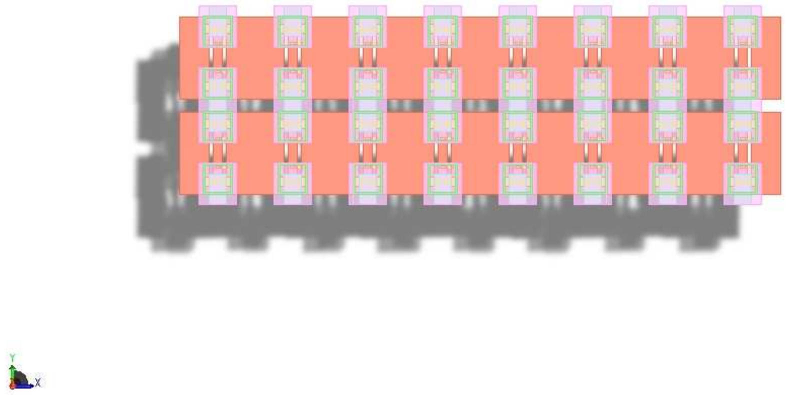

Figure 25: Artist impression of a *differential* slot-line TTD reflection phase shifter based on Radant RMSW200 SPST RF MEMS switches.

Brick Assembled p-i-n Diode Reflect Array Patents

United States Patent [11] 3,569,974

[72] Inventor **Willard W. McLeod, Jr.**
Lexington, Mass.
[21] Appl. No. **693,531**
[22] Filed **Dec. 26, 1967**
[45] Patented **Mar. 9, 1971**
[73] Assignee **Raytheon Company**
Lexington, Mass.

[54] **DUAL POLARIZATION MICROWAVE ENERGY PHASE SHIFTER FOR PHASED ARRAY ANTENNA SYSTEMS**
12 Claims, 12 Drawing Figs.

[52] **U.S. Cl.** **343/754,** 333/21, 333/24.1, 333/24.3, 333/98, 343/756, 343/778, 343/854
[51] **Int. Cl.** **H01p 1/16,** H03h 5/12, H01g 19/06
[50] **Field of Search** .... 343/754-—756, 854, 778, 909 (Cursory); 333/24.1, 24.3, 21 (A), 21

[56] **References Cited**

UNITED STATES PATENTS

3,100,287	8/1963	Scharfman et al.	333/24.1
3,109,152	10/1963	Dachert	343/778
3,154,784	10/1964	Allen	343/18
3,161,879	12/1964	Hannan et al.	343/756X
3,162,828	12/1964	Schmidt et al.	343/756X
3,166,724	1/1965	Allen	333/24.1
3,277,401	10/1966	Stern	333/24.3X
3,290,624	12/1966	Hines	333/31
3,305,867	2/1967	Miccioli et al.	343/754X
3,316,506	4/1967	Whicker et al.	333/24.1
3,387,301	6/1968	Blass et al.	343/854
3,401,361	9/1968	Schloemann	333/31(A)
3,425,003	1/1969	Mohr	333/24.1X
3,445,851	5/1969	Sheldon	343/754
3,453,563	7/1969	Maurer	333/24.3X

FOREIGN PATENTS

612,683	1/1961	Canada	333/24.1

OTHER REFERENCES

Frank et al., " Latching Ferrite Phase Shifter for Phased Arrays," The Microwave Journal March 1967, pp. 97— 102

Nolen, J. C., " Phased Array Polarization Agility" IEEE Trans. on Antennas & Propagation, Vol. AP— 13, 1965 pp. 820— 821

Primary Examiner—Eli Lieberman
Assistant Examiner—Wm. H. Punter
Attorneys—Harold A. Murphy, Joseph D. Pannone and Edgar O. Rost

ABSTRACT: A phase shifter is disclosed for supporting dual orthogonal polarization modes of propagated microwave energy in tactical electrically beam scanning phased array antenna systems of the optically fed reflector type. Reentrant single port antenna array elements provide a predetermined electrical phase shift of linear as well as circular polarized energy. Incident waves received by each element oriented in one plane of polarization, for example, a vertical wave, will be electrically shifted and launched after traversal of the device as, illustratively, a horizontally oriented wave. Each element incorporates a circular polarizer as well as reflective termination member together with solid state phase shifting means.

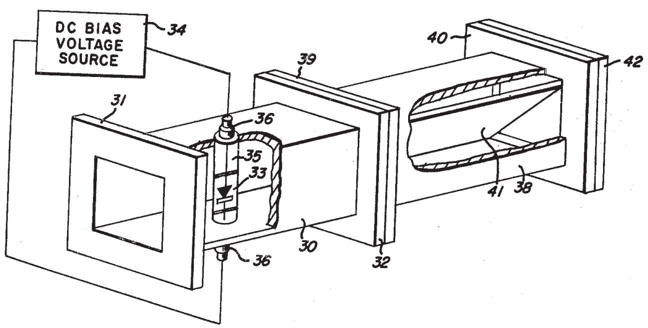

United States Patent [19]

Chekroun

[11] **4,320,404**
[45] **Mar. 16, 1982**

[54] **MICROWAVE PHASE SHIFTER AND ITS APPLICATION TO ELECTRONIC SCANNING**

[75] Inventor: **Claude Chekroun,** Bures Sur Yvette, France
[73] Assignee: **Societe d'Etude du Radant,** Orsay, France
[21] Appl. No.: **237,642**
[22] Filed: **Feb. 24, 1981**

Related U.S. Application Data

[63] Continuation of Ser. No. 971,546, Dec. 20, 1978.

[30] **Foreign Application Priority Data**

Dec. 20, 1977 [FR] France 77 38354

[51] **Int. Cl.**[3] **H01Q 3/26**
[52] **U.S. Cl.** **343/854;** 343/754; 343/786
[58] **Field of Search** 343/854, 754, 756, 909, 343/755, 757, 778; 333/21, 24.1, 24.3, 98

[56] **References Cited**

U.S. PATENT DOCUMENTS

3,276,023	9/1966	Dorne et al.	343/854
3,569,974	3/1971	McLeod Jr.	343/854
3,708,796	1/1973	Bony	343/754
4,212,014	7/1980	Chekroun	343/754
4,266,203	5/1981	Saudrean et al.	343/756

FOREIGN PATENT DOCUMENTS

1329686	5/1962	France .
2224887	10/1974	France .

OTHER PUBLICATIONS

Hanson, *Microwave Scanning Antennas,* vol. III, 1966, pp. 102–121.

Primary Examiner—David K. Moore
Attorney, Agent, or Firm—Finnegan, Henderson, Farabow, Garrett and Dunner

[57] **ABSTRACT**

A plurality of metallic wire conductors are fitted in shunt along a shorted wave guide parallel to a dielectric field of electromagnetic wave incident to the wave guide. At least some of the wires have diodes mounted on them such that selective biasing of the diodes renders these wires discontinuous and causes a controlled phase shift of the incident wave.

10 Claims, 6 Drawing Figures

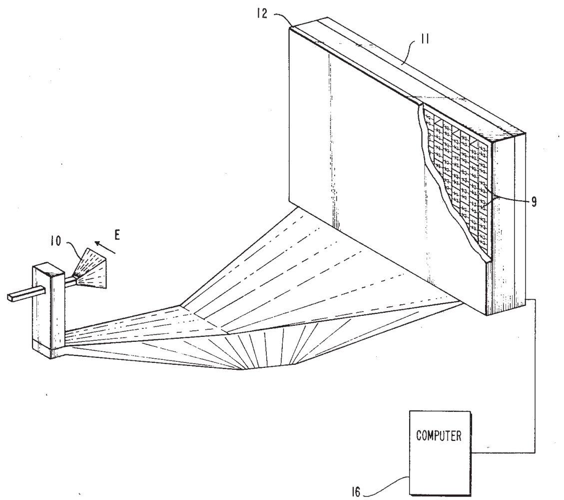

Reflect Arrays: References

[1] A. Dorne, R. G. Malech, and W. Statre, "Grid array antenna," U.S. Patent 3,276,023, May 21, 1963.

[2] W. W. Lam, C. F. Jou, H. Z. Chen, K. S. Stolt, N. C. Luhmann, and D. B. Rutledge, "Millimeter-wave diode-grid phase shifters," *IEEE Trans. Microwave Theory Tech.*, vol. 36, no. 5, pp. 902–907, May 1988.

[3] P. Naudin, M. Soiron, and C. Chekroun, "Microwave phase-shifter and electronic scanning antenna with such phase-shifters," U.S. Patent 6,429,822 B1, March 30, 2001.

[4] D. F. Sievenpiper, J. H. Schaffner, H. J. Song, R. Y. Loo, and G. Tangonan, "Two-dimensional beam steering using an electrically tunable impedance surface," *IEEE Trans. Antennas Propagat.*, vol. 51, no. 10, part 1, pp. 2713–2722, October 2003.

[5] C. Chekroun, T. Dousset, C. Renard, M. Déjus, and J.-M.Lopez, "ERASP: A light weight, low power consumption phased array antenna concept for a X-band spaceborne SAR system," *International Radar Conference Digest*, October 2004.

[6] H. Legay, G. Caille, A. Laisne, D. Cadoret, and R. Gillard, "Phase shifter module whose linear polarization and resonant length are varied by means of MEMS switches," U.S. Patent 7,358,915, March 23, 2005.

[7] W. W. McLeod, Jr., "Dual polarization microwave energy phase shifter for phased array antenna systems," U.S. Patent 3,569,974, December 26, 1967.

[8] J. H. Schaffner, D. F. Sievenpiper, R. Y. Loo, J. J. Lee, and S. W. Livingston, "A wideband beam switching antenna using RF MEMS switches," *IEEE AP-S International Symposium Digest*, vol. 3, pp. 658–661, July 2001.

[9] K. Van Caekenberghe, "RF MEMS on the radar," *IEEE Microwave Magazine*, vol. 10, no. 6, pp. 99–116, October 2009.

RF MEMS Switched Beamformers

- **Principle of operation**: It is a cascade of an RF MEMS single pole N throw (SPNT) switch and a beamformer (beamforming matrix or lens or reflector based focal plane scanner [1–3]).
- **Advantages**:
  - Bandwidth: TTD-capable, if based on focal plane scanner (parabolic reflector, Luneburg or Rotman lens)
- **Disadvantages**:
  - Bandwidth: coupler limited, if based on beamforming matrix (Blass, Butler, Nolen)
  - Beam pointing error: high, B beam positions versus 2^{2P} beam positions for (TTD) phase shifter based ESA
  - EIRP $\times$ G_r/T: P_T limited by linearity and cold-switched power handling of SPNT switch. G lowered by insertion loss (IL) of SPNT switch and beamformer.
  - Field of view: related to f/D (IL, size)
  - Not monopulse-capable

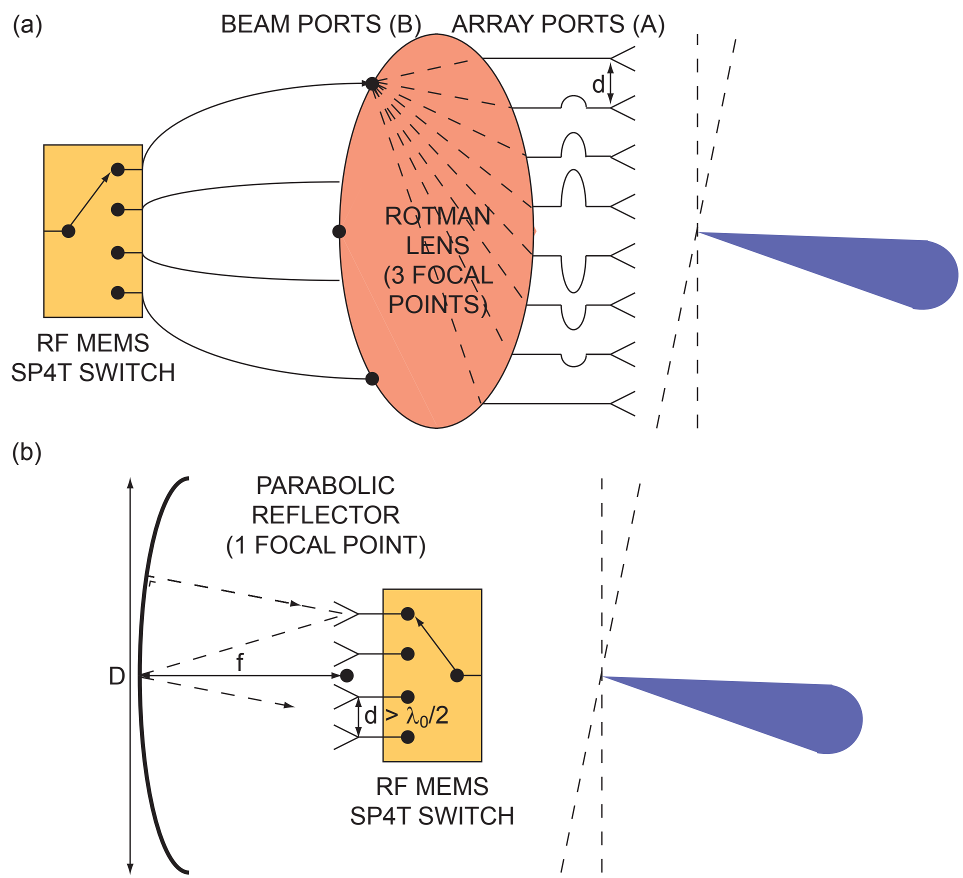

Figure 26: Switched beamformers based on an RF MEMS single pole 4 throw (SP4T) switch and a focal plane scanner: (a) the Rotman lens based focal plane scanner, (b) parabolic reflector based focal plane scanner.

Switched Beamformers: References

[1] R. C. Hansen, *Phased Array Antennas*. John Wiley & Sons, 1998.

[2] J. Schöbel, T. Buck, M. Reimann, M. Ulm, M. Schneider, A. Jourdain, G. J. Carchon, and H. A. C. Tilmans, "Design considerations and technology assessment of phased-array antenna systems with RF MEMS for automotive radar applications," *IEEE Trans. Microwave Theory Tech.*, vol. 53, no. 6, part 2, pp. 1968–1975, June 2005.

[3] M. V. Ivashina, M. Kehn, P.-S. Kildal, and R. Maaskant, "Decoupling efficiency of a wideband Vivaldi focal plane array feeding a reflector antenna," *IEEE Trans. Antennas Propagat.*, vol. 57, no. 2, pp. 373–382, February 2009.

Radomes

RF MEMS Radomes

- **Primary function**: Protection of ESA against adverse environmental conditions
- **Secondary functions**:
  - (Tunable) Frequency selective surface (FSS) [1]
  - Limiter
  - (Reconfigurable) Polarization transformer [2]
  - Shutter (RCS control) [3]

Radomes: References

[1] B. Schönlinner, A. Abbaspour-Tamijani, L. C. Kempel, and G. M. Rebeiz, "Switchable low-loss RF MEMS Ka-band frequency selective surface," *IEEE Trans. Microwave Theory Tech.*, vol. 52, no. 11, pp. 2474–2481, November 2004.

[2] L. Saudreau and J.-P. Biansan, "Microwave polarization transformer," U.S. Patent 4,266,203, Feb 22, 1978.

[3] J.-C. Sureau, "Electromagnetic energy shield," U.S. Patent 5,621,423, August 29, 1983.

Conclusion

Radar

Figures of merit:

- ☐ Radars for moving point targets:
  - Angle (field of view, angular resolution)
  - Doppler (maximum Doppler frequency shift, Doppler frequency shift resolution)
  - Range (maximum range, range resolution)
  - Probability of detection (P_D), false alarm rate (P_{FA})
- ☐ Radars for distributed targets:
  - Angle, Doppler and range (swath size, voxel resolution)
  - amplitude (contrast), phase
  - Polarization

Design trade-offs:

- ☐ Application: AMRFS, autonomous cruise control (ACC), autonomous landing guidance (ALG), altimetry, air traffic management (ATM), ground penetrating radar (GPR), weather forecasting
- ☐ Architecture: monostatic or bistatic, pulse-Doppler or FMCW. Pulse-Doppler extensions are monopulse and pulse compression. An FMCW extension is FM interrupted CW (FMICW).
- ☐ Platform: airborne, car-borne, naval, ground-based, space-borne. Clutter models are platform dependent.
- ☐ Propagation window: 3 GHz (S), 10 GHz (X), 24 GHz (K), 35 GHz (Ka), 77 GHz (W), 94 GHz (W), 210 GHz (G). The propagation window is chosen based on the RCS of the target and the size of the radar sensor.
- ☐ Radar modes: search, track (point targets), imaging, mapping (distributed targets). The radar mode sets the radar waveform.

Electronically scanned array

Figures of merit:

- ☐ Bandwidth
- ☐ Beam pointing error
- ☐ EIRP $\times$ G_r/T, scan loss
- ☐ Field of view
- ☐ Half power beam width
- ☐ Phase center stability
- ☐ Polarization purity
- ☐ Radar cross section
- ☐ Scalability
- ☐ Sidelobe level
- ☐ Size
- ☐ Thermal dissipation
- ☐ Weight

Design trade-offs:

- ☐ Aperture: real beam or synthetic aperture (SAR)
- ☐ Antenna: connected or folded dipole, microstrip, tapered slot, waveguide antenna
- ☐ Beamforming: digital (DBF), IF, optical, RF
- ☐ Geometry: conformal, distributed, planar, spherical
- ☐ Feed network: constrained (corporate, series) or space-fed (lens array, reflect array). Extensions include monopulse and calibration networks.
- ☐ Grid: periodic (hexagonal, rectangular, or triangular) or aperiodic (sparse)
- ☐ Manufacturing: 2-D arrays: brick, stick, tile or tray, 3-D arrays: geodesic dome, multifaceted (pyramidal frusta)
- ☐ Polarization: vertical (taking advantage of Brewster angle for ground-based and naval platforms), polarimetric (all-weather, FOPEN, SAR/ATR)
- ☐ RF power amplification: active (SSPA), passive subarrays, passive (VED)
- ☐ Scanning:
  Scanning: frequency-, space-, or time-orthogonal waveform-coherent pencil beams, or MIMO waveform-orthogonal wide beams

(TTD) Phase shifter

Figures of merit:

- ☐ Distortion (GVD)
- ☐ Gain if active, loss if passive
- ☐ Linearity (IP3, P1dB)
- ☐ Number of effective bits, if digital
- ☐ (TTD) phase shift / noise figure
- ☐ Power consumption
- ☐ Power handling
- ☐ Size
- ☐ Switching time

Design trade-offs:

- ☐ Analog or digital
- ☐ Biasing: current-controlled, voltage-controlled (electrodynamic (current flow), electrostatic (no current flow))
- ☐ Design: (distributed) loaded-line, reflect-type, switched LC network (high-pass, low-pass), switched-line, vector modulator
- ☐ Differential (CPS, slotline) or single-ended (CPW, microstrip) transmission line
- ☐ Phase shift or TTD phase shift
- ☐ RF power amplification: active (unilateral) or passive (reciprocal)

Conclusion

- Using a bottom-up approach, the figures of merit for RF MEMS technology are related to the figures of merit of radar subsystems. Particular emphasis is put on UWB RF MEMS T/R modules and passive electronically scanned reflect arrays.
- Thank you for attending. Any questions?

Open-Source Software

- Elsie 2.34 (shareware): Elsie is an uncommon commercial-grade lumped-element ("L-C") electrical filter design and network analysis program, directed toward the engineer or technician involved in that line of work. http://www.tonnesoftware.com/elsie.html

- GNU Octave 3.3.51: GNU Octave is a high-level language, primarily intended for numerical computations. It provides a convenient command line interface for solving linear and nonlinear problems numerically, and for performing other numerical experiments using a language that is mostly compatible with Matlab. It may also be used as a batch-oriented language. http://www.gnu.org/software/octave

- rfMaxima 0.1: rfMaxima is an RF toolbox for the wxMaxima computer algebra system[2]. rfMaxima symbolically derives 2-port network parameters (ABCD, G, InverseABCD, H, S, Y, and Z) from the solution of the set of Kirchoff current and voltage law equations representing the 2-port. In addition, it allows for symbolic derivation, as well as numerical evaluation (plotting), of microwave noise (experimental), stability and power parameters. http://rfmaxima.sourceforge.net

- Sugar 3.1: Much like SPICE does for circuit designers, SUGAR provides for MEMS designers a tool for quickly specifying their devices in a netlist type format and analyzing their devices with different simulation and mathematical techniques. http://sourceforge.net/projects/mems/files

- Qucs 0.0.15: Qucs is an integrated circuit simulator which means you are able to setup a circuit with a graphical user interface (GUI) and simulate the large-signal, small-signal and noise behaviour of the circuit. After that simulation has finished, you can view the simulation results on a presentation page or window. http://qucs.sourceforge.net

[2] Please assure that wxMaxima is working properly by calculating factor(50!), especially if you are using the Ubuntu 9.10 default install. If you are working on Ubuntu 9.10, please consider upgrading to Maxima 5.20.1 and wxMaxima 0.8.4-1.